Technical Report Documentation Page

1. Report No. FHWA/TX-04/0-1700-1	2. Government Accession No.	3. Recipient's Catalog No.
4. Title and Subtitle ESTIMATING IN SITU STRENGTH OF CONCRETE PAVEMENTS UNDER VARIOUS FIELD CONDITIONS		5. Report Date June 2001 Rev. August 2003
7. Author(s) Shantala V. Ramaiah, B. Frank McCullough, Terry Dossey		6. Performing Organization Code
		8. Performing Organization Report No. 0-1700-1
9. Performing Organization Name and Address Center for Transportation Research The University of Texas at Austin 3208 Red River, Suite 200 Austin, TX 78705-2650		10. Work Unit No. (TRAIS)
		11. Contract or Grant No. 0-1700
12. Sponsoring Agency Name and Address Texas Department of Transportation Research and Technology Implementation Office P.O. Box 5080 Austin, TX 78763-5080		13. Type of Report and Period Covered Research Report (9/1/99—8/31/04)
		14. Sponsoring Agency Code

15. Supplementary Notes

Project conducted in cooperation with the Texas Department of Transportation and the U.S. Department of Transportation, Federal Highway Administration.

16. Abstract

During the past few years, the transportation industry has expressed the desire to create performance-based specifications. One of the key developments required to characterize and improve the performance of (PCC) pavements is a better understanding of its in situ properties. Of great importance is the accurate estimation of in situ concrete strength. There are currently many methods used to estimate in situ strength, each providing unique benefits. However, many of these techniques can introduce variables that affect accurate estimation. Thus, a reevaluation of current procedures is required to appropriately reflect sound engineering principles and to produce a quality product. This project addresses many factors, which arise in practice, but whose effects on strength need to be determined, quantified, or reevaluated. These include the effects of core diameter, cylinder curing regime, pavement curing history, presence of reinforcement in a core, vertical location of core, aggregate type, and surface evaporation on both compressive and tensile strength.

This project is different from previous research in that in situ strength is determined directly from tensile strength test. If pavement strength is to be determined, it is suggested that indirect tensile tests should be conducted rather than estimating tensile strength from compressive or flexural tests, because of the fact that pavements fail in tension.

17. Key Words in situ strength, concrete pavements, tensile strength, compressive tests, flexural tests		18. Distribution Statement No restrictions. This document is available to the public through the National Technical Information Service, Springfield, Virginia 22161.	
19. Security Classif. (of report) Unclassified	20. Security Classif. (of this page) Unclassified	21. No. of pages 186	22. Price

Form DOT F 1700.7 (8-72) Reproduction of completed page authorized

Estimating In Situ Strength of Concrete Pavements Under Various Field Conditions

Shantala V. Ramaiah
B. Frank McCullough
Terry Dossey

Research Report 0-1700-1

Research Project 0-1700
Improving Portland Cement Concrete Pavement Performance

Conducted for the
Texas Department of Transportation
in cooperation with the
U.S. Department of Transportation
Federal Highway Administration
by the
Center for Transportation Research
Bureau of Engineering Research
The University of Texas at Austin

June 2001
Revised August 2003

Implementation Statement

The observations and recommendations developed in this report provide excellent additions to the existing improvement program for (PCC) pavements. An implementation plan reflecting this new information is provided in Chapter 9 in terms of specific recommendations for continued improvement of high performance concrete (HPCP) pavement concerning developments in specifications, testing, construction, monitoring, design, and condition evaluation. The objective of this program is to increase pavement life and quality leading to pavements that serve for 25 to 40 year on high-volume facilities with minimal maintenance.

The reader is referred to Chapter 9 for specific recommendations in five basic areas discussed in the following sections.

Abstract

During the past few years, the transportation industry has expressed the desire to create performance-based specifications. One of the key developments required to characterize and improve the performance of (PCC) pavements is a better understanding of its in situ properties. Of great importance is the accurate estimation of in situ concrete strength. There are currently many methods used to estimate in situ strength, each providing unique benefits. However, many of these techniques can introduce variables one that affect accurate estimation. Thus, a reevaluation of current procedures is required to appropriately reflect sound engineering principles and to produce a quality product. This project addresses many factors which arise in practice but whose effects on strength need to be determined, quantified, or reevaluated. These include the effects of core diameter, cylinder curing regime, pavement curing history, presence of reinforcement in a core, vertical location of core, aggregate type, and surface evaporation on both compressive and tensile strength.

This project is different from previous research in that in situ strength is determined directly from tensile strength tests. If pavement strength is to be determined, it is suggested that indirect tensile tests should be conducted rather than estimating tensile strength from compressive or flexural tests, because of the fact that pavements fail in tension.

Disclaimers

The contents of this report reflect the views of the authors, who are responsible for the facts and the accuracy of the data presented herein. The contents do not necessarily reflect the official views or policies of the Federal Highway Administration or the Texas Department of Transportation (TxDOT). This report does not constitute a standard, specification, or regulation.

There was no invention or discovery conceived or first actually reduced to practice in the course of or under this contract, including any art, method, process, machine, manufacture, design or composition of matter, or any new and useful improvement thereof, or any variety of plant, which is or may be patentable under the patent laws of the United States of America or any foreign country.

NOT INTENDED FOR CONSTRUCTION, BIDDING, OR PERMIT PURPOSES

B. Frank McCullough
P.E. License: Texas No. 19914
Research Supervisor

Acknowledgments

The authors would like to thank the many engineers, TxDOT staff, and the El Paso District for their input, supply of equipment, testing technicians, mobilization, and execution of the project in the El Paso area. Appreciation is also expressed to Jobe Materials whose input, services, construction material contribution, and labor were invaluable to the success of this project. Additionally, appreciation is expressed to the research teams of the University of Texas at El Paso, the University of Texas at Houston, and the Texas Transportation Institute from Texas A&M University for equipment and time contributions involving nondestructive testing (seismic), microwave sensors, and dew point sensors, respectively. Finally, the authors would like to thank CTR employees Tracy Pilson and Dave Merritt, Nancy Kurio, Jerrie England, and John Miller for their assistance in this project.

Research performed in cooperation with the Texas Department of Transportation and the U.S. Department of Transportation, Federal Highway Administration.

Table of Contents

List of Tables

List of Figures

List of Photos

1. Introduction

The studies discussed herein represent the continuation of 23 years of research conducted in Texas to understand the reasons for differences in pavement performance around the state. In 1974, the Texas State Department of Highways and Public Transportation (now the Texas Department of Transportation [TxDOT]) began condition surveys to periodically survey continuously reinforced concrete pavements (CRCP) and establish a database that would help develop design methods and construction specifications, monitor maintenance effects, and compare pavement type. Findings from these studies indicated significant effects of aggregate type of pavement performance. Thus, coarse aggregate studies Project 422 and subsequently Project 1244 were commissioned to understand the material properties (including aggregate type) causing the differences. Results of these studies yielded many findings; most significantly the recommendations that night placement and the use of blended aggregate should be implemented. Many programs that can be used for design and analysis were developed, but shall not be discussed in this report.

Results of findings from Projects 422 and 1244 led to the commission of Project 7-3925. Some of the accomplishments of these studies were to perform early-age and later-life conditions surveys of test sections, monitor performance based on coarse aggregate type, refine thermal coefficient testing and crack control techniques considering concrete coefficient of thermal expansion (COTE), develop a spalling model, and support the quality control/quality assurance (QC/QA) specification development.

Out of the results of Project 7-3925 came the large scale Project 1700. This project continues detailed analyses of a wide array of influences affecting the performance of CRC pavements. As part of Project 1700, Task 5.2 calls for the study of specific variables on a series of Small Slab Studies. This report covers the need for, design, and results of these first two studies and is the second report in a series of Project 3925 reports.

1.1 BACKGROUND

In this section, several PCC pavement developments in Texas and elsewhere are discussed first. This is followed by a review of the current practices and deficiencies, which leads to a definition of needs to be studied in this phase. The last section describes the responsibility of several agencies involved in the partnering effort.

1.1.1 PCCP Developments

During the past few years, the transportation industry has expressed the desire to create performance-based specifications. One of the key developments required to characterize and improve the performance of portland cement concrete (PCC) pavement is a better understanding of its in situ properties. Of great importance is the accurate estimation of in situ concrete strength, because it has a major impact on concrete performance. Currently there are many methods used to estimate in situ strength, each providing unique benefits. However, many of these techniques can introduce variables that affect accurate estimation. Examples include the type of specimen used, test employed, or unavoidable/incompatible field conditions. If true QC/QA is desired, one should step back and revisit concepts for total quality-control testing with PCC pavements. This requires reevaluating current procedures and modifying them, as appropriate, to reflect sound engineering principles and to produce a quality product.

For the rigid pavement database, maintained since 1974, a number of factors should be added to the database and developed using it, given that these studies have shown their importance. Those pertaining to this report are listed below:

(1) The evaporation rate (relative to curing effectiveness) at the time of the PC placement for the test section should be added.

(2) The vertical distribution of the tensile strength has been identified as an important factor affecting concrete pavement performance, especially in the spalling area. Thus it is recommended that the vertical tensile strength distribution be determined for a subsection of the rigid pavement database in order to determine what is an acceptable range.

(3) Once the vertical strength distribution is ascertained from the additions to the database, as described in item (1), then an acceptable level of difference between top and bottom may be established by examining the pavement's performance at various levels.

Performance-based specifications for PCC pavement should be developed using these studies, insofar as significant information has been derived and may be used to improve the overall level of rigid pavement performance in Texas. Those issues pertaining to this report are listed below:

(1) The evaporation rate on every project should be monitored in real time and for use by the contractor to adjust the curing conditions of placed pavements to ensure that a desirable set of conditions are realized.

(2) The desire to develop an NDT of measuring in situ strength. To ensure that proper concrete conditions are achieved so as to provide acceptable PCC pavement in place, an equation with tensile strength as a function of temperature, moisture, and density should be developed. At the present time, only temperature is used in a maturity equation, but in order to ensure that the in situ strength is adequate, the moisture and density should be considered.

Ultimately, the goal to be achieved is to design and build quality, high-performance pavements. Accurate estimation of in situ strength is of paramount importance in assuring pavement performance. If loads are applied to concrete before it reaches sufficient strength, severe reduction in life or even catastrophic failure may result. This report presents and discusses experimental results concerning the most common and significant variables affecting the accurate estimation of in situ strength. A clear understanding of the advantages, practicality and accuracy of various methods of estimating in situ strength and their associated variables are also presented. This study differs from previous research in that in situ strength is also determined directly from tensile strength tests, as well as compressive strength tests. The effects of most of the variables investigated in this project on compressive strength have been researched heavily. However, virtually no research has been conducted on the variables impact on tensile strength. If pavement strength is to be determined, it is suggested that indirect tensile tests should be conducted rather than estimating tensile strength from compressive or flexural tests, because of the fact that pavements fail in tension. This project also addresses the necessity, feasibility, and effects of using tensile tests as the standard for estimation of in situ concrete pavement strength.

Current developments on COTE include the implementation of QC/QA specifications in which the aggregate and concrete COTE are determined using either of three tests, with results used for the design of pavement considering site-specific factors (Schindler 2001). The method is designed to increase pavement life as the COTE of concrete dramatically affects ESALs, leading to failure. A major benefit of the COTE-based design is that no reference is made to a specific aggregate type, but only to the engineering property (Schindler 2001).

1.1.2 Review/Critique of Current Practices

The following section introduces the reader to current issues and practices on the design of high performance concrete (HPC) pavement. Issues specified in coarse aggregate Report 3925 are provided, as well as discussions on the use of tensile tests for pavement strength assessment, selection

1.1.2.1 Report 3925 Issues

The two Small Slab Studies discussed in this report implement testing of some recommendations in the first Project 3925 study. As progressive steps are being taken to implement the evolution of HPC pavement, issues addressed in this report represent some of the action items that will be achieved over the next few years. The first issue addressed is the control of construction/specification items to monitor and manage surface moisture evaporation such that acceptable stress levels are maintained. In times of critical evaporation, monomolecular film (MMF) and expedited curing compound application, and possible application of two coats of curing compound are recommended for investigation. The benefits of these procedures are evaluated in Small Slab Study II (SSII).

The second issue this report addresses is vertical strength loss because of excessive surface moisture loss and associated delamination. Recommendations include: developing a technique for cutting a core into segments (two or three levels) and testing them; developing a correlation between vertical strength distribution and spalling; and instrumenting test slabs of varying curing types for maturity and moisture to develop a relationship between strength loss-based maturity and the parameters investigated. This model can then be used to determine acceptable/unacceptable evaporation rates and quantities. All of these recommendations are investigated in SSII.

A third issue concerns ambient and concrete temperatures. It has been shown that ambient temperatures above 32 °C 90°F and/or high set temperatures can be detrimental to concrete. The concrete, setting at high temperatures, contracts when temperatures drop, inducing higher than design tensile stresses and thus increased cracking. Specifications on concrete and ambient temperatures need to be included in construction manuals to minimize these detrimental temperature effects.

1.1.2.2 Tensile Testing for Pavement Strength Estimations

The acceptance testing of PCC is based on flexural testing of specimens. Because concrete fails in tension, splitting tensile strength testing should be considered for acceptance testing. Report 3925 recommends the use of splitting tensile testing as the official TxDOT tool for the planning, design, and construction of PCC pavements. As suggested in Report 3925, the Small Slab Studies utilize a testing program on cores and cylinders from small slabs to investigate the relation between in situ cores and cylinders cured with simulated field conditions, effects of reinforcement

The nature of cracking in concrete pavements demonstrates that a tensile failure, not a compressive failure, is experienced. When development of tensile strength testing began, the method was viewed as difficult giving to the obstacles preventing obtaining precise values the secondary stresses induced from clamping devices. At the same time, flexural tests were available, and because of the lack of development of the tensile test methods, the flexural test was used as a surrogate test for tensile strength. Tensile failure is usually caused by fracture due to the initiation and propagation of tensile cracks, resulting in a brittle failure (compressive failure involves connecting cracks rather than propagating, making failure much less brittle).

Generally, for quality control of PCC pavement, current practice uses the flexural test. Regardless of whether third-point loading or center-point loading is used, many problems have been encountered relative to sample preparation, storing, and testing. For example, if in situ strength is desired, cores can be extracted from the pavement by cutting, whereas beams cannot be removed easily. Merits of the flexural test, however, are that it simulates the bending of a pavement under a wheel load, but not the entire action of the pavement structure.

To minimize the problems introduced by using the flexural test, some elements of the concrete pavement industry have turned to compressive tests. Generally, this decision has been made on the basis of sharing test equipment with those used in the structural field. Although employing a direct tensile test is still problematic, the indirect tensile test, which had not yet been developed when the flexural test was selected, is now the best available predictor of pavement performance. In contrast, compressive strength testing is poorly correlated to flexural strength and less representative of the type of failure experienced in pavements. For these reasons, all current design methods for PCC utilize a limiting tensile stress value, whether directly or indirectly, for determining thickness.

1.1.2.3 In Situ Strength Estimations: Cylinders and Cores

When estimating the strength of PCC pavement, not only must a test be selected that accurately represents the expected failure mode, but also a representative sample of in situ concrete must be chosen. Because molded specimens have the advantage of being economical, quick and easy to make, repeatable, and relatively controllable, they are often used in tests for estimates of in situ strength. These strength measurements are ultimately used to estimate when a structure or pavement has reached sufficient strength such that it can be opened to traffic, formwork can be removed, or post-tensioning can be applied. They can also be used to determine load-bearing capacity, compliance with specifications, and eventually warranty acceptance and/or payment level.

If in situ strength is to be estimated from the strength of molded specimens, it is critical that compatibility of comparisons exists. For example, a common method of determining when a pavement can be opened to traffic is based on the flexural strength of water-cured molded beams. Concrete pavements in Texas are currently designed on the basis of achieving in situ flexural strength of 720 psi at 28 days. Acceptance testing, however, is based on molded flexural beams tested at an age of 7 days. If these 7- and 28-day strengths are not compatible, a pavement may be opened to traffic prior to development of sufficient strength and thus experience greater damage and decreased performance. In addition to compatibility between ages, compatibility issues are likely to exist between the curing experienced by molded specimens and a pavement. Often lab-cured specimens have water continuously available for hydration of cementitious particles; whereas in a pavement, evaporation of water may drastically reduce water availability, preventing proper hydration and reducing strength. Thus, resulting strengths can be very dissimilar, making comparisons between the two problematic. For example, lab-cured specimens are more likely to reach their maximum potential strength because water is continuously available for hydration. Additionally, the strength of molded specimens may differ from that of cores because of differences in casting, degree of compaction, conditions of restraint, ambient vapor pressure differential, heat retained from hydration, damage during cutting, and water gain during cutting (Simons 1990, Kesler 1966). These differences must be accounted for when estimating in situ strength from lab-cured cylinders. Otherwise, the molded specimens only provide an estimate of the concrete quality as delivered to the project.

When the strength of molded specimens does not reflect actual in situ strength or suggests in situ strength is below the specified strength, it is often necessary to directly determine in situ strength from cut cores. This is often a difficult, expensive, and time-consuming task. Unfortunately, many situations arise during construction and testing that cannot be avoided, and again affect the accurate prediction of in situ concrete strength. For example, the pavement may be too thin to obtain a standard-sized sample, or perhaps the pavement contains a large amount of reinforcement and obtaining a sample without steel is not possible. Another very common situation is the delayed application of a curing compound after concrete placement. These and many other variables are often present when one should determine in situ strength from a core.

Because molded cylinders may not accurately reflect in situ strength and obtaining cores is a laborious, time-consuming, and expensive process, other means of determining in situ strength are continually being developed and tested. One of these is the maturity method, a procedure in which in situ strength is estimated from the time-temperature history of concrete. The method is simple and nondestructive to a pavement. At this time, however, it is known that the maturity index used needs adjustments to reflect the effects of moisture loss. If the maturity method can be adjusted for the effects of surface moisture loss, QC/QA issues will benefit greatly as the proper curing of a pavement can be ensured rather than assuming the supplied curing regime is satisfactorily implemented. This would give contractors the freedom to select the type of curing regime implemented, so long as it can be demonstrated that a specified moisture level is maintained for the required time period. Contractors could then choose the most economical curing method, while engineers could be assured that specified strength is reached.

If surface moisture loss can be accurately measured, the proper curing of a pavement would be more accurately estimated rather than assuming the standard curing regime yielded satisfactory strength. Knowing when the concrete has sufficiently cured will improve QC/QA activities for pavement construction and ensure accurate opening time for traffic. Additionally, necessary modifications to current specifications on the use of maturity measurements for strength may be discovered. With proper quantification of the moisture in a pavement and performance-based specifications, a contractor would have greater flexibility in his work. For example, the contractor may be allowed to select the type of curing regime implemented, so long as it is demonstrated that some yet-determined critical moisture level is maintained for the required period of time.

1.1.3 Defining Study Needs

In the previous section, a detailed discussion of developments in the concrete industry was presented along with development needs. This section defines some of the needs studied in the first two small scale slabs studied in connection with Task 5.2 of Project 1700. Small Slab Studies I and II were developed and planned as a part of Project 1700 to quantify the effects of numerous variables affecting the accurate estimation of in situ strength. Small Slab Study I (SSI) was developed first to address a specific set of issues described later. After the analysis of data from the experiment, SSII was formulated to address specific issues not fully explained or additional issues surfacing from the SSI results. These include, but are not limited to, the effects of reinforcement, curing history, sample size, sample position, and aggregate type. Relationships between in situ, molded cylinder, and maturity method predicted strengths are developed and a comprehensive set of comparisons is established. All tests focus on the accurate estimation of pavement tensile strength rather than its prediction from compressive or flexural tests, as this test method is the most accurate in establishing pavement strength that may be correlated with pavement performance and the likelihood of failure.

1.1.4 Partnering

This project is a partnering effort of state agencies, academia, and private enterprises. It involves the work of the Center for Transportation Research of the University of Texas at Austin for the design, direction, data analysis, and reporting of all results. It also includes the Design, Construction, Materials and Research branches of TxDOT and the El Paso District for the supply of coring equipment, testing technicians, mobilization, and execution of the project in the El Paso area. The above parties desire to address issues affecting recent loss of pavement life observed in concrete pavements around Texas and investigate methods of increasing performance of future concrete pavements. Jobe Materials' involvement included volunteering construction materials, labor, and input due to interest in development of high-quality concrete pavement. The University of Texas at El Paso, the University of Texas at Houston, and Texas Transportation Institute from Texas A&M University were responsible for nondestructive testing (seismic), microwave sensor equipment and measurements, and dew point sensors and measurements, respectively, to investigate the feasibility and applicability of each instrument for HPC pavement monitoring.

1.2 OBJECTIVES

The overall objectives of SSI and SSII are to address the impact of specific specimen characteristics, destructive- and nondestructive-testing procedures, pavement construction, sampling techniques, and environmental conditions on strength. Nearly all tests represent scenarios that occur often in the field, but whose effects have not been quantified. SSI addresses an array of issues, whereas SSII focuses on specific aspects of SSI that required additional study and a more rigorous testing plan. In general, these aspects are the effects of a curing compound on strength and characterizing the vertical strength profile. A detailed list summarizing the objectives of each study is provided in the following sections.

1.2.1 Small Slab I Objectives

The specific objective of SSI was to determine the accuracy of various procedures commonly used to estimate strength and also to investigate the effects of specific variables commonly encountered in the field on compressive, splitting tensile, and flexural strength. Each item listed below describes variables whose effects must be quantified if concrete strength is to be accurately estimated. The objectives of SSI include:

(1) Determine the effects of core diameter and presence of reinforcement in a core on the measurement of strength and elastic modulus (to be referred to as elastic modulus).

(2) Determine the effects of curing history, aggregate type, and vertical location of a core in a slab or cylinder, core, and/or pavement strength.

(3) Evaluate current strength relationships adopted in codes and compare to research data.

(4) Determine the feasibility of developing non-destructive methods to measure the in situ elastic moduli and estimate strength of a portland cement concrete (PCC) pavement using seismic equipment. As a satellite objective, determine the effects of reinforcement and curing on seismic testing.

1.2.2 Small Slab II Objectives

The overall objective of SSII is to achieve a full understanding of the moisture losses from various curing conditions and their effect on in situ strength, and to compare strengths from maturity measurements to molded specimens cured under ideal conditions. The following subobjectives are required to achieve this primary objective:

(1) Evaluate which curing conditions decrease vertical strength differentials and increase strength.

(2) Characterize the moisture profile in a concrete pavement under different curing conditions.

(3) Determine the effects of moisture loss on the tensile strength vertical profile.

(4) Determine the feasibility of using maturity meter readings to predict strength and determine if adjustments for moisture loss are required.

(5) Evaluate dew point, microwave, and capacitance moisture sensors for accuracy and variability, and develop correlation models if possible.

1.3 Scope

SSI and SSII are the first of what shall hopefully become a series of slab studies designed to clarify issues currently affecting determination of in situ properties and to study issues affecting the development of high-performance pavements. SSI is extensive enough to establish the relative sensitivity of a wide array of variables on the compressive, tensile, and flexural strength of concrete. SSII focuses on the effects of delayed application of a curing compound with the effects on the resulting pavement moisture loss and vertical tensile strength. The maturity method is incorporated into this study to determine the effects of moisture loss on the accuracy of the maturity curve.

The large number of variables investigated in SSI prevented the detail necessary to satisfactorily capture the effects of vertical location of a sample and the presence of a curing compound on strength. For example, only two curing scenarios and two vertical positions were tested in SSI. The design of SSII includes an experimental plan tailored to determine the specific effects of moisture. SSII focuses on the characterization of the moisture profile, utilizes a progression of curing compound application times from six different curing conditions, and calls for much smaller test specimens than those used in SSI to determine the vertical tensile strength profile. In SSI, top and bottom specimens were obtained from the top and bottom 6 inches of the slab, trimming off the top-most concrete where delicate strength differential due to moisture loss is most clearly seen. Experience from SSI indicated the need to test thinner sections for SSI tests.

The results from both SSI and SSII will be condensed into an implementable document. This document will be similar in content to Chapter 8 of this report.

1.3.1 Scope of Small Slab I

A smaller core is often required because of constraints imposed by the size of the pavement, steel congestion, or cutting equipment/testing machine capabilities. At times, smaller cores may be used for their economic advantages. This study specifically addresses the feasibility of using 4 x 8 in. diameter cores in lieu of 6 x 12 in. cores for compressive and tensile strength tests.

Currently, the standard-cure (water) cylinder is used to determine in situ strength. Water-cured cylinders are more often used to obtain consistency in testing and for acceptance testing than for estimation of in situ strength. This study investigates the tensile and compressive strengths obtained from using sand-cured cylinders in lieu of lab-cured cylinders, as they are economical, easily implemented in the field, and may better reflect the effect of moisture loss experienced by a pavement.

Though many strength relationships between compressive, splitting tensile, and flexural strength have been published, they are not consistent. Accurate relationships can provide a very powerful tool in construction and design, whereas code relationships are often intentionally conservative to provide a built-in safety factor. In this investigation, currently accepted relationships will be compared to those developed from SSI experimental data to demonstrate the relative accuracy and applicability of each.

When estimating in situ pavement strength from cores rather than a molded sample, it is very possible that reinforcement will be present in the core. If the presence of reinforcement in a core is found to have negligible effects on strength, then the time-consuming step of steel locating can be eliminated. This study investigates the effects of reinforcement on compressive and tensile strength tests.

Curing compound is commonly applied to reduce water loss during curing and reduce the likelihood of drying/shrinkage cracks. Tining may be applied to produce a safer riding surface. Both procedures have an effect on concrete strength, especially near the surface. This study will attempt to quantify how concrete compressive and tensile strength are affected when these procedures are bypassed.

When a sample is trimmed or cut in preparation for testing, or when a structure is large and cores are taken near the surface, the core may not be as representative of the overall concrete strength. This study compares the strength of cores from the upper and lower sections of a slab to determine the effects of vertical position on compressive and tensile strength.

Both limestone (LS) and siliceous river gravel (SRG) are commonly used in Texas' concrete pavements due to their relative abundance; this study investigates concrete strength effects due to aggregate.

1.3.2 Scope of Small Slab II

TxDOT standards state that a pavement finished to standards will include both a coating of (MMF) and a curing compound applied at sheen loss. As a result of problems during construction, one or more of these procedures is often missed or delayed. This study simulates different combinations of curing techniques with a slab cured using plastic sheeting, a retired but reliable method of ensuring proper curing, to determine the effects on the relationship between surface moisture loss and strength.

When curing compound is not applied and the evaporation rate is high, it is possible that concrete near the surface will be weakened due to insufficient water availability. It is beneficial to know the depth at which surface moisture loss ceases to affect strength and how a curing compound affects this gradient. The tensile strength profile will be estimated in this study as it is the most pertinent strength in the design of pavement and the length to diameter ratio of the sample is not as significant in tensile tests as it is in compressive tests (Wright 1955).

The maturity index is a function of time and temperature; currently the effects of moisture loss are not taken into account in strength predictions. It is likely that when a pavement experiences high evaporation, strength is lowered by insufficient availability of water for hydration. However, it is not known how well this is addressed by the nature of the existing maturity method. It is possible that increased evaporation rates are partially offset by decreases in the concrete temperature in such a way that the maturity index automatically adjusts for moisture loss and, to some extent, is independent of curing history.

Concrete temperature will be recorded using the traditional thermocouple with maturity meter as well as the new Thermacron i-Button. Each button is approximately the size of six dimes with sensors encased in stainless steel and provides continuous time-temperature. They can be missioned, remissioned, or have data downloaded at any time. This study will evaluate the feasibility of using the Thermacron i-Buttons in concrete for future use in long-term temperature monitoring, short-term temperature monitoring, and establishing maturity curves.

Moisture measurements will be made using four separate devices: dew point sensor, humidity sensor, microwave sensor, and the Aquameter. Each sensor utilizes a different technology for estimating moisture and differs greatly in cost, sensitivity, and history of use in concrete. Each will be discussed below.

The dew point sensor is the most expensive, but has been used frequently in previous projects for moisture monitoring. The microwave sensor and Aquameter measure the capacitance (dielectric constant) change in concrete. The microwave sensor has traditionally been used in soil applications and its use in concrete is still being investigated. The Aquameter, on the other hand, provides moisture content up to 1 in. below the surface. The procedure is quick and requires only a few seconds for a reading to be made. The gauge is approximately 2 x 3 x 5 in. This instrument has been precalibrated by the producers from 140 different mix designs.

The duplication in moisture content measurements will not only increase the accuracy of data, but also will assess the devices for practicality, accuracy, and price.

1.4 Report Organization

This report is organized into ten chapters, including the current Chapter 1. This report presents the need for this research, the literature reviewed in preparation for this project, the design of the slabs selected for testing, the results of SSI and SSII, discussions of the results, and conclusions derived from data analyses. Below is a list of all Chapters 2-10, followed by a brief description of each.

Chapter 2 describes the approach taken in the design of the slabs so that objectives could be achieved.

Chapter 3 presents results of the literature review conducted in preparation for both Small Slab Studies. Factors that affect the measurement of concrete strength, as well as actual strength, are discussed.

Chapter 4 provides the designs of the slabs used in both Small Slab Studies. The slab sizes, core locations, testing equipment used, specimen factorials, and layouts are provided.

Chapter 5 provides analysis results of destructive test data for SSI. Significance of variables is determined for all analyses. Where beneficial, models have been developed. This chapter sheds new light on the effects of many variables on the accurate estimation of tensile strength, a concrete property arguably more useful than compressive strength in the design of pavements.

Chapter 6 provides modulus values obtained in SSI. Young's modulus is measured using seismic and mechanical tests on the slab, cylinders, beams, and cores. Comparisons are made to determine if the seismic modulus can be correlated accurately to concrete strength development. Study results on the effects of variables on modulus, discussed in *Chapter 3,* are also presented.

Chapter 7 provides data results from SSII. Results of the new equipment used for temperature and moisture content estimation, and results of preparatory lab experiments conducted prior to SSII construction are presented.

Chapter 8 discusses the results of all data analyses from both Small Slab Studies (*Chapter 5–Chapter 7).* Interpretations and causes of trends observed in results are examined.

Chapter 9 is a brief chapter providing a short discussion of items for implementation derived from the two studies. Based on previous experience with PCC pavement, the implementation topics are categorized.

Chapter 10 provides the conclusions developed from the study.

2. Study Approach

The construction sites for both Small Slab Studies were in El Paso, Texas, because of the volunteering of construction materials and labor by Jobe Materials of that area. Small Slab Study I (SSI) was constructed on March 2, 1999, at Jobe's McKelligon Canyon site. Small Slab Study II (SSII) was constructed March 28, 2001, at Jobe's Plane Port Batch Mixing Plant. In both projects, the Center for Transportation Research was the main coordinator, in charge of data collection, analysis, and reporting.

Both studies use cores for estimation of in situ strength, and compare results to strength predicted by cast specimen and nondestructive means. Every method introduces unique obstacles and yields results of varying accuracy and variability. To conform to current standards, in this study in situ strength was assumed to be that exhibited by the standard 6 x 12 in. core. Both studies then use specimen strengths for all comparisons, whether 6 x 12 in. sand-cured cylinders or 4 x 8 in. cores. There are exceptions to this rule however. Some comparisons are made that exclude 6 in. cores, such as in tests determining effects of the presence of reinforcement on 4 in. limestone (LS) cores.

2.1 Small Slab I Study Approach

In SSI, 4 in. cores are cut and tested at 1, 3, 7, 14 and 28 days from the limestone (LS) and siliceous river gravel (SRG) slabs (three replicates per test). Similarly, LS and SRG water-cured cylinder, sand-cured cylinders and water-cured beams are tested at these ages. Along with 6 in. cores cut and tested at 7- and 28-day strength, these specimens make up most of the sample pool required for testing. Additional samples used in separate comparisons include 4 in. cores from the reinforced LS slab, cores from the designated tined, and "cardboard covered" areas, and cores cut into top and bottom portions.

2.2 Small Slab II Study Approach

As described in Chapter 1, the purpose of the SSII was to better characterize the moisture profile in a concrete pavement under various curing conditions, as well as to assess its effects on strength and maturity. To satisfy these objectives, six different curing environments were created, each representing varying severities of evaporation. Tensile cores were cut into 2.5 x 6 in. disks to capture vertical strength differentials. To simulate field conditions, the following six curing environments were selected:

- Application of a curing compound at sheen loss (with monomolecular film [MMF]). This represents ideal compound application time.

- Application of a curing compound at sheen loss (without MMF) to determine and quantify any strength loss by not using MMF.

- Application of a curing compound 2 hours after concrete placement, or as deemed proper at the time of construction based on the concrete behavior. This represents slightly delayed application as is common in the field.

- Application of the curing compound 8 hours after concrete placement. Cases have been reported where application is this severely delayed. Though this is not a desired construction practice, it is beneficial to quantify the strength loss that could be experienced in these situations.

- A section with no curing compound. This scenario is provided for comparison to an extreme case.

- A section covered with plastic sheeting as soon as is feasible. This case represents an ideal case where moisture loss is minimized. This method is usually considered too tedious for normal paving practice.

Moisture measurements were taken on each slab by four types of sensors. Continuous moisture measurements were logged for 2 days by the dew point sensor and 3 days by the four microwave sensors. Humidity and Aquameter readings were taken manually for 3 days from time of placement. Cores samples were drilled from each slab section and tested for splitting tensile and compressive strength for construction of maturity curves and comparisons to in situ strength.

In the SSI, only the dew point sensor was used for moisture measurements. In SSII, a range of complex and expensive moisture equipment was used. The equipment is listed below with the more complex and expensive listed first:

- Dew Point Sensor: The sensor obtains readings from the top inch of the slab. In the simplest terms, the sensor works by measuring the condensation formed on internal chilled mirrors. The entire unit can be removed from the concrete once tests are completed. One drawback to this type of sensor is that the time required for condensation may prevent obtaining immediate humidity readings. More research is still required on this matter.

- Microwave Sensor: The sensor requires embedment for anchoring of the sensors, and thus obtains readings at least 3 inches below the concrete surface. Because all other sensors obtain moisture readings within the top surface of the concrete, compatibility between measurements taken by this and other sensors will be compromised. Moisture readings are not expected to vary as much 3 inches below the concrete surface than those moisture readings at one inch below the surface.

- Humidity Sensor: Five capsules were placed in all slabs but the slab with plastic sheeting and concrete pans. Readings were taken in each slab with each sensor by continuously rotating them between capsules and recording readings manually. The humidity sensors are connected to capsule caps. When capsules were not in use, noninstrumented caps were left on the capsule to maintain moisture conditions as much as possible until a cap with a sensor was utilized again.

A water pan was also instrumented to determine maximum potential water loss. Additionally, two concrete pans made of the same concrete were continuously weighed at the same times as the water pan for comparison and calibration with in situ water loss and evaporation. One pan was allowed to cure next to the slab, but was shielded from wind by a windscreen whereas the other was open to the wind.

Temperature was logged in both studies using the standard thermocouple and maturity meter. SSII also introduced the use of the Thermacron i-Button for continuous monitoring of concrete temperatures. Data was retrieved from an RJ-11 female telephone plug soldered to the i-Button. After rigorous testing, it was decided that the i-Button would be best protected from the high alkaline environment of concrete, which tended to obstruct connections, by soldering the female adapter to wires and subsequently encasing all connections and buttons in a JB weld epoxy allowed to cure fully prior to placement in concrete. The buttons were soldered to telephone wires with RJ-11 (two-wire) jacks that extended beyond formwork. It was shown during 28 day downloads that these telephone jacks are very reliable. As long as the jack is not shattered, all mud and sand can be scraped off and connection established. In the event that jacks are destroyed, new connections can easily be constructed with new adapters.

2.3 DATA ANALYSIS

Data for this investigation was examined using analysis of variance (ANOVA) procedures via Statistical Analysis Software (SAS). Significance of variables was defined by the standard 95% confidence interval, or $\alpha = 0.05$. Using this criteria, it can be said with 95% confidence that whenever the p value (as provided in appendices) is less than 0.05, the null hypothesis can be rejected, indicating a significant difference between levels of the test variable (SAS 1985). Statistical result tables provided in the body of this report are simplified for quick reference: checkmarks indicate $p \leq 0.05$, dashes indicate that a variable was not applicable to the analysis, and empty cells indicate that the variable was included in analysis but was found to be insignificant. Actual data and statistical result values can be found in Appendices C, D, and F. These appendices include both raw and corrected data with associated statistical analysis results. Only in the appendices are statistical analysis results provided for raw data. All statistical results tables included in the body of this report reflect analysis results conducted on “corrected” data, or data in which values that deviated significantly from their category’s mean were eliminated (denoted by a “strikethrough” in the appendices). Raw data is provided for reference.

In some analyses, Fisher’s Least Significant Difference Test (LSD) is used. This parametric analysis is used to perform simultaneous, multiple tests while controlling the comparison-wise error rate, CER (SAS 1985). Controlling the CER means that the 95% confidence criteria is used to determine significance between pairs of data, but the probability that at least one incorrect decision between pairs will be made is greater than 5% (SAS 1985). In the LSD test, variables grouped with the same letter (T-value) cannot be said to be significantly different at the 95% confidence level.

3. Literature Review

Prior to beginning the design of each Small Slab Study, a literature review of selected topics was conducted. This enabled evaluation of the Small Slab results in light of current published data and theories. The literature review conducted addresses the effects of core diameter, curing, reinforcement, and vertical location of the sample on strength, as well as brief discussions on the maturity method and strength relationships.

As reflected in the following literature review summary, compressive strength and the variables that influence it have been researched extensively. Comparatively, minimal research has been done regarding the effects of the variables listed above on tensile strength. Depending on the application, concrete tensile strength is often neglected due to the presence of stress-absorbing reinforcement. However, tensile strength becomes critical for high-performance pavements where close cracking is unacceptable because of its effect on performance, failures, serviceability, and durability. This should be kept in mind regarding theories traditionally associated with compressive strength.

It is important to note that the topics covered in this literature review address two issues: factors that affect the measurement of concrete strength and factors that affect actual concrete strength. The factors influencing the measurement of strength discussed in this chapter include the effects of decreasing core diameter, core versus cylinder strength, moisture content at time of testing, strength relationships, presence of reinforcement, use of the maturity method, and nondestructive testing (NDT) procedures for strength prediction. The factors influencing the actual strength of concrete that are discussed in this chapter include the effects of cylinder-curing history and vertical location in a sample.

3.1 Factors Affecting Measurement of Concrete Strength

When determining concrete strength, it is crucial that the parameters, accuracy, and variability of specimens to be tested and procedures to be used are understood and properly addressed. This section discusses the effects of using small diameter cores, cores with steel, strength comparisons, maturity methods, and NDT for the estimation of in situ strength.

3.1.1 General Effects of Decreasing Core Diameter

The standard 6 x 12 in. core is often difficult or even impossible to obtain when a pavement is too thin, congestion of reinforcement exists, or pavement integrity would be compromised. These obstacles can sometimes be circumvented through the use of smaller cores. The use of small-diameter cores is also advantageous as they reduce damage to a pavement, are easier to cut, do not require high-capacity testing machines, and facilitate sample handling and storage.

Currently, the dimension of the standard core used in the United States and the United Kingdom is 6 x 12 in. Though not recommended, both countries allow the use of 4 in. diameter cores if necessary. In comparison, Australia and Switzerland allow the use of 3 in. and 2 in. cores, respectively (Concrete Society 1987; Bungey 1989). The use of 1.5 in. diameter cores or smaller has been found to yield very unreliable results and should not be allowed (Concrete Society 1987). This variety in the size of specimens worldwide demonstrates the widespread movement in using small-diameter cores.

The large majority of research found states that compressive strength decreases with core diameter (Carrasquillo 1994; Bungey 1989; Keiller 1984; Aïtcin 1994). However, many find this increase small enough to be considered negligible (Meininger 1968; Mather 1961; Yip 1988; Concrete Society 1987). Table 3.1 provides a summary of popular research concerning the effects of core diameter on compressive strength. It provides the relative strengths of cores of varying diameters, each with length to diameter (L/D) ratios of 2. The Concrete Society has used data in this table in its decision to allow the use of 4 in. cores. Results show that though most researchers found that strength increases with decreasing core diameter, the differences are small. This explains why most countries have not introduced correction factors for core diameter on compressive strength.

Table 3.1 Relative Compressive Strengths of Cores with L/D = 2.0 (Concrete Society 1987)

Reference	Ratio of Strength for given core diameter ratios				
	2"/3"	2"/4"	3"/4"	2"/6"	4"/6"
Meininger 1968		1.04		1.06	1.02
Henzel 1969		1.06			1.04
Campbell 1967					0.80
Perestons 1967	1.01				
Petersons 1967			0.93		
Bhargava 1971					1.00
Petersons 1973			1.02		
Lewandowski 1971					1.05
Sangha 1972		1.02	1.02		
Buo 1973				1.05	
Keiller 1984	1.00				
Lewis 1976	1.10	1.03	0.94		
Kemi 1979					1.00
Ramirez, 1979		0.90	0.95		
Munday 1984			1.08		0.91
Bungey 1982		0.99	1.01		

A popular explanation for the increased strength of smaller specimens is provided by Weibull's "weakest link theory" (Bloem 1960). In 1939, Weibull obtained a significant size effect through applications of probabilistic principles to the behavior of brittle materials. The theory states that specimens with larger volumes are more likely to contain critical defects and so fail at lower stresses. A less-accepted explanation involves the decreased relative stiffness of larger cores to the loading machine (Bartlett 1994). Stresses in small specimens are more uniformly distributed and thus the sample can fail at higher loads. However, this effect can be avoided by using an appropriate loading pad (Bartlett 1994). In cylinders, large-diameter specimens often exhibit lower strength because of the increased depth of cracking due to drying shrinkage (Aïtcin 1994). This explanation may not be applicable to cores, however, because of the lack of a surrounding mortar layer (Yip 1988).

Figure 3.1 shows the decrease in compressive strength of cylinders with diameter. The figure agrees with the work of Price that showed that the compressive strength of a 36 x 72 in. cylinder was approximately 82% of a 6 x 12 in. cylinder (Mather 1961; Kesler 1966). The shape of the curve suggests that the effects of core diameter decrease as the diameter increases.

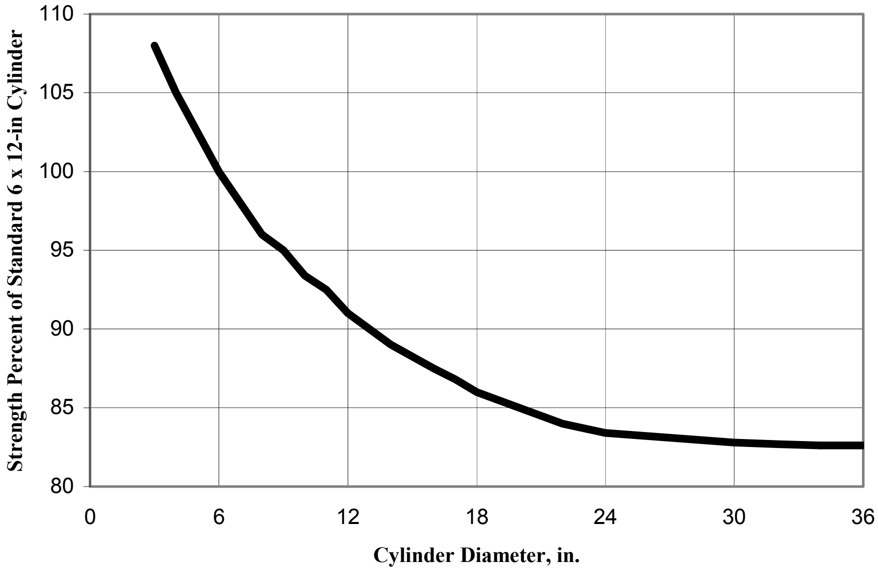

Figure 3.1 Effects of Diameter on Cylinder Compressive Strength (L/D = 2:1) (Kesler 1966)

A small number of researchers have found compressive strength to be lower for small-diameter cores (Campbell 1967; Concrete Society 1987; Ahmed 1999; Bungey 1979; Elimov 1997). A possible explanation for these results may be that the damaging effects of coring were greater than the benefits presented by the Weibull theory (Bartlett 1994). Assuming that the coring process damages a set thickness, *t*, of a core, the percent of the core damaged from coring will increase as core size decreases. That is, as core size decreases less of the core will remain intact and able to contribute to strength. As the volume to surface area ratio decreases, damage caused from coring and sawing of the sample during removal increases (Bungey 1989; Ahmed 1999). This damaging effect may be critical for cores with diameters below 4 in. (Bungey 1989).

There is very little research if any on the effects of core diameter on tensile strength. One investigation by Wright comparing the tensile strength of 4 x 4 in. and 6 x 6 in. cylinders has shown that 4 x 4 in. cylinders were 10% stronger than 6 x 6 in. cylinders in tensile strength. Similar results have been found by Miels (Carrasquillo 1994). Again, this can be explained by the Weibull theory stating that smaller specimens are less likely to contain defects, and thus will fail at higher stresses.

3.1.1.1 Core Length to Core Diameter Ratio L/D

One of the disadvantages of obtaining 6 in. cores is that the pavement or structure may be too thin or small to obtain a sample with an L/D ratio of 2:1. When this situation exists, either a smaller diameter core must be cut or the L/D ratio must be modified. It is commonly accepted that, for a given diameter, compressive strength increases as its length decreases (Carrasquillo 1994; Yip 1988). In the United Kingdom, a ratio between 1.0 and 1.2 is preferred to reduce costs, damage to the structure, and material variability along the specimen length (Bungey 1989). However, in the United States specimens are constructed with a standard L/D ratio of 2:1. This is done primarily to eliminate multiaxial stress states at the center of the specimen and to facilitate comparison of data with most other research.

The most convincing argument for constructing a sample with an L/D ratio of 2:1 is that a sample should be in a state of uniaxial stress if accurate compressive strength measurements are to be made. Testing equipment itself induces lateral stresses at specimen ends due to friction between the bearing faces of the testing machine and specimen ends, resulting in a state of multiaxial stress in the sample (Carrasquillo 1994). These stresses are greatest at specimen ends and decrease towards the core center. At a distance from the specimen ends equal to the specimen diameter, lateral stresses are negligible and the sample can be assumed to be in a state of uniaxial compression (Carrasquillo 1994). Thus, an ideal specimen with an L/D ratio of 2:1 will be in a state of uniaxial compression in its center, where cracking leading to failure usually originates.

When specimens with a L/D ratio of 2:1 cannot be obtained, correction factors exist that can be applied to obtain the strength of an equivalent sample with an L/D ratio of 2:1 (Carrasquillo 1994). Correction factors have been empirically determined for specimens with L/D ratios between 1.0 and 2.0 by many researchers and are summarized in Table 3.2. For comparison to the standard 6 in. core and to facilitate comparisons with published data, values are normalized as a percentage of strength of specimens with L/D = 2:1 (Yip 1988). Thus, if a 6 in. x 6 in. core exhibited 5,000 psi compressive strength, the compressive strength of a 6 x 12 in. sample of the same material would be near 4,100 psi. Figure 3.2 provides the percent of compressive strength of cylinder to the standard 6 x 12 in. cylinder. When L/D is less than 1, strength is drastically affected by changes in the L/D ratio, significantly increasing as L/D decreases (Munday 1984). For example, the correction factor for an L/D ratio of 0.50 has been found to be as small as 0.60 (Carrasquillo 1994). It has also been shown that L/D effects are more significant for 2 in. cores than 4 in. diameter cores (Bartlett 1994). The following describes the effects of varying the L/D ratio near equality:

$0 \leftarrow L/D \leq 1$	Dramatic increases in compressive strength
$1 \leq L/D \leq 2$	Noticeable changes in strength
$2 \leq L/D \leq 3$	Strength remains relatively constant
$3 \leq L/D \rightarrow \infty$	Strength decreases at a decreasing rate

Table 3.2 L/D Compressive Strength Correction Factors (Yip 1988)

Reference	L/D ratio		
	1	1.5	2
Meininger, Wagner and Hall	0.87	0.96	1.00
Kesler	0.84	1.01	1.00
Hofsoy	0.75	0.91	1.00
Lewandowski	0.81	0.82	1.00
Sangha and Dhir	0.82	0.98	1.00
Bungey	0.79	0.89	1.00
Tam, Ooi and Ooi	0.77	0.87	1.00
Yip (1982)	0.80	0.91	1.00
Yip (1988)	0.88	0.96	1.00
BS 1881 : Part 120	0.80	0.92	1.00
ASTM C 42-84a	0.87	0.96	1.00
Average	0.82	0.93	1.00
Converse of Average	1.00	1.07	1.22

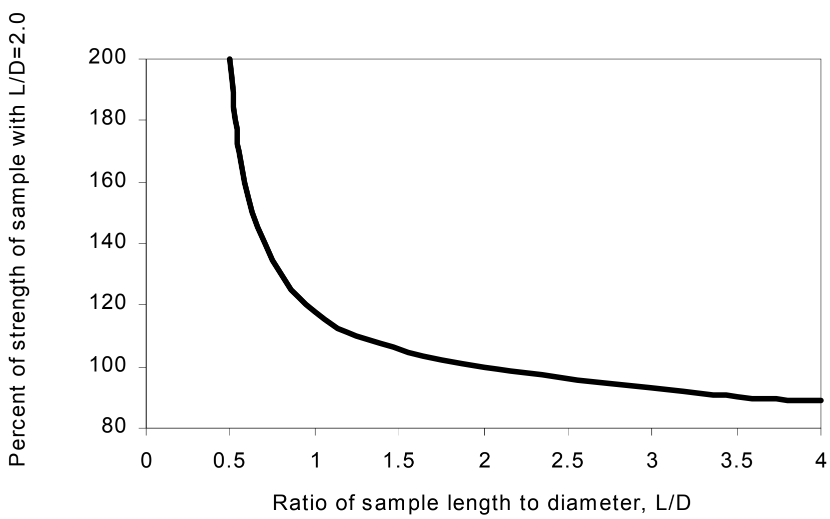

Figure 3.2 Effects of L/D Ratio on Cylinder Compressive Strength (Carrasquillo 1994)

Unlike compressive strength, the tensile strength of a cylinder has been shown to be independent of the length of the specimen and thus independent of the L/D ratio (Wright 1955). This is logical as the L/D requirement was due to the excessive friction of the bearing plates with the specimen ends. However, in the split tensile test a line load is applied, virtually eliminating the introduction of lateral stresses. It has been shown, however, that increasing the length of a sample does decrease the variability in data (Wright 1955).

3.1.1.2 Core Diameter to Nominal Aggregate Diameter Ratio D/d

A change in core diameter also affects the core diameter to nominal aggregate diameter ratio (D/d). The smallest D/d value possible is equality, representing a solid aggregate sample. Assuming a sufficiently strong aggregate, when D/d is equality, strength values should be very high (this is solely an academic point as the sample would no longer be defined as concrete). Contrary to this theory, most tests have shown that increasing the maximum size of coarse aggregate decreases strength (Bloem 1960).

Though most research shows that for a given diameter, increases in nominal aggregate size diameter will decrease strength, the effects are complex. For example, increasing aggregate size reduces the required amount of mixing water and, thus, the water/cement (w/c) ratio. Low w/c ratios are commonly associated with high strengths (Bloem 1960). Additionally, for well-graded mixes of the same w/c ratio, research has shown higher strengths for smaller, rather than large, aggregates (Bloem 1960). Conversely, the use of large aggregates is often found to decrease strength because of increased effects of aggregate loosening during extraction/coring of the core (Bungey 1979). These effects may be significant in the case of mass concrete projects where large aggregates are often used. Additionally, the strength of the aggregate itself can affect sample strength (Tanigawa 1978). Therefore, the net effect of varying the D/d ratio is difficult to determine as the individual effects are interrelated, possibly canceling each other out, and making them hard to differentiate (Bungey 1979).

Changing the D/d ratio also affects the variability. The D/d ratio can be interpreted as a measure of the degree of homogeneity of the sample. For specimens of the same diameter, homogeneity decreases and variability increases when a larger aggregate is used (Bungey 1979; Mather 1961).

As reflected in current American, German, and Australian standards requiring that the D/d ratio be greater than 3:1 in *molded* specimens used for compressive strength tests, research has shown that the effects of D/d can be considered negligible when the *core* diameter to nominal aggregate diameter ratio is greater than 3:1 (Bungey 1979; Carrasquillo 1994; Malhotra 1977). According to Carrasquillo, cores with D/d ratios of 2:1 are satisfactory though not ideal (Carrasquillo 1994). This is supported by investigations on specimens with ratios of 1.0 in which no significant D/d effects were exhibited (Concrete Society 1987).

3.1.1.3 Accuracy of Results

The most common criticism of small-diameter cores is their unreliability. Virtually all research shows that core variability decreases with diameter (Yip 1988; Bungey 1979; Carrasquillo 1994; Bartlett 1994; Bungey 1989; Ahmed 1999; Mather 1961). To obtain the same degree of testing accuracy as large-diameter cores, a larger number of small-diameter cores are required. This variability is due largely to the sensitivity of smaller specimens to critical failure mechanisms and their reflection of the heterogeneity of the parent concrete. Thus, American Concrete Institute (ACI) 318 requires a minimum of three standard specimens per test to ensure acceptable accuracy in data. According to Tucker, equal accuracy is achieved when the number of cylinders tested is such that the summation of the cross-sectional areas of the specimens of two sizes is equal (Malhotra 1977). Thus, five 4 in. cores (area = 20 in.^{2}) would provide approximately the same accuracy as three 6 in. cores (area = 18 in.^{2}). Thus, the advantage of reduced damaged area, costs, and time provided by the use of small-diameter cores is negated by the fact that more specimens are needed to achieve the same accuracy. If small-diameter cores must be used, the number that should be used depends on the reason for testing, the volume of concrete being evaluated, and the acceptable accuracy.

3.1.1.4 Strength Effects

Some research has shown that the effects of core diameter are dependent on the strength of the concrete mix (Bungey 1979; Carrasquillo 1994; Lamond 1994). According to Forstie and Schnormeier, a trend reversal occurs at 2,875 psi (Date 1984). If concrete strength is below 2,875 psi, increasing core diameter will decrease strength. However, if concrete strength is above 2,875 psi, increasing core diameter will increase strength. More research is still needed in this area.

3.1.2 Effects of Reinforcement

When cutting cores in reinforced concrete, it is often difficult or time-consuming to determine the exact horizontal location of reinforcement. Thus, it would be useful to know if the presence of steel in a sample does not affect strength so that the time-consuming process of determining steel location can be eliminated.

Because the effects of reinforcement on compressive strength from published data are variable, a core should be cut to avoid steel (Carrasquillo 1994; Malhotra 1977). Though undesirable, it may be unavoidable to obtain a sample free of reinforcement when there exists high steel congestion. According to Malhotra, it is better to cut a core to a L/D ratio less than 2:1 if it eliminates reinforcement, rather than to include steel in the sample (Malhotra 1977). According to the Concrete Society, the presence of steel is usually accompanied by reductions in strength of up to 10%, as based on results of tests on cylinders (Concrete Society 1987). The only study referenced on the effects of reinforcement on cores show reductions are generally less than 5% (Concrete Society 1987). Compressive strength correction factors to account for the presence of steel in cores are shown below. The model is only an estimate, and its use is not suggested for correction factors in excess of 10% (Concrete Society 1987).

- For a core containing a single bar perpendicular to the axis of the core:

  $$1 + 1.5 * (\Phi_r * h) / (\Phi_c * L)$$

- For a core containing multiple bars perpendicular to the axis of the core:

  $$1 + 1.5 * [\Sigma (\Phi_r * h)] / (\Phi_c * L)$$

where
Φ_r = diameter of bar
Φ_c = diameter of core
h = distance of bar axis from nearer end of core
L = length of core

When using cores that contain steel for tensile tests, it is critical that the reinforcement is not in the tensile region of the sample. The occurrence of steel in the path of failure significantly affects tensile strength test results (Carrasquillo 1994). This can usually be avoided by aligning the specimen carefully during testing.

3.1.3 Strength Relationships

Many investigations have been conducted in attempts to develop an accurate relationship between compressive, tensile, and flexural strength. Though many investigations have been conducted, results have been conflicting (Raphael 1984). ACI has adopted the relationship that flexural strength is 7.5 times the square root of the specified concrete compressive strength (see below). Though it underestimates strength, it continues to be used because it is conservative and simple to manipulate. In 1984, Raphael developed a relatively accurate model based on results of 1,500 specimens obtained from three other researchers' investigations (Raphael 1984). All compressive strength results were obtained from 6 x 12 in. cylinders, tensile strength results from 6 x 12 in. cylinders and 6 in. square prisms, and flexural strength results from 6 x 6 in. beams and square prisms (Raphael 1984). From this data, he developed the following strength relationships:

Raphael (1984): $f_r = 2.3\ f_c^{2/3}$ in psi
$f_t = 1.7\ f_c^{2/3}$ in psi
thus, $f_t = 0.74\ f_r$ in psi

where
f_r = flexural strength, psi
f_t = splitting tensile strength, psi
f_c = compressive strength, psi

The most utilized relationship is that between compressive and flexural strength. As discussed previously, it has long been known that concrete pavements fail in tension. Thus, using compressive tests to estimate flexural strength and then to estimate tensile strength is highly undesirable. In addition to being nonrepresentative of the type of failure experienced by pavements, compressive strength correlates poorly to tensile strength. Thus, if possible, some form of a tensile strength test should be utilized for performance-based specifications. We should avoid, therefore, the use of a surrogate test to arrive at the desired value. Examples of strength relationships used in codes of various countries are shown below and plotted in Figure 3.4. Note that these are in terms of ultimate strength, whereas Raphael's models apply at any age.

New Zealand (1995): $f_r = 0.8\ f_c^{.5}$ in MPa
Canadian (1994): $f_r = 0.6\ f_c^{.5}$ in MPa
American (1995): $f_r = 7.5\ f_c^{.5}$ in psi

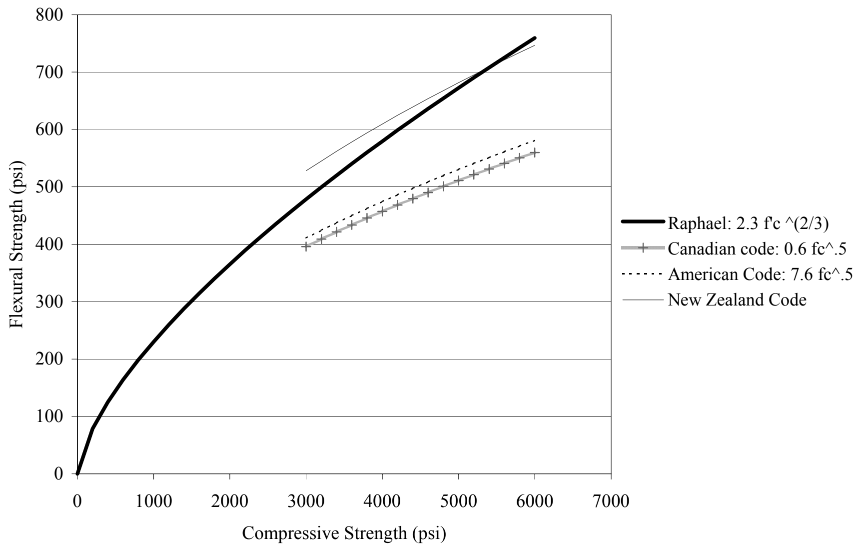

Figure 3.3 Compressive versus Flexural Strength: Raphael versus Codes

3.1.4 Maturity

The maturity method is based on the principle that the temperature history of concrete is indicative of strength development (Carino 1994). The strength of a concrete is dependent on the degree of hydration on the cement, which is dependent on how long and at what temperature the concrete has cured (Holland 1987). Specimens of the same concrete mix that have cured under different temperatures for different amounts of time are assumed to have reached the same strength, if their maturity values are equal (Holland 1987).

The procedure is straightforward and has been adopted by the American Society for Testing and Materials (ASTM) as shown in the chapter entitled *Practice for Estimating Concrete Strength by the Maturity Method* (ASTM 1998). A pair of lab-cured cylinders are continuously monitored for temperature to yield a maturity index while pairs of identically lab-cured cylinders are tested for strength, usually at 1, 3, 7, 14, and 28 days. A maturity curve is then constructed with time-temperature readings on the abscissa and corresponding strengths from cylinders on the ordinate. The curve should be used only for comparisons between identical concrete mixes. Adjustments can be made at the discretion of parties involved if changes in mix design or any other variables are present. The strengths of in situ concrete can thus be estimated from the curve using maturity indexes, regardless of the amount of time provided for hydration or temperature.

The maturity curve developed by Plowman has been adopted by many others, including ASTM. It proposes that the time-temperature and compressive strength relationship is semi-logarithmic. This is logical as the time component of the maturity value will increase indefinitely as strength gain diminishes. Other curves have been developed, including linear curves, but they have been shown to be inaccurate (Malhotra 1994). An alternative curve is also used which is more complex but provides more accurate results. The method expresses maturity as an equivalent age at a given temperature (Holland 1987). The equation provides reasonable accuracy for strengths between 1 and 28 days and temperatures below 100 °F, though research suggests that the method is accurate for ages greater than 1 year (Plowman 1956; Oluokun 1990).

Some researchers claim that the maturity method is not applicable to concrete cured at temperatures greater than 100 °F or at ages prior to 3 days or after 28 days (Oluokun 1990). Plowman's model is as follows:

$$S = a + b * \log M$$

where

S = compressive strength, psi
M = maturity index
a, b = regression constants

The maturity index, used in all maturity equations, is a function of time, temperature, and age. The temperature should be that of the concrete, preferably at mid-depth. The datum temperature, the temperature at which hardened concrete ceases to hydrate, has been shown to be between 11 and 14 °F (Plowman 1956; Oluokun 1990). ASTM currently allows the use of two equations for development of the maturity curve: the time-temperature factor (TTF) and equivalent age. TTF is commonly used as the calculations are simpler. Equivalent age is more accurate, but requires knowledge of certain concrete properties and is more complex. TTF can be calculated using the following equation (Holland 1987):

$$M = \Sigma\Delta t * (T_c - T_o)$$

where

Δt = time interval, days, or hours
T_c = average concrete temperature during time interval, °F
T_o = datum temperature, 11°F

The equivalent age of a concrete can be calculated using the following equation (ASTM 1998):

$$te = \Sigma e\text{-}Q(1/Ta\text{-}1/Ts)\ \Delta t$$

where

t_e = equivalent age at a specified temperature Ts, days or hours
Q = activation energy (J-mol) divided by the gas constant (J/(K-mol), K
Ta = average temperature of concrete during time interval, Δt, *K*
Ts = specified temperature, K
Δt = time interval, days or hours

Once equal maturity values have been reached, specimens of the same concrete batch are assumed to have reached the same strengths regardless of temperature and curing histories (Holland 1987).

3.1.5 Nondestructive Testing

The resonant frequency (RF) of vibration of a concrete specimen is directly related to its dynamic modulus of elasticity and density (Malhotra 1994). Resonant frequency is best suited to homogenous, solid, isotropic media, though the method can be used as long as the size of a specimen is large compared to the size of its constituent materials (Malhotra 1994). The method can be used to determine the uniformity of concrete, indicate the presence of voids and cracks or changes in the properties of concrete, and to estimate deterioration. Further research is required before the method will be incorporated into specifications as a method for assessing strength. For a thorough look into the use of NDT testing, the article *Nondestructive Tests* by V.M. Malhotra is suggested.

In pulse velocity tests, the travel time of stress pulses passing through concrete is determined. The technique can be used for in situ concrete as well as samples, and is unaffected by the sample's size or shape so long as they remain within the limitations of the pulse-generating device (Malhotra 1994). This flexibility in sample size and shape gives pulse velocity testing a very attractive attribute. Generally, small samples are used rather than structural members in the field because of their sensitivity to boundary conditions and shape.

3.2 FACTORS AFFECTING CONCRETE STRENGTH

This section discusses the effects of curing history, moisture loss, and depth of a core in a sample on strength test results.

3.2.1 Curing Method Effects

The compressive and tensile strength of concrete is very influential in the design of concrete structures and pavements, respectively. As the size of members is based on strength, it is critical that the specified strength be reached so that the structure or pavement can support anticipated design loads without failure. Additionally, it is critical that proper estimation of in situ strength be obtained so that a pavement is not opened to traffic prior to achieving the specified strength. This prevents unnecessary damage and loss of life to the pavement.

Cores undergo virtually the same curing as the parent structure and are thus assumed to give the best indication of in situ strength. However, obtaining cores is time-consuming and destructive to a structure. The commonly utilized alternative is to determine strength from molded specimens. The problem with molded specimens is that they may not reflect the compactive efforts and curing conditions experienced by the parent pavement. It is well known that water-curing a sample will generally result in higher compressive strength than that exhibited by cores. However, the effects on tensile strength have not been researched to as great an extent. Research on the effects of sand-curing on tensile strength is especially lacking.

There are currently a number of methods utilized for the storage and preparation of specimens to be used in strength measurements. The most common methods for making and curing concrete test specimens is the field and laboratory. Field specimens are intended to undergo curing similar to that of the structure and can be used to determine in situ strength, check adequacy of the laboratory mix, or to measure and control the quality of concrete (Kesler 1966). Laboratory-prepared specimens, though they may not represent the actual strength of a pavement or structure, are consistent and thus used for research and mix-proportioning studies (Carrasquillo 1994). Push-out specimens, or in-place specimens, are extruded from molds placed within the structural slab at the time of casting and are subsequently "pushed-out" at the time of testing. Accordingly, push-out specimens receive virtually identical curing to that of the concrete in the structure and provide strength values that are more representative of actual strengths than lab-cured cylinders (Carrasquillo 1994).

The compressive strength obtained from lab-cured cylinders is often used as an indication of in situ strength. However, differences in curing between standard cylinders and in situ concrete have been found to yield significant effects in strength. Even push-out cylinders, which undergo virtually identical curing to that of the parent concrete have been shown to yield higher compressive strength than cores (Bloem 1968). The incompatibility between in situ strength and cylinder strength can be attributed to many factors, including differences in thermal effects, casting, degree of compaction, conditions of restraint, ambient vapor pressure, curing history, and moisture condition at time of testing (Concrete Society; Simons 1990, Kesler 1966).

The following sections will discuss the effects of curing regime and moisture condition on sample strength at time of testing as well as their influence on the compatibility of strengths between cylinders and cores.

3.2.1.1 Poor Curing versus Good Curing

The curing of fresh concrete is the process by which fresh concrete is converted into a solid mass through hydration of its cementitious materials (Senbetta 1994). Reducing moisture loss during the curing process (i.e., water-curing in place of air-curing) increases the degree of hydration experienced by the concrete, resulting in increased concrete compressive strength (Aïtcin 1994; Senbetta 1994; Lamond 1994; Bloem 1965; Ahmed 1999). Standard moist curing for cylinders is achieved by curing the specimen at a temperature of approximately 73 °C. This is done in a moist condition whereby free water is maintained on the surface of the specimen, with clean and lime-saturated water (Senbetta 1994). For concrete structures, wet curing can be achieved through continuous sprinkling, prolonging formwork removal, ponding, sealing the surface or covering the surface with materials such as burlap, sand or straw that are kept continuously wet, or other such methods in which moisture loss is kept to a minimum (Senbetta 1994; Concrete Society 1987). Some researchers have also found that the effects of curing manifest only after 7 days (Aïtcin 1994). For example, the work of Aïtcin showed that the difference between water-cured, sealed, and air-cured cylinders was identical before 7 days, with strengths decreasing by up to 20% thereafter (Aïtcin 1994).

3.2.1.2 Core Strength versus Standard Cylinder Strength

Most researchers have found that strength is lower than standard in cores than in cured specimens (Concrete Society 1987; Bloem 1968; Elimov 1997; Meininger 1968; Simons 1990), though some controversy exists. Some researchers have found strengths to be greater for cores (Yip 1988) and others found that no difference exists (Mather 1961). This suggests that other factors may be affecting results. These include the selected curing regime, ambient temperatures present, core size, quality of cutting equipment, damage and loss of entrained air during extraction and handling, and water absorbed during cutting (Malhotra 1977; Kesler 1966; Simons 1990). As with cylinders, some research has also shown that the lowered strengths of cores are apparent only after 7 days (Simons 1990). In general, lower strengths should be anticipated for cores than standard-cured molded specimens.

Figure 3.3 below summarizes research results comparing the strength of standard-cured cubes to that of cores from slab under varying curing regimes (Concrete Society 1987). It shows that compressive strength is lower for cores than standard-cured cubes, with core strength increasing as slab moisture loss decreases [for comparison with the standard American cylindrical sample: true cube strength is 1.25 times the standard-cured cylinder strength, with L/D ratio of 2:1 (Concrete Society 1987)]. Thus, the 28 day compressive strength of the concrete determined from cores from an concrete cured under average, nonextreme conditions is approximately 77% of its potential strength as determined from true cube strength, all specimens being soaked for 48 hours before testing (Concrete Society 1987). The figure also shows that most strength gain is achieved by 28 days from time of placement. The curves in Figure 3.3 correspond to the following conditions:

(1) Water-curing

(2) Concrete protected from all water loss

(3) Concrete protected from water loss for 12 days, then allowed to dry in air

(4) Concrete protected from water loss for 5 days, then allowed to dry in air

(5) Concrete allowed to dry continuously in air

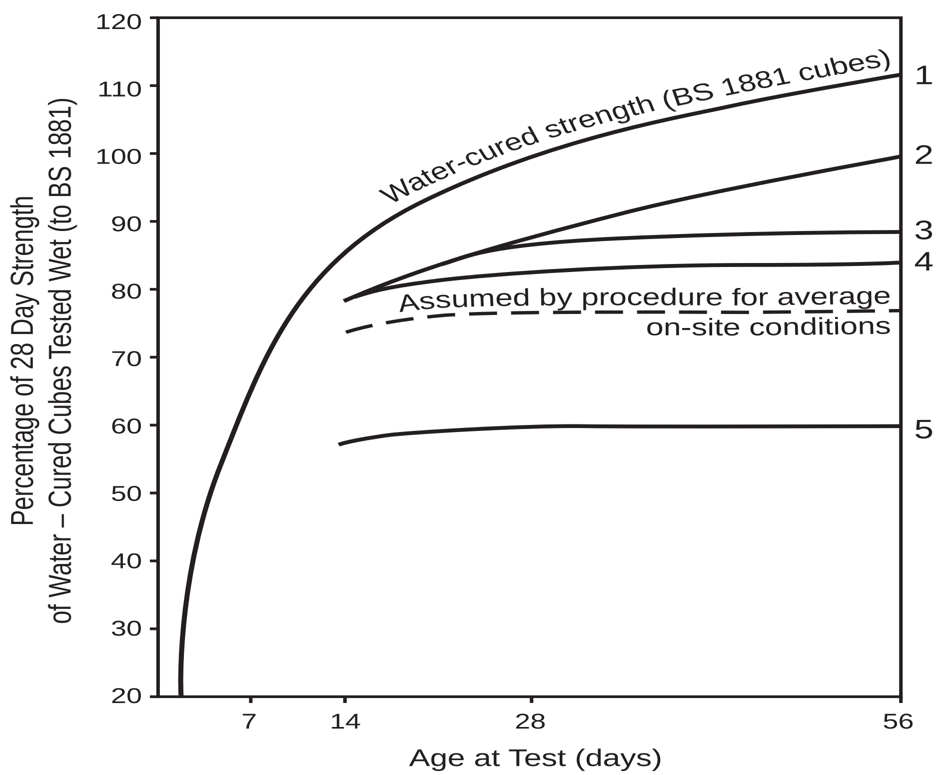

Figure 3.4 Effect of Curing on In Situ Compressive Strength as a Percent of Water-Cured Cube Strength (Concrete Society 1987)

Bloem warns that "They [core tests] cannot be translated to terms of standard cylinders strength with any degree of confidence" (Bloem 1965). For one, it is not possible to determine the effect of curing on in situ strength, and thus core data cannot be related with any certainty to potential strength determined by standard cylinders (Dhir 1984). Additionally, simulating field conditions in a lab is very difficult. Even cylinders that have been cured to simulate field curing conditions indicate only quality of concrete and do not quantitatively measure strength. Even field-cured and push-out cylinders whose curing regimes were tailored to simulate in situ curing conditions produced 10% and 7% higher strengths than cores, respectively (Bloem 1968). As mentioned previously, differences in strength may occur as a result of differences in casting, degree of compaction, conditions of restraint, ambient vapor pressure differential, and heat retained from hydration (function of the thermal mass of the member) (Kesler 1966; Simons 1990). According to the Concrete Society, differences in compaction can be assumed to be insignificant (Concrete Society 1987).

To simulate field curing accurately in the laboratory, the fact that the full thickness of lab specimens is affected by the curing regime must be considered. In a structure or pavement, concrete within an element will often be protected from moisture loss by concrete nearer the surface, with reductions in strength resulting from surface moisture loss being noticeable only within the top 2 inches from the surface (Concrete Society 1987). This is supported by Sheriff's research showing that cores cut from the bottom of slabs gave similar results regardless of whether they are subjected to very good or very poor curing (Concrete Society 1987). Another factor that can affect core and cylinder strength compatibility includes decreased core strength due to water gain and damage during cutting (Malhotra 1977; Carrasquillo 1994). There is validity to Bloem's claim that strengths obtained from core tests cannot be translated to terms of standard cylinders with any degree of certainty.

3.2.1.3 Moisture Condition at Time of Testing

It has been found by many investigators that specimens tested in a moist condition, which can be obtained by presoaking, yield compressive strengths up to 20% lower than if tested in a dry state (Bloem 1965; Kesler 1966; Carrasquillo 1994; Yip 1988). This is partially explained by the fact that in drying specimens, as the specimens' outer surfaces attempt to shrink compressive lateral stresses are induced, which increases the strength of secondary bonds within the paste structure (Carrasquillo 1994). Some researchers, however, state that dry specimens may result in lowered strength because of the formation of tensile stresses in the outer fibers caused by differential volume changes and nonuniform drying, which leads to premature surface cracking (Kesler 1966). For the same reasons, similar trends should be anticipated when conducting tensile strength tests.

Standard procedures often require cores taken from in situ concrete to be soaked for the 2 days prior to testing. The moisture content at the time of testing does not affect its inherent strength, but rather is a testing parameter technique providing for controlled testing procedures and yielding uniform results (Concrete Society 1987). The procedure eliminates the need to account for differences in moisture conditions at the time of testing. However, if determination of the in situ strength is desired, a specimen should be tested in as close to the same moisture condition as that which exists in the structure (Carrasquillo 1994). Some drying time may be required to allow water absorbed due to wet cutting to evaporate (Yip 1988).

3.2.2 Effects of Vertical Location

For cores, it is possible that strength is variable along the specimen's longitudinal axis. A possible cause is the settling of larger aggregates because of gravity, resulting in a nonhomogenous sample where strength increases with depth. The same result also may be due to the migration of water to the top of the sample from capillary action, increasing the water-cement ratio and consequently decreasing strength near the surface. Similarly, moisture loss on the surface of the pavement as a result of high evaporation rates can further decrease the strength of a pavement. When reinforcement is present in a slab or pavement, these effects may be cancelled with lower strength near the bottom portion of a sample due to inadequate compaction of the concrete caused by the steel preventing the passage of aggregates. All of these effects must be considered when evaluating sample strengths.

Findings from the literature review state that compressive strength increases with depth by up to 10% (Yip 1988; Meininger 1968). Usually this is due to the migration of water towards the surface of the pavement, increasing the water cement ratio, and thus decreasing strength. Research by Ingvarsson has shown that this effect only affects the top 2 inches from the concrete surface (Concrete Society 1987). Some researchers have stated that there is a possibility that this migration increases the amount of water available for hydration near the surface where the effects of evaporation and associated reductions in strength are anticipated, serving to increase strength.

3.3 SUMMARY OF LITERATURE REVIEW

Changing the diameter of a core can have an impact on its strength because of its effect on the following variables:

- Diameter:
  Most investigators have found compressive strength to be negligibly higher for small-diameter cores than larger-diameter cores (L/D = 2:1). Comparatively little research has been conducted on the effects of core-diameter on tensile strength. Of the research conducted, tensile strength has been found to increase by approximately 10-15 percent if small-diameter specimens are used.
  - L/D: Compressive strength increases as L/D decreases, with significant changes when L/D is below equality. To avoid using correction factors and to test specimens in pure uniaxial compression, specimens should be cut to an L/D value of 2:1. Tensile strength is not affected by the L/D ratio (Carrasquillo 1994).
  - D/d: The effects of changing the D/d ratio are variable, though most research shows strength increases with D/d. The effects can be assumed to be negligible when $D/d \geq 3$ or when $D/d_{max} \geq 2$.
  - Strength Variability between Specimens: The same degree of accuracy is obtained between specimens of varying core diameter if the sufficient specimens are used such that the summation of their surface areas (with respect to diameter, not length) is equal.
- Reinforcement
  Reinforcement has been shown to reduce compressive strength by 0-10%. When possible, its inclusion in a sample should be avoided. If this is not possible, correction factors from the Concrete Society are available when corrections are smaller than 5%. In tensile tests, specimens that contain steel in the tensile stress region should not be used.
- Strength Relationships
  Though much research has been conducted in attempt to accurately model strength relationships, no model has been universally accepted. The work of Raphael, utilizing the data of others' research and totaling over 1,500 specimens, has produced models that very accurately predict strength. Unlike conventional models used in codes, Raphael's model utilizes a two-thirds exponential relationship.
- Maturity
  The strength of concrete has been estimated from its time-temperature history with reasonable accuracy, and thus the maturity method has been adopted by ASTM as a viable means of determining compressive strength. The method should not be used prior to 3 days, and may be used after 28 days' strength with more caution. The maturity curve is only applicable for comparisons between identical concrete mixes/batches.

- NonDestructive Tests

  Nondestructive seismic tests are currently used to estimate modulus and deterioration in concrete. There is still a push, however, to correlate modulus development with strength development. Current standards have accepted seismic tests only as a measure of concrete deterioration indicated by reductions in modulus measurements.
- Curing Effects

  Compressive strength increases as the water available for hydration increases. The effects of curing on tensile strength need further investigation. It is recommended that specimens be soaked for 2 days prior to testing to provide uniform results unaffected by moisture conditions at the time of testing.
- Vertical Location

  Though some researchers state that higher strengths may exist near the surface of a concrete pavement, most research has shown that strength increases with depth.

4. Experimental Design

The design of the slabs for each Small Slab Study was tailored to meet the specific needs of each investigation. The slab designs were intended to accurately simulate a typical concrete pavement, associated field conditions, and standard construction and testing procedures. An appropriate number and type of specimens needed to be obtained to ensure no damage to nondestructive testing (NDT) equipment or specimens because of coring, equipment loads, or poor design. Additionally, monitoring of climatic and in situ parameters had to be accurate and well defined.

4.1 BACKGROUND

Typical of a standard concrete pavement, both Small Slab Study I (SSI) and Small Slab Study II (SSII) were constructed with an average thickness of 14 inches, using a standard limestone and/or siliceous river gravel mix design. Construction took place in El Paso, Texas, where suppliers interested in the study's results volunteered their materials, services, and labor.

In both experiments, it was decided that at least three specimens would be obtained for each test performed to ensure acceptable accuracy in data and to provide sufficient replicates for statistical analysis. All data compilation and analysis was conducted by the Center for Transportation Research (CTR).

4.2 SMALL SLAB I TESTING PROGRAM

For all variables to be examined, plans were developed and test schedules and procedures prepared. This section focuses only on the design of the slab itself. Procedures followed the Texas Department of Transportation (TxDOT) standards and were executed as planned. The slab was constructed on March 1, 1999, at the Jobe Materials plant in El Paso, Texas, with tests and monitoring terminating on March 29, 1999.

4.2.1 Layout

The slab design of SSI consisted of three sections, each 15 x 24 ft. to accommodate the large quantity of specimens to be cut and an undisturbed NDT area. The three sections can be identified as the nonreinforced siliceous river gravel (SRG) slab, the nonreinforced limestone (LS) slab, and the reinforced LS slab (Photo 4.1). The 8 ft. wide midsection along the center of the slab served as the undisturbed area for NDT testing as well as an area where equipment could be operated from or placed during the early life of the slab. Cores were cut from the two outer sections as shown in Figure 4.2. Cores were staggered as shown to provide the necessary randomness. A minimum separation of 10 inches between cores, and 4 inches between cores and slab edges, was specified.

Photo 4.1 Side View of Small Slab Study I Layout

NDT equipment consisted of dew point sensors (moisture meter), maturity probes, a weather station, temperature gauges, and seismic equipment. Maturity meters (4 channel) were placed as shown in Figure 4.1, at depths of 2 in., 3 in., and 10 in. Moisture meters were placed as shown in Figure 4.1 with a 3.25 ft. separation, 6 in. from the slab edge. One meter was in the cured section of the SRG and the other was in one of the sections covered with cardboard, as will be shown later. Seismic tests were conducted on the slab, cores, and molded specimens.

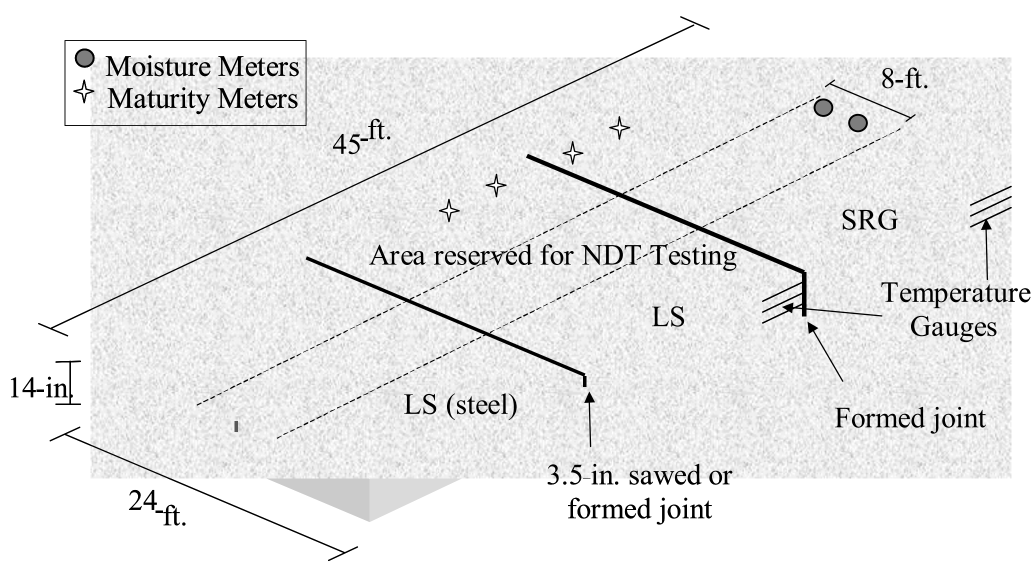

Figure 4.1 General Layout of SSI (N.T.S.)

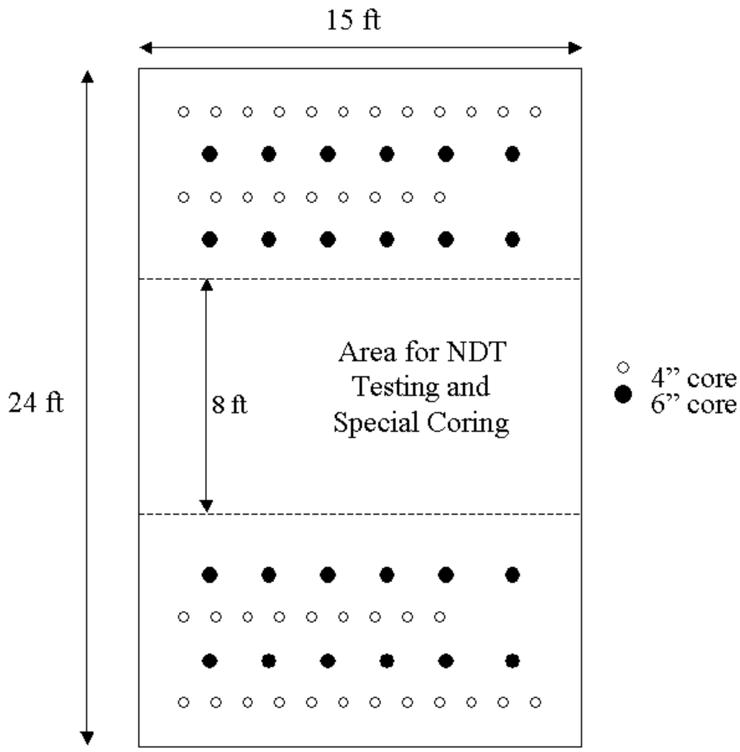

Figure 4.2 Typical Coring Locations for SSI

The reinforced slab was designed to represent several typical reinforcement designs used in pavements. Two steel configurations were selected: a single mat layer of 43 - #7 bars at 6.5 in. spacing at a 7 in. depth (0.661%) and a double mat section of 30 - #6 bars at 9.5 in. spacing at 5.5 and 10.5 in. depth (0.664%) (Figure 4.3, Photo 4.2). A minimum 5 in. separation between reinforcement and slab edges was specified to provide adequate densification. The single- and double-mat sections were each 7.5 x 24 ft., respectively. Four 24 ft. #4 bars spaced at 2 ft. c/c were used along the longitudinal length for both slab sections. Cores of 4 x 8 in. rather than 6 x 12 in. were specified to facilitate cutting.

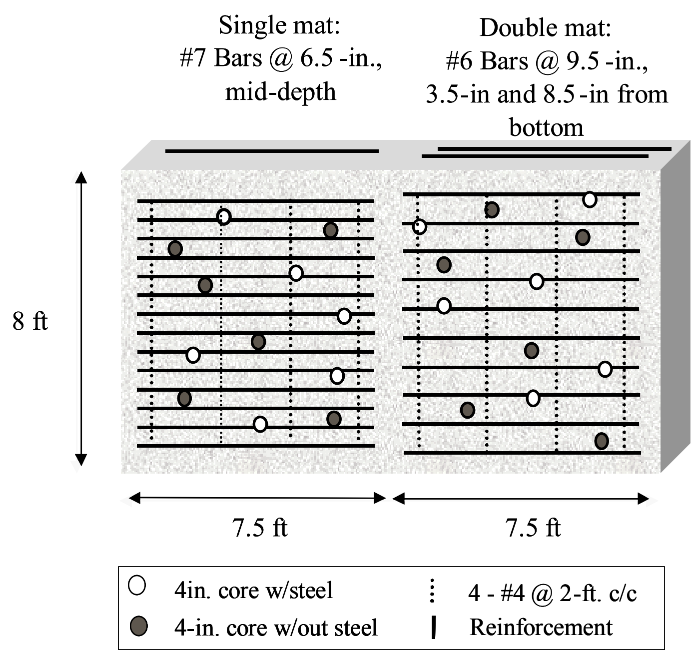

Figure 4.3 Layout of Reinforced LS Section for SSI (N.T.S.)

Photo 4.2 Closeup of Double Mat Reinforcement Setup Prior to Concrete Placement

The effects of various pavement surface treatments on strength were tested on central portions of the slab set aside for this purpose. Figure 4.4 shows the layout of the areas designated for specific surface treatments. A curing compound was applied to all sections except those marked *cardboard* which were covered when the compound was applied.

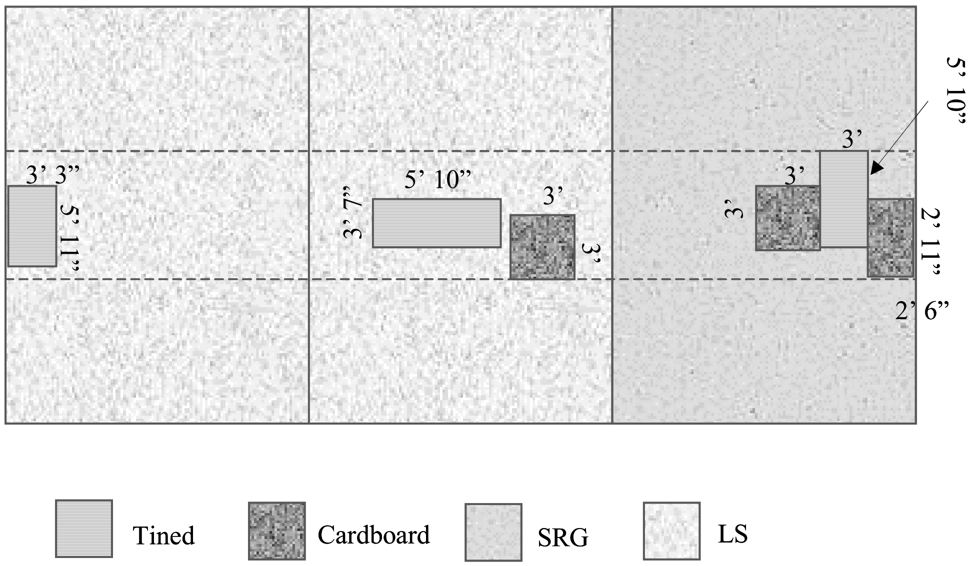

Figure 4.4 Layout of Pavement Surface Treatment Experimental Areas for SSI

After placement, the slab was carpet dragged and a curing compound was applied (except for areas covered by cardboard). Appendix A provides additional design information including the mix design of the LS and SRG batches, a chronological listing of activities for the first 3 days, placement and curing compound application times, concrete batch properties, the distribution of batches in each slab section, and a few photographs depicting the slab. Appendix B provides details on core locations, identification/nomenclature, and strengths.

In addition to cores, 6 x 12 in. cylinders and 6 x 6 x 21 in. beams were molded. All beams and one-half of the cylinders were cured in a water bath, with the remaining cylinders cured under moist sand conditions. Some cylinders were sand-cured to determine if they better reflected in situ curing than water-cured cylinders due to similarities in curing history. All cylinders were placed in their respective curing conditions 1 day after casting. Specimens from coring operations were immersed in water 30 minutes prior to testing to eliminate variation in moisture conditions at the time of testing, though this may not have been a sufficient amount of time to eliminate variance because of drying effects (some codes require a 2 day soaking period).

Because the slab thickness was 14 in., cores used to test the effects of vertical location on strength could not satisfy the standard length to diameter (L/D) ratio requirement of 2:1 and still be 4 in. or 6 in. in diameter; this would require a 16 in. or a 2 ft. thick slab, respectively. Thus, the full 14 in. core was cut into two 4 x 6 in. specimens for tests on 4 in. diameter cores or two 6 x 6 in. specimens for tests on 6 in. diameter specimens.

4.2.2 Specimen Details

To accommodate the large number of tests proposed for SSI, many specimens were required; Figure 4.5 shows the coring factorial for this study. White cells indicate that tests were conducted on three and black cells indicate that no tests were required. The factorial specifies a total of 132 cores. Full cores refer to those with an L/D ratio of 2:1. Specimens used for modulus testing were subsequently used for compressive strength tests as allowable.

Additional cores not shown in the factorial were required for secondary objectives: fifteen cores were required for pavement surface treatment tests and forty-eight for reinforcement tests (see Figure 4.4). As discussed in Section 4.5, the cores used for pavement tests were not suitable for this use. They varied in L/D ratio (i.e., eight for tensile tests and twelve for compressive tests) and location (i.e., top and bottom cores were used in tensile tests with no specification on sizes used for compressive strength).

The factorial for molded cylinders is provided in Figure 4.6. Again, white cells indicate that tests were conducted on three specimens. One hundred eighty molded cylinders were required for this study.

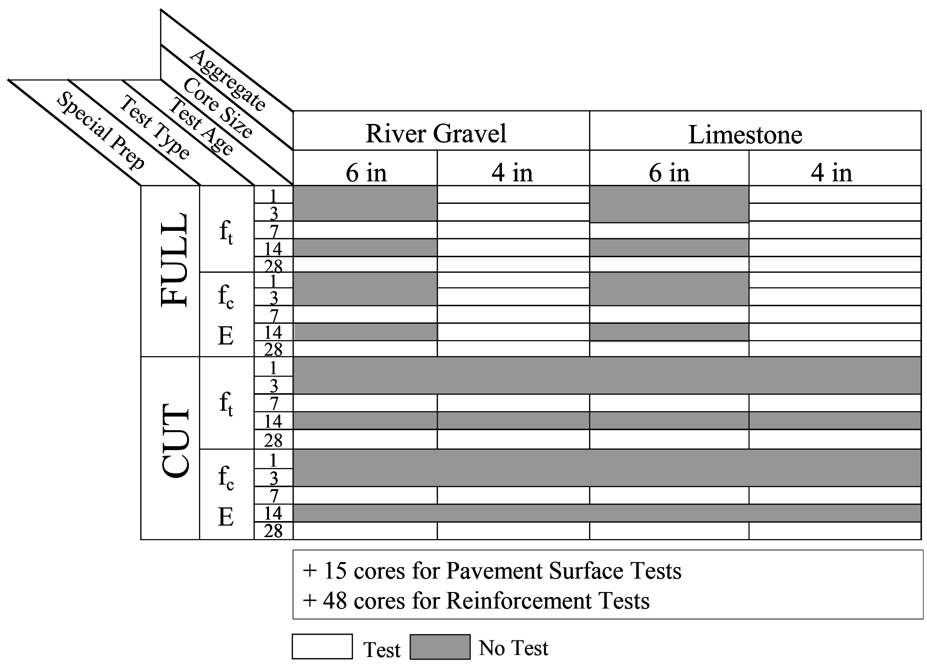

Figure 4.5 Cored Specimen Factorial for SSI

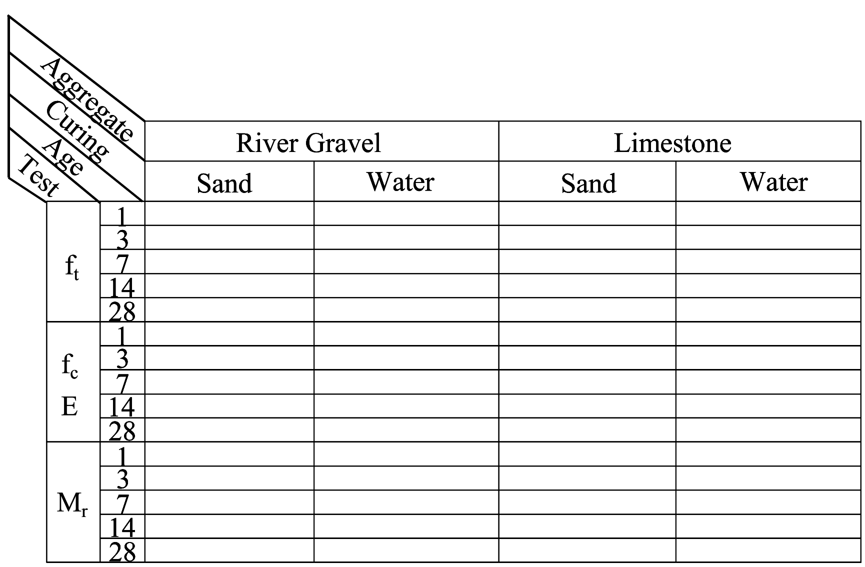

Figure 4.6 Molded Specimen Factorial for SSI (three test specimens for each cell)

A system of nomenclature was developed to keep track of the specimens. Table 4.2 gives a list of labels used for identification. As an example, let us consider a specimen represented by the upper-left corner of the factorial in Figure 4.6, *T1SGa*. This refers to the first 4 in. diameter SRG sand-cured cylinder tested for splitting tensile strength 1 day after placement, the first of three tests in that test series.

Table 4.1 Nomenclature for SSI Specimens

Designation	Description
T, C, F	Tensile, compressive, or flexural tests conducted
1, 3, 7, 14, 28	Age at time of testing, days
S, W	Sand curing or water curing for molded specimens
L, G	Limestone or siliceous river gravel specimens
a, b, c	Specimen designation for 4 in. cores (3 per test)
d, e, f	Specimen designation for 6 in. cores (3 per test)
X	Indicates specimens with steel

The following variables were held constant throughout the investigation to minimize variability in measurements: concrete compaction, curing technique, sample end conditions, loading apparatus, rate of load application, moisture condition at time of testing, orientation of specimen removal, and concrete design strength.

4.3 SMALL SLAB II TESTING PROGRAM

A general layout for the entire slab is shown in Figure 4.7 below. The slab was 14 in. thick to easily provide undamaged 6 x 12 in. specimens, as well as to reflect typical pavement thickness, and was cast on a 5 in. asphaltic base. Formwork was made of steel, and Styrofoam held by rebar embedded in the base was used for construction (Photo 4.3). To simulate standard practice, developed with recent special provisions, a monomolecular film (MMF) was applied to designated slabs immediately after the burlap finish. This is shown in Photo 4.4 where sections with MMF are more reflective. The curing compound was applied to slab *S* at sheen loss (Figure 4.7). No curing compound or MMF was applied to the *No Compound*, *N,* section to reflect a worst-case scenario. No compound was required in the *Plastic Sheeting, P*,' slab because this would be redundant. A uniform amount/weight of curing compound was applied to the other sections at the specified times: sheen loss (*S*), 2 hours after the compound was applied to the sheen loss slab (*2*) and 8 hours after the compound was applied to the sheen loss slab (*8*). An additional slab was constructed to evaluate the effects of not using MMF. In this slab, *O*, only a curing compound was used, applied at sheen loss, which simulates the practice prior to the special provision requiring the use of MMF. Photo 4.5 shows the final slab after insertion of instruments, application of the MMF, curing compound, and plastic sheeting. Two concrete trucks were required for placement of this slab. To reduce variability due to this difference, sections were cast as a mix of the two batches. That is to say, portions of each batch were placed in each slab with a vibrator used for partial mixing.

Photo 4.3 Formwork and Foam Separation Prior to Concrete Placement

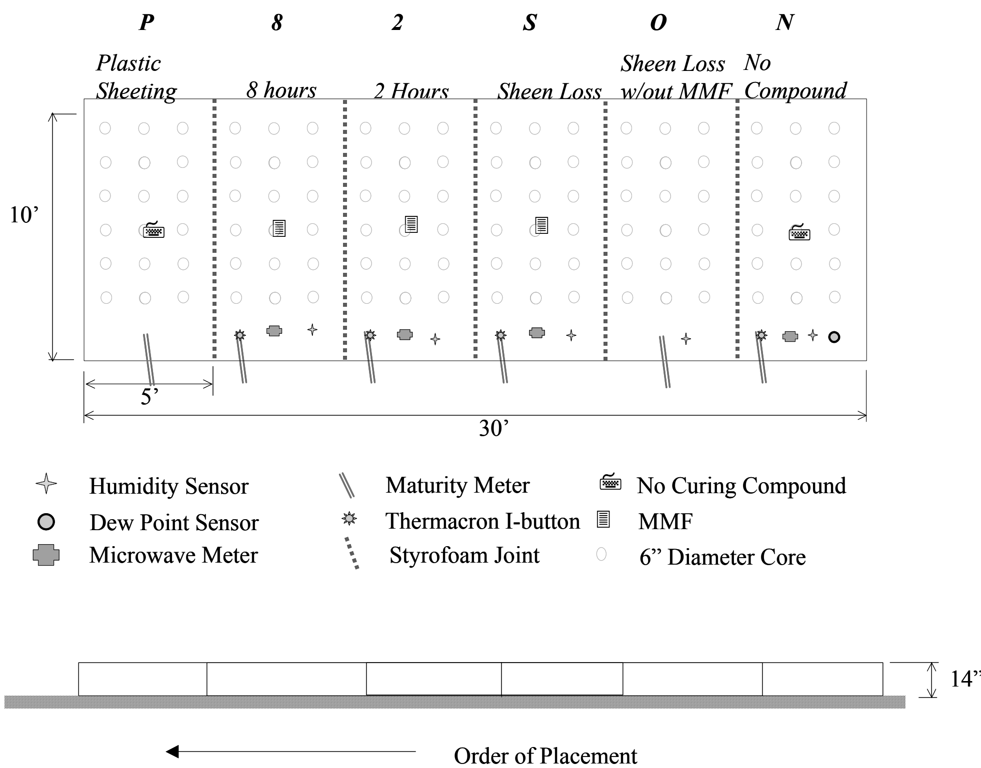

Figure 4.7 General Layout of SSII

Photo 4.4 Slab after Concrete Placement, Burlap Finish, and MMF Application

Photo 4.5 Slab after Concrete Application of Curing Compound and Plastic Sheeting

Cores were distributed with a minimum of 8 in. between any two adjacent cores, slab edges, or embedded equipment to ensure moisture conditions were not affected by edge effects and equipment was not damaged during coring (see Figure 4.8). Cores were cut by a coring truck located off the slab and not in an area that was yet to be cut or that contained NDT equipment. A typical coring truck has a 2-foot reach, and thus coring began at the outer edge of the slab, moving inward. Photo 4.6 shows the slab after the coring of 3-day cores. Note that the water required for cutting wets the slab preventing further moisture analyses. Once the outer cores were cut, subsequent cores were reached by moving the truck onto the slab. Half of the cores in each section were used for splitting tensile tests and the other half for elastic modulus and compressive strength determination.

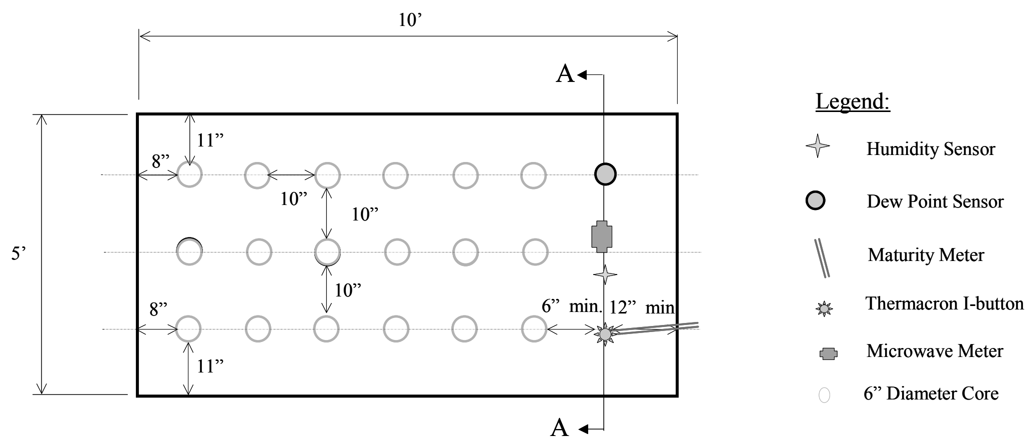

Figure 4.8 Typical Coring Layout for SSII

Photo 4.6 Slab after 3-Day Coring and Construction of Ramp for Coring Truck

4.3.1 Equipment Details

To achieve the objectives of SSII, six slab sections with varying curing histories were constructed. Continuous moisture measurements were logged for 2 days by the dew point sensor and 3 days by the four microwave sensors. Humidity sensor and Aquameter readings were taken manually for 3 days from the time of placement. In the SSI, only the dew point sensor was used for moisture measurements. In the SSII, the moisture equipment utilized represented a range of complexity and expense. The equipment is listed below with the more complex and expensive listed first:

- Dew point sensors: A probe was placed in the slab with neither curing compound nor MMF and was used for calibration and comparisons to other devices. Originally intended for placement in slabs *N*, *S*, *2*, *8* and a concrete pan to be weighed, four gauges were stolen the night prior to construction. Because only one sensor was left, it was placed in the uncovered slab, the worst-case placement scenario.
- Microwave meters: Four probes were placed in all but the plastic sheeting and sheen loss. The microwave sensor was embedded to a depth of approximately 2 - 3 inches to anchor the weight of the metal converter box. Thus, the microwave sensors record moisture slightly below the surface. Once all readings have been obtained, the wires are cut and the box is salvaged, whereas, the sensors are sacrificial.
- Aquameter: Readings were taken on the surface of each slab (except the plastic covered slabs as the repeated lifting of the plastic would alter curing) every half hour. Readings were taken initially in various locations in each slab section to obtain an average moisture content. By the second day after placement, one location was selected on the slab for all future readings. Selected locations represented concrete areas that had a smooth finish. This was done because it appeared that the variability due to concrete surface is greater than that due to moisture content.
- Humidity sensors: Five capsules used with two sensors were placed in all slabs (except the slab with plastic sheeting) and in the concrete pan without a windscreen. The bottoms of the capsules were cut off of all casings. Capsules were embedded to a depth of about ¾ in. Two humidity sensors, *1* and *A*, were used to determine variability between sensors.
- A water pan was utilized to determine maximum potential water loss. Additionally, two concrete pans made of the same concrete batch were continuously weighed at the same times as the water pan for comparison and calibration with in situ water loss and evaporation. One pan was allowed to cure next to the slab, but was shielded from wind by a windscreen whereas the other was open to the wind.

Temperature was logged in both studies. In SSII, an additional sensor, the Thermacron i-Button was used. Both studies are described below:

- Standard maturity meters (thermocouples): Placed in all slab sections and molded specimens, one per cylinder. Gauges were approximately at mid-depth in each slab. Independent meters logged slab and cylinder probes.
- The Thermacron i-Button was used to obtain continuous time-temperature (maturity) readings. Temperatures were recorded every 30 minutes in SSII to match thermocouple readings. Photo 4.7 shows a typical Thermacron i-Button, female attachment, and a probe that can be used for obtaining readings (not used in SSII). Buttons were embedded to depths of 1 in and 13 in., thus 1 in. from the top and bottom of the slab. They were placed in four slabs, *N*, *S*, *2*, and *8*, as shown in Figure 4.8. They were connected by wires with the top i-Button tied to a hole in the top of an 18 in. PVC pipe to prevent slippage, and the bottom i-Button tied around the pipe to keep it from drifting laterally (Figure 4.8). The PVC pipe was embedded 5 inches into the asphaltic base to prevent

overturning during concrete placement and placed 1 foot from the slab edges (Photo 4.9). The thermocouple was tied around the midsection of the pipe, and the gages placed in all six slabs. The pipe was inserted to serve only as a platform to tie the gauges to. Two additional probes were provided to monitor maturity in the standard-cured cylinders.

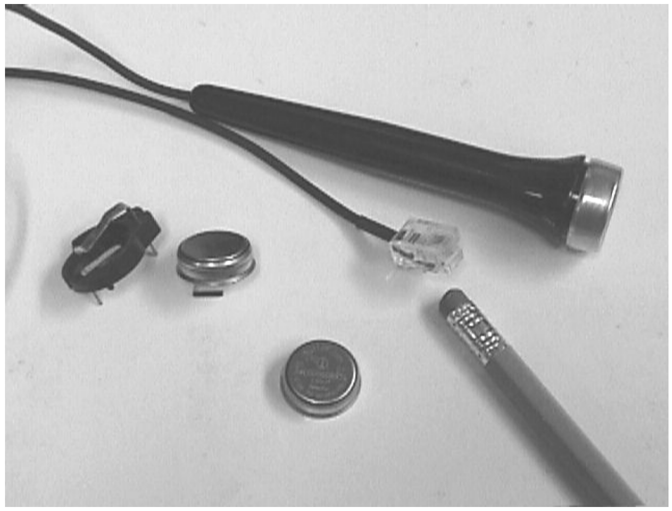

Photo 4.7 Typical Thermacron i-Button, Female Adapter and Probe

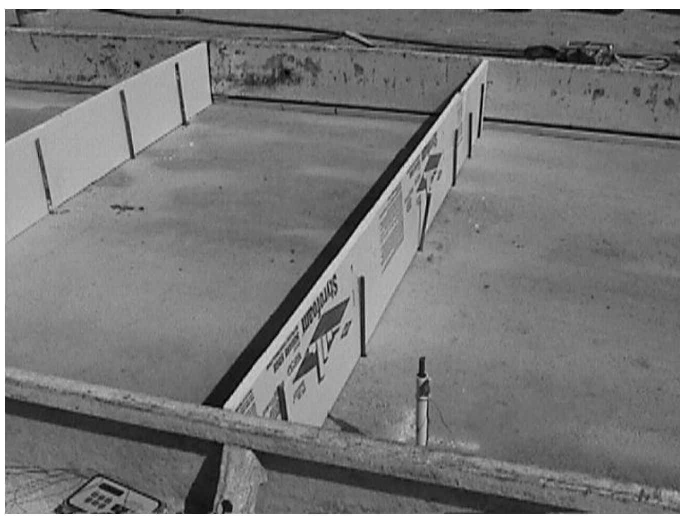

Photo 4.8 Setup of i-Button on Slab Prior to Concrete Placement

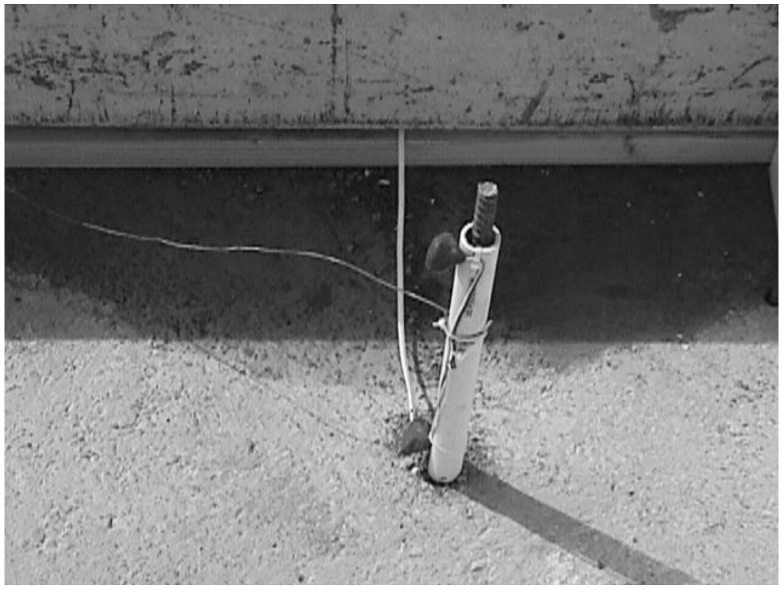

Photo 4.9 Location of i-Buttons 1 Foot from Slab Edges

In addition to concrete moisture and temperature sensors, ambient conditions were measured using a weather station run continuously for 30 days after time of concrete placement.

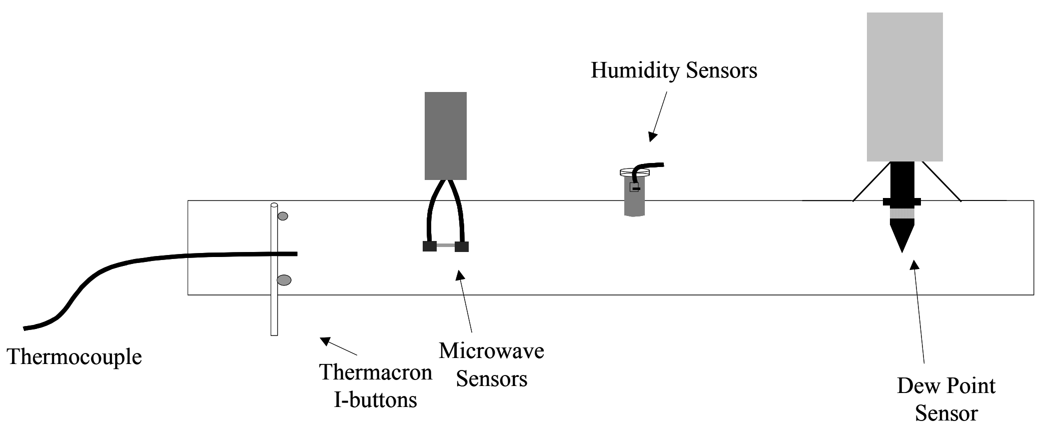

Figure 4.9 Slab Cross Section Showing Equipment Locations for SSII

4.3.2 Specimen Details

Cores and molded cylinders were used in this investigation. All specimens had a 6 in. diameter. Cylinders and cores used for elastic moduli /compressive strength tests were 6 x 12 in. and cores used for splitting tensile tests were 6 x 2.5 in.

Cores used for tensile strength tests were cut such that two specimens from the top and one from the bottom, each 2.5 x 6 in., could be obtained (Figure 4.10). Thus, three splitting tensile test specimens were obtained per core. The top 1/8 in. was **not** trimmed as is customary, because moisture is most variable near the surface and trimming would potentially result in the loss of valuable data. Thus, the 2.5 x 6 in. specimens included the uppermost 5 in. and lowermost 2.5 in. of the core. The midsection, *y*, was labeled and stored for possible future use.

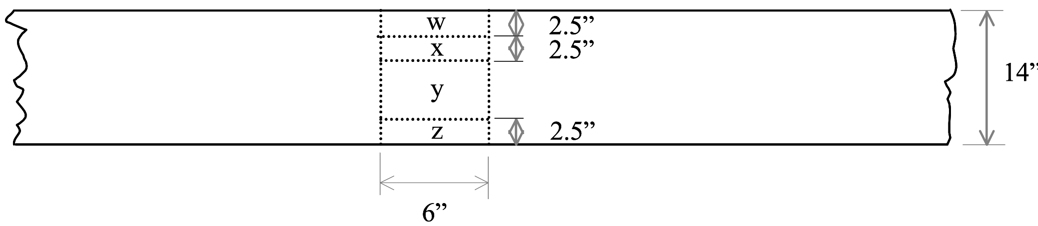

Figure 4.10 Cross Section Showing Labels and Location of Cuts for Tensile Cores

Elastic moduli and compressive strengths were determined from cores cut at 3, 7 and 28 days from each of the six slab sections. These cores were 6 x 12 in., with the bottom 2 in. cut to preserve top concrete affected most by the curing regime selected.

Figure 4.11 provides a factorial summarizing the cores required for the investigation. Each cell represents a test in which three replicate specimens are used. Thus, to conduct these tests at three ages with three replicates per test from six different slab conditions, a total of 108 cores were required for this investigation. Fifty-four of the one hundred eight cores were cut for tensile strength tests, resulting in one hundred sixty two tensile strength tests. The remaining Fifty-four cores were used for modulus and compressive tests, resulting in an additional one hundred eight tests (where modulus and compressive strength determination represent separate tests). Therefore, a total of two hundred seventy tests were conducted on cut specimens.

On each core testing day (3, 7, and 28 days after placement), thirty-six cores were cut and ninety tests were conducted. Eighteen of these cores were cut into four sections, with sections *w, x,* and *z* tested for splitting tensile strength, for a total of fifty-four splitting tensile tests per day. The remaining eighteen cores cut on core test days were tested for elastic modulus and compressive strength, adding thirty six tests per day. Thus, on days in which core tests were scheduled (3, 7, and 28 days after placement), thirty-six cores were cut and ninety tests conducted.

Test Type	Age (days) / Curing Regime	Plastic Sheeting	Sheen Loss (No MMF)	Sheen Loss	2 Hours	8 Hours	No Compound
Tensile	3						
	7						
	28						
Modulus/ Compressive	3						
	7						
	28						

Figure 4.11 Coring Factorial for SSII

Molded specimens were 6 x 12 in., standard water-cured cylinders. Figure 4.12 provides a factorial for the molded specimens. White cells indicate that three specimens were utilized per test (unless specified otherwise), and a black cell indicates that no tests were conducted. The second of two cylinders used for maturity readings was provided in case a probe malfunctioned, as well as to average measurements. These cylinders were not tested for strength as the presence of the probe may affect strength. A total of thirty-four cylinders were required, with a total of forty cast. A maximum of six cylinders were tested for tensile strength, compressive strength and elastic modulus per day, resulting in a maximum of nine cylinder tests per day.

Test / Age (days)	Tensile	Modulus / Compressive	Maturity
Early		(two samples)	
1			
3			
7			
14			
28			(two samples)

Figure 4.12 Cylinder Factorial for SSII

Because of the large number of specimens and tests in this investigation, a system of labeling was assigned to all specimens in order to prevent specimen identification errors. Table 4.2 lists nomenclature used and Figure 4.13 shows a typical coring layout and associated core labels. Cores *w*, *x*, and *z* were 2.5 x 6 in. and tested for splitting tensile strength, whereas section *y* was 6.5 x 6 in. and stored for possible future tests. Below is a list of parameters and codes associated with each variable.

Table 4.2 Nomenclature for SSII Specimens

Designation	Description
P, O, S, 2, 8, N	Curing compound application time/designation: Plastic, Sheen loss (no MMF), Sheen loss, 2 hours, 8 hours, No compound
T, C	Test type (tensile and compressive/modulus
1, 3, 7, 14, 28	Age at time of testing, days
a, b, c	Specimen designation for 4-in. cores (3 per test)
w, x, y, z	Vertical location (top to bottom), see Fig. 4.10

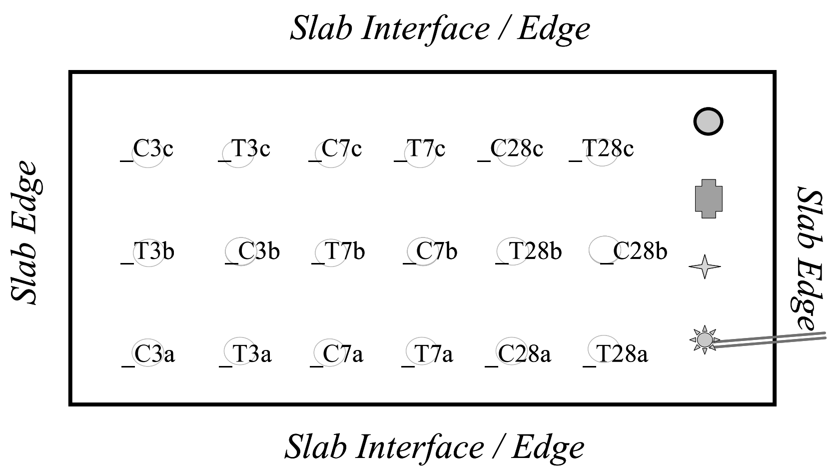

Figure 4.13 Coring Layout with Associated Identification

5. Small Slab I Destructive Test Results and Analyses

The following section presents data obtained from the Small Slab Study I (SSI) along with associated statistical analysis. Results corresponding to objectives outlined in Chapter 1, along with an additional section addressing the significance of age on strength are provided. This is done to avoid redundancy, as the influence of age (curing time) is part of every analysis.

5.1 CORE DIAMETER

Results presented in this section compare the 7- and 28-day compressive strength of limestone (LS) and siliceous river gravel (SRG) concrete using 4 x 8 in. and 6 x 12 in. cores. Analyses show that the use of 4 x 8 in. cores in lieu of 6 x 12 in. cores significantly increases both compressive and tensile strength (see Appendices C-1 and C-2 for strength values and detailed statistical analysis results).

5.1.1 Compressive Strength

As shown in Table 5.1 and Figure 5.1, the compressive strength of 4 in. cores is significantly higher than that of 6 in. cores for all ages and aggregate types tested. As mentioned in Section 2.3, *Data Analysis*, checkmarks indicate that a variable is statistically significant; $p \leq 0.05$ for that variable. On average, the 4 in. diameter LS cores were 20% stronger than the 6 in. diameter LS cores. Similarly, the 4 in. SRG cores were 6% stronger than the 6 in. diameter SRG cores. Though the effects of age and aggregate type are discussed in separate sections, it is worthwhile to briefly discuss the statistical results. Figure 5.1 graphs the average 7- and 28-day strengths of the 6 in. LS and SRG cores tested in compressive strength. The graphs show that SRG cores exhibit higher compressive strength than LS cores only at 7-day strength. After 28 days, LS cores exhibit the higher strength. The significance of age is apparent in Figure 5.1. Additionally, both SRG and LS specimens increase in compressive strength between 7 and 28 days. The independence of aggregate type on strength is also apparent in Figure 5.1.

Table 5.1 ANOVA Results of Core Diameter Data (α= 0.05)

Variable	Compressive Strength	Tensile Strength
Aggregate Type		
Age at Testing	✓	
Core Diameter	✓	✓

✓ Variable statistically significant

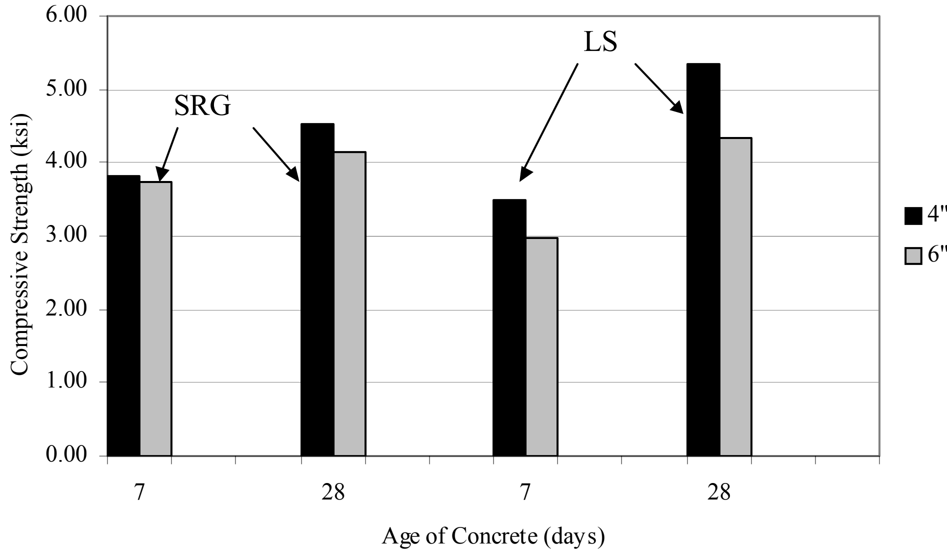

Figure 5.1 Average Compressive Strength of 4 in. and 6 in. Cores

From the statistical analyses, Equation 5.1 was developed and can be used to estimate the 7- and 28-day compressive strength of 4 in. and 6 in. diameter, LS and SRG cores. The model indicates that the use of an LS aggregate in place of SRG increases compressive strength by 17 psi (3% on average), that the use of 4-in cores in place of 6 in. cores increases compressive strength by 552 psi (13% on average), and tests conducted at 28 days rather than 7 days will yield 1,086 psi (24% on average) higher compressive strength on average. It is clear that the increases in strength because of age and core diameter are greater than those caused by differences in aggregate type. Though the effects of aggregate type do not significantly affect strength, the variable is included in the model for completeness. Data, p-values and r^2 values associated with this equation can be found in Appendices C-1 and C-2.

$$f_c = 4.503 - 0.2760 * diam + 0.0517 * age + agg \quad \text{(Eq 5.1)}$$

where

fc	=	compressive strength, ksi
diam	=	diameter of core with an L/D ratio of 2:1 between 4 and 6 in., in.
age	=	age of concrete at time of testing between 7 and 28 days, days
agg	=	aggregate type
	=	0.0165 for LS specimens
	=	0 for SRG specimens

5.1.2 Tensile Strength

As shown in Table 5.1 and Figure 5.2, the tensile strength of 4 in. cores is significantly higher than that of 6 in. cores for all ages and aggregate types tested. On average, the 4 in. diameter LS cores were 10% stronger than the 6 in. diameter LS cores. Similarly, the 4 in. SRG cores were 15% stronger than the 6 in. diameter SRG cores. Again, though the effects of age and aggregate type are discussed in separate sections, their effects will be discussed briefly here.

As shown in Figure 5.2, though LS cores are consistently stronger than SRG cores, the effects are insignificant. Similarly, no significant increase in strength is present in either LS or SRG cores between 7 and 28 days. This independence of age and aggregate type is easily seen in Figure 5.2. Discussions concerning discrepancies of the significance of variables between compressive and tensile strength results are provided in Section 7.1.

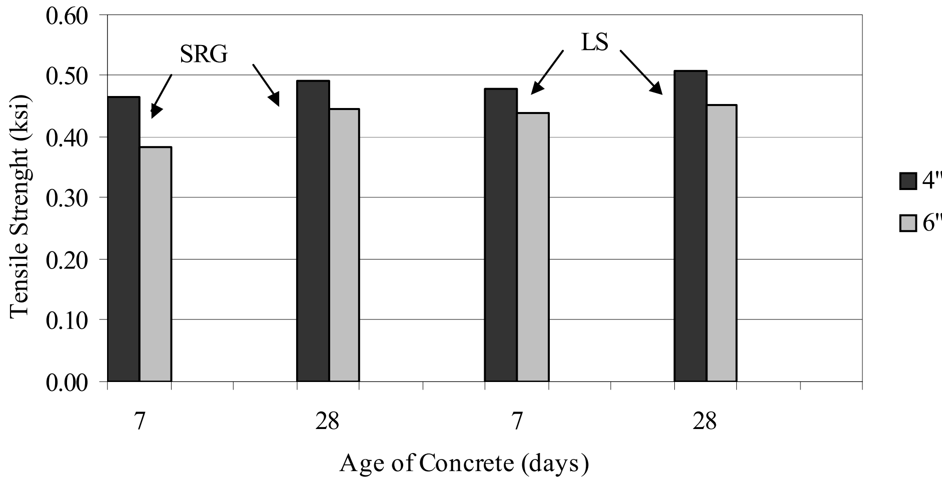

Figure 5.2 Average Tensile Strength of 4 in. and 6 in. Cores

From the statistical analyses, Equation 5.2 was developed and can be used to estimate the 7- and 28-day tensile strength of 4 in. and 6 in. diameter LS and SRG cores. The model indicates that the use of an LS aggregate in place of SRG increases tensile strength by 23 psi (4% on average), that 28-day concrete is stronger than 7-day concrete by 34 psi (6% on average), and that the use of 4 in. cores in place of 6 in. cores increases tensile strength by 54 psi (10% on average). It is clear that the increases in strength due to core diameter are greater than those caused by differences in aggregate type and age. Though the effects of aggregate type and age do not significantly affect strength, the variable is included in the model for completeness. Data, p-values, and r^2 values associated with this equation can be found in Appendices C-1 and C-2.

$$f_t = 0.553 - 0.0268 * diam + 0.0016 * age + agg \qquad \text{(Eq 5.2)}$$

where

ft	=	tensile strength, ksi
diam	=	diameter of core with an L/D ratio of 2:1 between 4 and 6 in.
age	=	age of concrete at time of testing between 7 and 28 days, days
agg	=	aggregate type
	=	0.0230 for LS specimens
	=	0 for SRG specimens

5.2 CYLINDER CURING METHOD

Results presented in this section compare the 7- and 28-day compressive and tensile strengths of LS and SRG, 6 x 12 in. cores, water-cured cylinders, and sand-cured cylinders (see Appendices C-3 and C-4 for strength values and detailed statistical analysis results). Two analysis types were used to determine significance of variables: analysis of variance (ANOVA) and Fisher's Least Significant Difference (LSD) Test (a post hoc comparison of means). The ANOVA consisted of separate analyses between cores for each cylinder type, while the Fisher's test allowed simultaneous multivariable analysis. Significance in Fisher's test is denoted by differences in T-groupings, providing a concise method of comparing multiple data types. Results are shown in Tables 5.2 and 5.3 below.

Table 5.2 ANOVA Results of In Situ and Molded Sample Strength Data

Variable	Compressive Strength		Tensile Strength	
	wtr vs. cor	snd vs. cor	wtr vs cor	snd vs. cor
Curing Method	✓			✓
Age at Testing	✓	✓	✓	✓
Aggregate Type				

Table 5.3 LSD Results of In Situ and Molded Sample Strength Data

Variables		n	Compressive Tests		Tensile Tests	
			T grouping	Avg. Strength (ksi)	T grouping	Avg. Strength (ksi)
CAT	srg	18	A	4.106	A	0.416
	ls	18	A	3.922	A	0.409
CUR	wtr	12	A	4.431	A	0.439
	snd	12	B	3.908	B	0.368
	cor	12	B	3.703	A	0.431
AGE	28	18	A	4.418	A	0.431
	7	18	B	3.61	B	0.394

Table 5.3 shows clearly that water-cured cylinders exhibited significantly higher compressive strength (14%) than cores and sand-cured cylinders, with cores and sand-cured cylinder strengths being virtually identical. This is indicated by the different T-groupings of water-cured cylinders *wtr,* and sand-cured cylinders, *snd,* and cores *cor*. Groups with the same letter are statistically indistinguishable. Conversely, sand-cured cylinders produced tensile strengths that were significantly lower (15%) than those obtained from water-cured cylinders and cores, with the tensile strength of cores and water-cured cylinders being virtually identical. It can be seen that a T-grouping that is lower in the alphabet denotes decreasing strength. Thus, differences in curing lead to differences in strength of up to 15%. Figures 5.3 and 5.4 plot the compressive and tensile strengths of each sample type, respectively.

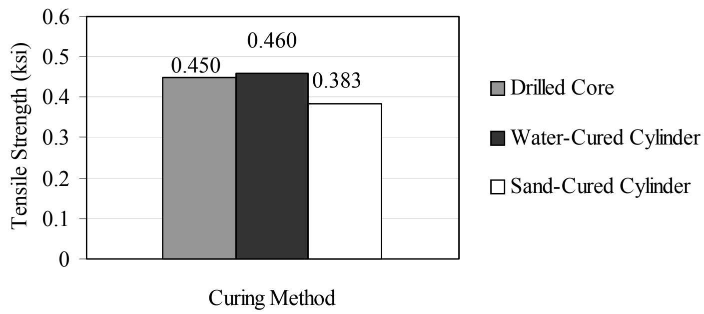

Figure 5.3 Average 28 Day Compressive Strength of Cores and Cylinders

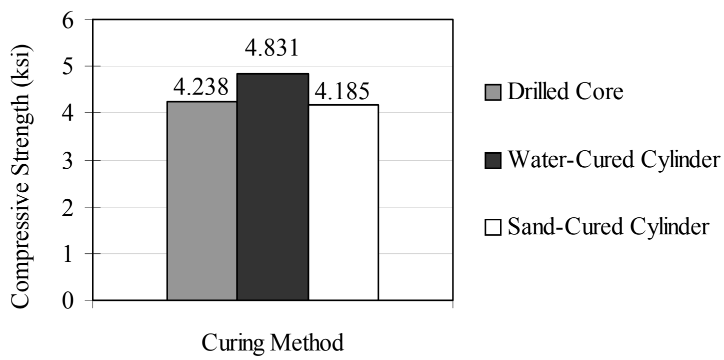

Figure 5.4 Relative 28 Day Tensile Strength of Cores and Cylinders

From the statistical analyses, Equation 5.3 was developed and can be used to estimate the compressive strength up to an age of 28 days for LS and SRG, 6 x 12 in. cores, water-cured cylinders, and sand-cured cylinders. The model indicates that the use of an SRG aggregate in place of LS increases compressive strength by 185 psi (5% on average), that water-cured cylinders exhibited compressive strength approximately 600 psi (16% on average) higher than sand-cured cylinders and cores, and that the effects of age between 7 and 28 days after placement contributed to an increase in strength of approximately 1,000 psi (26% on average). It is clear that the increases in strength due to water-curing and age are greater than those caused by differences in aggregate type selection. Though the effects of aggregate-type do not significantly affect strength, the variable is included in the model for completeness. Data, p-values for variables, and r^2 values associated with this model can be found in Appendices C-3 and C-4.

$$f_c = 3.8506 + cure + age * 0.0345 + agg \qquad \text{(Eq 5.3)}$$

where

fc	=	compressive strength, ksi
cure	=	curing method applied to the sample
	=	-0.7282 for cores
	=	-0.5231 for sand-cured cylinders
	=	0 for water-cured cylinders
age	=	age of concrete at time of testing, up to 28 days

agg	=	aggregate type used in sample
	=	-0.1846 for LS specimens
	=	0 for SRG specimens

From the statistical analyses, Equation 5.4 was developed and can be used to estimate up to 28-day tensile strength LS and SRG, 6 x 12 in. cores, water-cured cylinders, and sand-cured cylinders. The model indicates that the use of an LS aggregate in place of SRG increases compressive strength by 7 psi (2% on average), that sand-curing decreases strength by approximately 70 psi (17% on average), and that the effects of age 28 days after placement yielded an increase in strength by approximately 50 psi (12% on average). It is clear that the reductions in strength due to sand-curing and age are much greater than those caused by differences in aggregate-type selection. Though the effects of aggregate type do not significantly affect strength, the variable is included in the model for completeness. Data, p-values for variables, and r^2 values associated with this model can be found in Appendices C-3 and C-4.

$$f_t = 0.4048 + cure + age * 0.0017 + agg \qquad \text{(Eq 5.4)}$$

where

ft	=	splitting tensile strength, ksi
cure	=	curing method applied to the sample
	=	-0.0070 for cores
	=	0 for water-cured cores
	=	0.0708 for sand-cured cylinders
age	=	age of concrete at time of testing, up to 28 days, days
agg	=	aggregate type used in sample
	=	0.0069 for LS specimens
	=	0 for SRG specimens

5.3 STRENGTH RELATIONSHIPS

Strength relationships obtained in this experiment are compared to those of Raphael as discussed in Section 3.3. Statistical analyses of SSI data revealed much higher correlations using the 2/3 exponential relationship suggested by Raphael than by using the standard square root. This is indicated by the high r^2 values of 0.9781–0.9938 obtained from 2/3 exponential fits, as well as the plotting of experimental data on Raphael's model (Figures 5.5, 5.8, and 5.11). Statistical analyses were conducted on averages of data sorted by age and aggregate type. Figures 5.5–5.13 provide plots comparing regressions developed from SSI data *averaged* by aggregate type, curing method and age compared to Raphael's models, and standard deviation plots of SSI data and regression equations developed. Listed below are the regression equations developed from SSI, associated r^2 and coefficient of variation values, and the strength relationships suggested by Raphael.

SSI Results	Raphael's Results
$f_r = 2.5\ f_c^{2/3}$	$f_r = 2.3\ f_c^{2/3}$
$f_t = 1.67\ f_c^{2/3}$	$f_t = 1.7\ f_c^{2/3}$
$f_r = 1.51\ f_t$	$f_r = 1.35\ f_t$
-or- $f_t = 0.67\ f_r$	-or- $f_t = 0.74\ f_r$

where

ft	=	splitting tensile strength @ age í
fc	=	compressive strength @ age í
fr	=	modulus of rupture @ age í

Table 5.4 summarizes the statistical analysis results and comparisons to Raphael's equations. Columns 1 through 3 represent SSI data correlations to the SSI model by r^2 values, coefficient of variation values, and the percent of data values falling within one standard deviation of the SSI regression. Thus, column 3 refers to Figures 5.6, 5.9, and 5.12. For example, row 1 of column 3 in Table 5.4 corresponds to Figure 5.6 where 82% of the data points (18 out of 28) fall within one standard deviation of the SSI regression. Columns 4 and 5 of the table compare the fit of the data to the SSII and Raphael regressions. Column 5 is very revealing as it exhibits the agreement of the SSI data points with Raphael's models, as determined from over 1,500 specimens. For example, column 5 indicates the percentage of SSI values that cross Raphael's model within one standard deviation. Thus, in Figure 5.7, one can see that 60% (17 out of 28) of the SSI values are within one standard deviation of Raphael's model. Data and statistical analysis results for strength relationships can be found in Appendices C-5 and C-6.

Table 5.4 Statistical Analysis Results and Comparisons of Data

Model	SSI Regression				Raphael Regression
	r^2	C.O.V.	Percent of data within one S.D. of SSI Regression	Percent of data crossing SSI Regression, within one S.D.	Percent of data crossing Raphael Regression, within one S.D.
Compressive-Flexural	0.9938	8.5	64	82	61
Flexural-Tensile	0.9840	13		39	29
Compressive-Tensile	0.9781	16	71	64	85

Column 5 of Table 5.4 clearly indicates that the Small Slab Study data was best represented by Raphael's compressive-tensile model with 85% of the data crossing Raphael's model, within one standard deviation. The compressive-flexural and flexural-tensile models had only 61% and 29% crossing, respectively (see Figures 5.7 and 5.10).

It may appear from Figure 5.5 that 4 in. cores do not lie near the SSI regression line. However, removal of these specimens does not increase r^2 values significantly. Figures 5.6–5.8 provide the strength relationships developed by Raphael along with the regression line and original data points obtained from SSI.

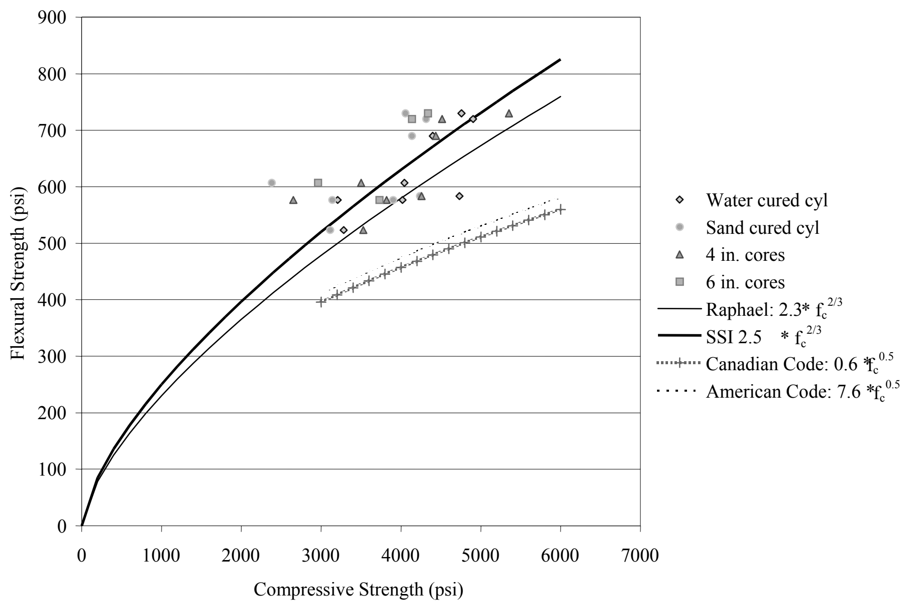

Figure 5.5 Compressive versus Flexural Strength Regressions and Comparisons with Codes

As shown in Figure 5.5, the relationships provided in the American and Canadian codes severely underestimate flexural strength. This may be due to the safety margin incorporated in most codes. Raphael's equations, derived from the data of other researchers and comprising approximately 1,500 cores, slightly underestimates flexural strength compared to experimental data, though the differences are small. The coefficient of flexural strength to compressive strength$^{2/3}$ for Raphael is 2.3 and for SSI is 2.5, a difference of approximately 8.5%.

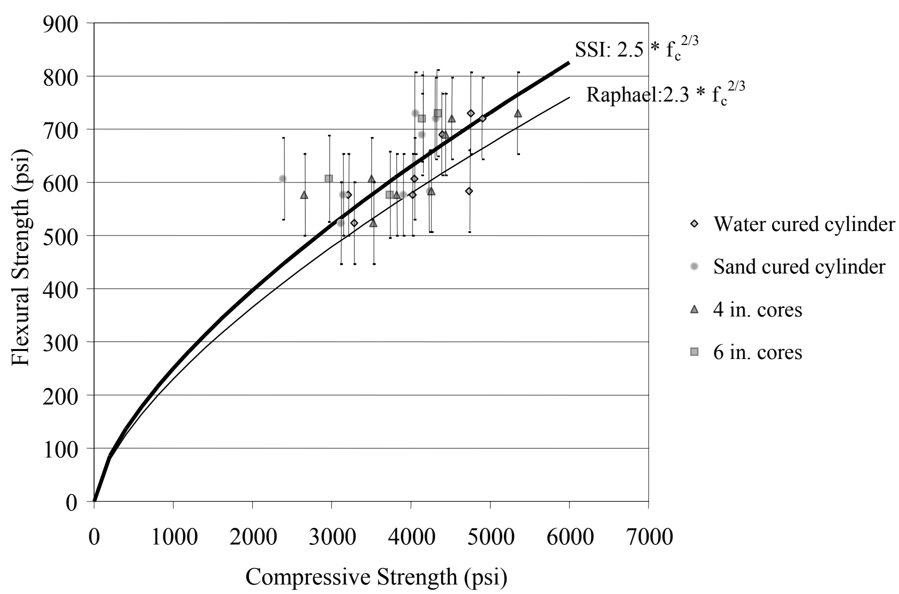

Figure 5.6 SSI Flexural versus Compressive Strength Regression

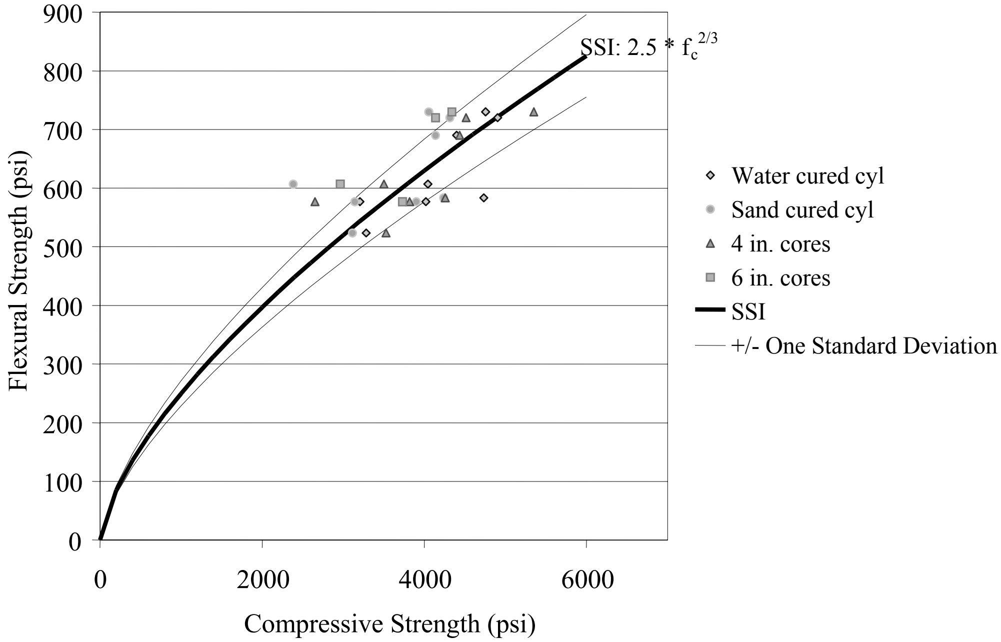

Figure 5.7 Comparison with Raphael's Flexural versus Compressive Strength Regression

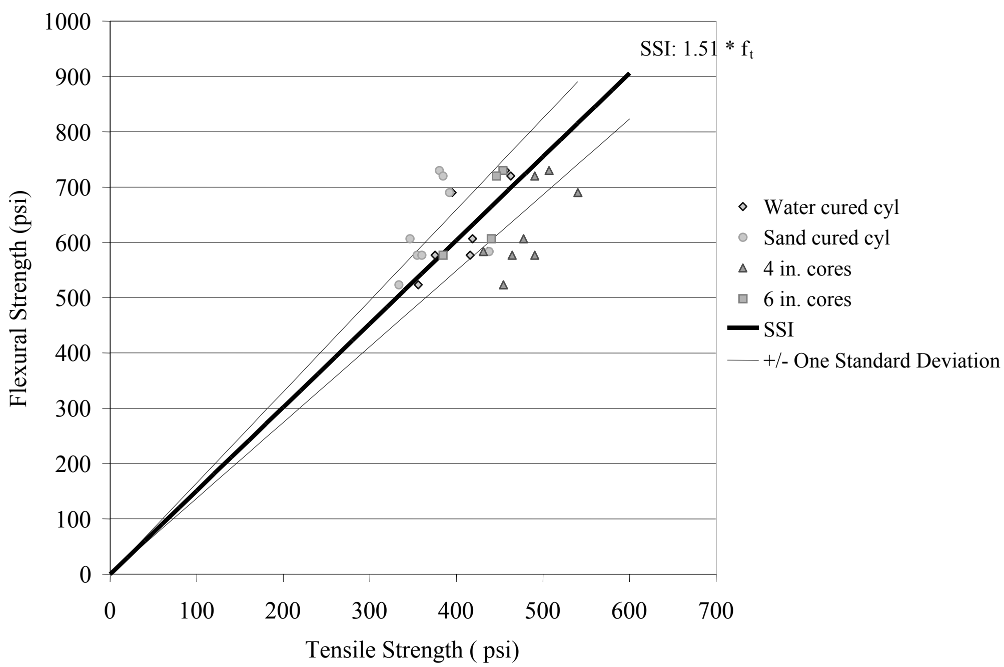

Figure 5.8 SSI Flexural versus Tensile Strength Regression

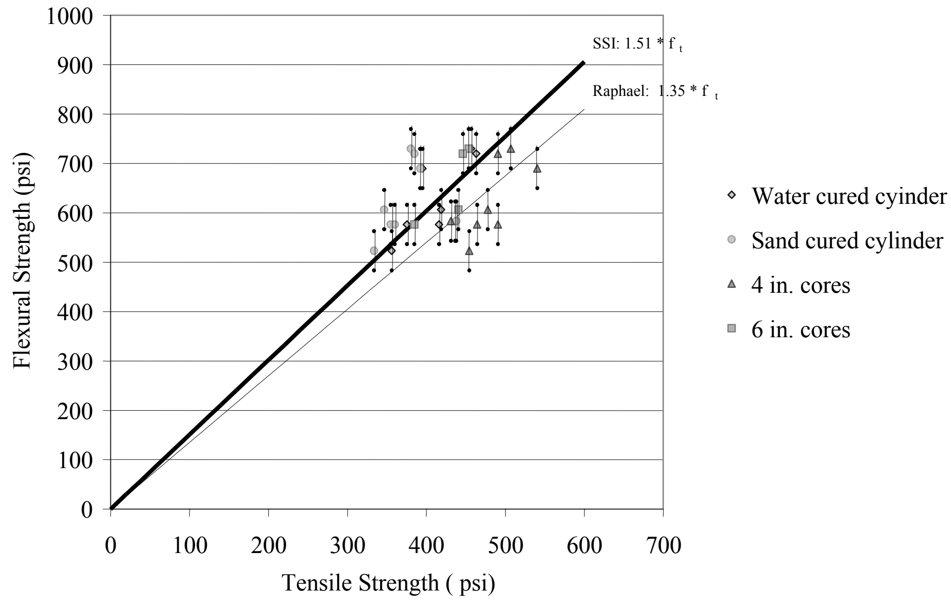

Figure 5.9 Comparison with Raphael's Flexural versus Tensile Strength Regression

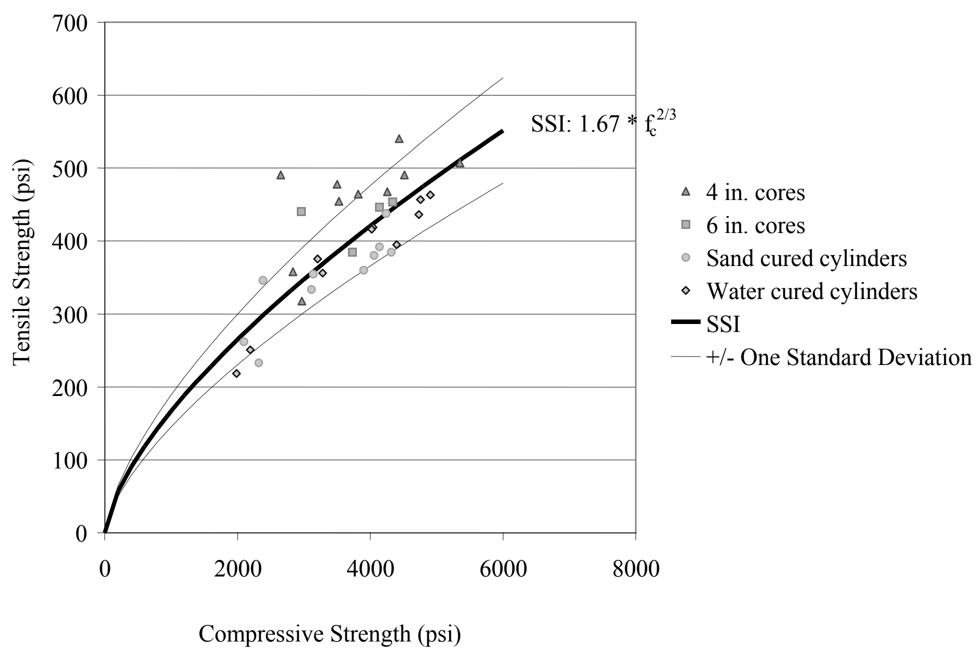

Figure 5.10 SSI Tensile versus Compressive Strength Regression

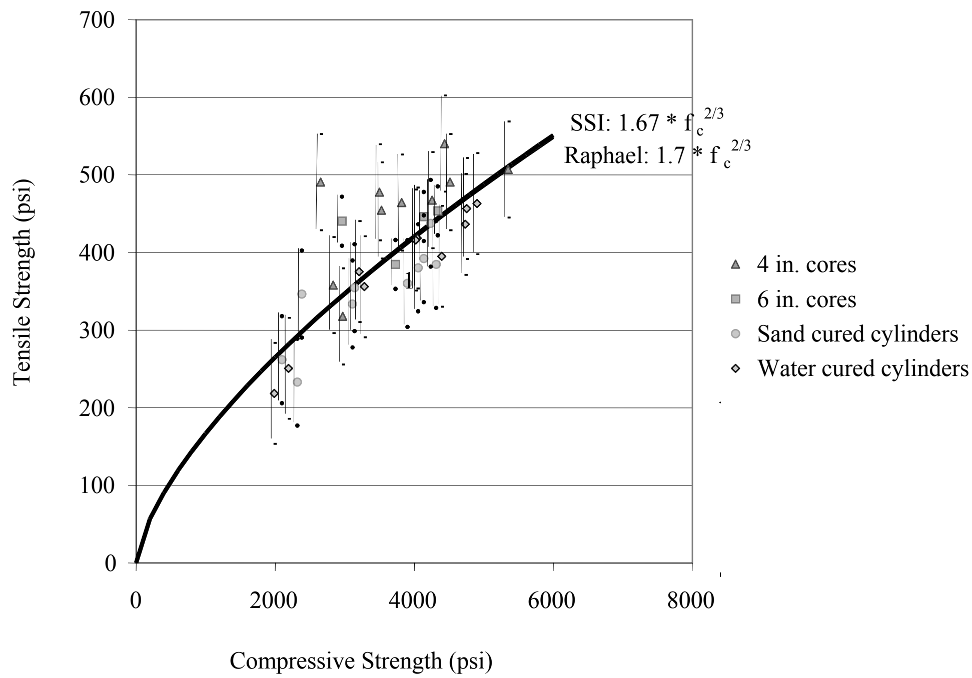

Figure 5.11 Comparison with Raphael's Tensile versus Compressive Strength Regression

As shown in Figure 5.11, the SSI regression lies nearly coincident with that developed by Raphael. Relative to the SSI regression, Raphael's model over-predicts strength by only 2%, a negligible amount. This complete agreement with Raphael and the high r^2 value (0.9840) of the SSI regression shows that relatively accurate predictions of tensile strength from compressive strength are possible.

5.4 REINFORCEMENT

Results presented in this section compare the 14- and 27-day compressive strengths and 3-day tensile strengths of 4 in. LS cores both with and without steel, from slab areas with zero, one, and two mats of reinforcement. Original plans called for both compressive and tensile tests to be done at 3-, 14-, and 28-day strengths. However, because of errors in coring, not all desired cores were obtained. Specifically, no 3-day specimens were cored for compressive strength tests, and thus only 14- and 28-day core strengths were used. Additionally, no 14- and 28-day cores to be used in tensile strength tests contained reinforcement. Therefore, only the 3-day specimens were used for tensile strength analyses. The data table in Appendix C-7 shows specimens containing reinforcement.

Table 5.5 shows the results of the statistical analyses conducted. Results indicate that only the presence of steel, not amount, affects the compressive strength of the cores. In other words, no significant changes in *compressive strength* were exhibited between cores obtained from slabs containing single and double mats, though specimens with steel were significantly stronger than those without. Table 5.5 also shows that tensile strength is independent of the presence and/or amount of steel in a core. These results confirm the hypothesis that reinforcement running parallel to the failure plane, though not within it, will not affect tensile strength. As explained earlier, the effects of age on tensile strength could not be determined as indicated by the dash in Table 5.5.

The 14-day tensile strength data, in which no specimens contained steel, was used to run an additional analysis to determine the effects of the amount of steel in a slab on specimens that do not include steel. In other words, it was used to determine the effects of having steel near a sample. As expected, the number of mats in the slab did not affect the strength of the cores (n=8, r^2= .3113). Figures 5.12 and 5.13 show the strength of cores from the reinforced slab as a percentage of strength of cores from the unreinforced slab.

Table 5.5 ANOVA Results of Reinforcement Data

Variable	Compressive Tests	Tensile Tests
No. of mats		
Presence of steel	✓	
Age		-

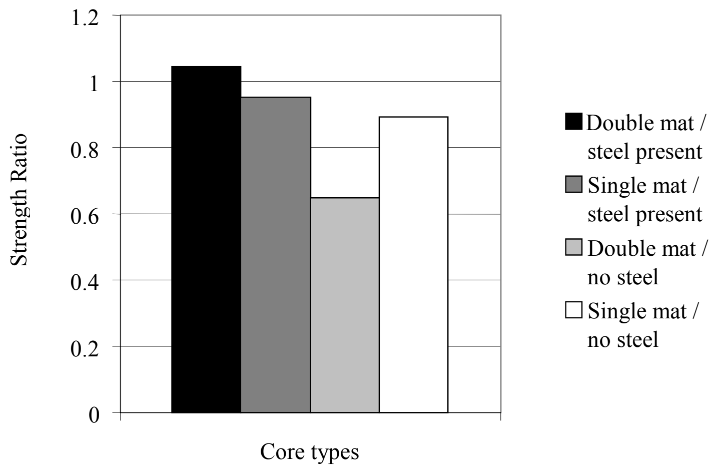

Figure 5.12 Average Compressive Strength of Cores in Reinforced Slab to Unreinforced Slab

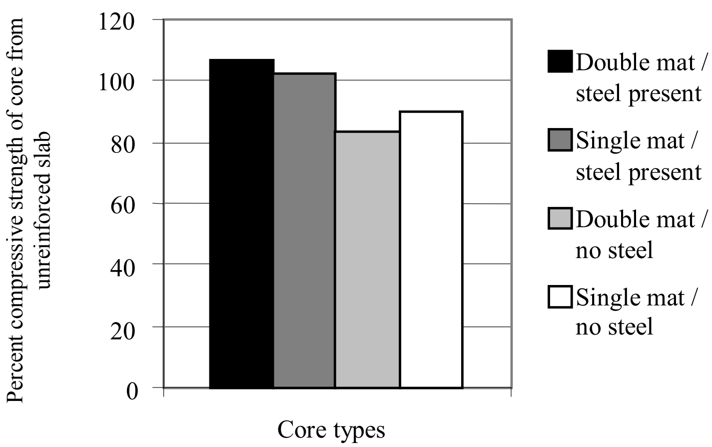

Figure 5.13 Average Tensile Strength of Cores from Reinforced Slab Cores to Unreinforced

From the statistical analyses, Equation 5.5 was developed and can be used to estimate the 14- and 27-day compressive strength of 4 in. LS cores with and without reinforcement from slabs with zero, one, and two mats of steel. All specimens were made of LS aggregate, and thus the *agg* variable is not a part of this analysis. The model indicates that if a sample contains steel, obtaining the core from a slab section with *double mats* rather than single mats *reduces strength by 64 psi* (1% on average). If *steel* is *present* in a core, compressive strength will *increase by 541 psi* (11% on average). Lastly, the model indicates that 28-day concrete is stronger than 14-day concrete by 250 psi (5% on average). It is clear that the increase in strength as a result of the presence of reinforcement is greater than the increase caused by the number of mats in the slab from which the cores were cut and age between 14-day and 28-day testing. Though the effects of aggregate type and age do not significantly affect strength, the variable is included in the model for completeness. Data, p-values for variables, and r^2 values associated with this equation can be found in Appendices C-7 and C-8. The reader should recognize the equation is only applicable to mixes similar to the one used.

$$f_c = 4.709 + stl + mat + 0.0179 * age \qquad \text{(Eq 5.5)}$$

where

fc	=	compressive strength, ksi
stl	=	presence of steel in the sample
	=	-0.541 if steel is not present in the core
	=	0 if steel is present
mat	=	number of mats of steel in the slab from which the sample is cut
	=	0.3515 if unreinforced
	=	0 for a single mat slab
	=	-0.0644 for a double mat slab
age	=	days from time of placement to testing

From the statistical analyses, Equation 5.6 was developed and can be used to estimate the 3-day tensile strength of 4 in. LS cores with and without reinforcement from slabs with zero, one, and two mats of steel. The model indicates that if a sample contains steel, obtaining the core from a slab section with double mats rather than single mats reduces strength by 47 psi (10% on average). If steel is present in a core, tensile strength will increase by 84 psi (17% on average). As only 3-day LS specimens were tested, the *age* and *agg* variables, respectively, are not a part of this analysis. It is clear that the increase in strength as a result of the presence of reinforcement is greater than the increase caused by the number of mats in the slab from which the cores were cut. Data, p-values for variables, and r^2 values associated with this equation can be found in Appendices C-7 and C-8.

$$f_t = 0.4858 + stl + mat \qquad \text{(Eq 5.6)}$$

where

ft	=	splitting tensile strength, ksi
stl	=	presence of steel in the sample
	=	-0.0845 if steel is not present in the core
	=	0 if steel is present
mat	=	number of mats of steel in the slab from which the sample is cut
	=	0.1157 if unreinforced

= 0 for a single mat slab
= -0.0467 for a double mat slab

5.5 PAVEMENT SURFACE TREATMENT

Results presented in this section compare the 28-day compressive and tensile strengths of 4 x 8 in. LS and SRG cores from slab sections in which tining has been introduced or a curing compound application has been eliminated. To determine the effects of the application of a curing compound on strength, tined specimens were excluded from the analysis as their strengths would not vary significantly from the carpet-dragged specimens as both had a curing compound. Thus, their inclusion would provide misleading results. Similarly, to determine the tining, specimens without a curing compound were excluded from the analysis. Because of decisions at the time of coring, specimens used in the tensile strength analyses consisted of specimens from the top and bottom of the slab. Therefore, the effects of the vertical location on tensile strength were a part of this analysis. The effects of vertical position on strength will not be discussed in this section as a separate section is dedicated to this subject.

As shown in Table 5.6, the application of a curing compound significantly affected only compressive strength. The table also shows that the presence of tining did not affect strength in any test. This was anticipated as tining only increases surface area, a change that should not affect strength if a curing compound is applied properly.

As mentioned previously, the vertical position of the sample was a variable in this experiment due to sample availability. Analysis shows that specimens from the bottom of the slab were significantly stronger. Because the specimens used in this portion of the investigation were not labeled, it is not possible to know their placement and curing compound application times. Thus, it cannot be determined if the low top strengths are due to high evaporation rates on the surface or inherent low strengths of top concrete. This issue will be thoroughly discussed in the following section.

As shown in Table 5.6 and Figures 5.14 and 5.15, LS was found to be significantly stronger than SRG for tensile strength. Because LS specimens were placed prior to SRG specimens, the decreased strength of the SRG cannot be attributed to increased moisture loss and associated lower strength. Therefore, the effect may be due to discrepancies in the diameter to diameter (D/d) ratio between the two mixes. As discussed earlier, smaller, well-graded aggregate was used in the LS batch, ultimately increasing its core-diameter to nominal-aggregate diameter ratio, a change known to increase compressive strength. It is not known why the same trends are not exhibited for compressive strength.

Table 5.6 ANOVA Results of Pavement Surface Treatment Data

Variable	Compressive Tests		Tensile Tests	
	No tine: No Compound vs. Compound	Compound: Tine vs. No Tine	No tine: No Compound vs. Compound	Compound: Tine vs. No Tine
Aggregate type			✓	✓
Compound or Tining	✓			
Position	-	✓	✓	✓

From the statistical analyses, Equation 5.7 was developed and can be used to estimate 28-day compressive strength of 4 x 8 in. LS and SRG cores from a pavement both with and without tining or a curing compound. The model indicates that applying a curing compound increases core compressive strength by 1,000 psi (25% on average). Tining decreases core compressive strength by only 40 psi (1% on average) and using LS in place of SRG decreases strength by 133 psi (4% on average). It is clear that the increase in strength due to the application of a curing compound is much greater than the loss of strength resulting from tining and using LS aggregate. Data, p-values for variables, and r^2 values associated with this equation can be found in Appendices C-9 and C-10. These results are reflected in Figure 5.13.

$$f'_c = 3.946 + cure + agg \qquad \text{(Eq 5.7)}$$

where

f'c	=	compressive strength, ksi
cure	=	type of curing method applied to pavement at core location
	=	0.9849 for untined cores with a curing compound
	=	0.9463 for tined cores with a curing compound
	=	0 for untined cores without a curing compound
agg	=	aggregate type used in sample
	=	-0.1333 for LS specimens
	=	0 for SRG specimens

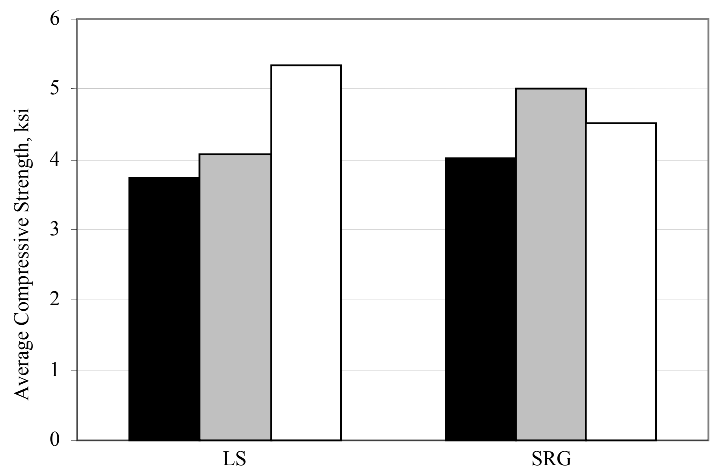

	LS	SRG
No compound / no tining	3.741	4.019
Compound / Tined	4.079	5
Compound / no tining	5.352	4.516

Figure 5.14 Average Compressive Strength of Cores from Slabs of Varying Surface Treatments

From the statistical analyses, Equation 5.8 was developed and can be used to estimate 28-day tensile strength of 4 x 8 in. LS and SRG cores from a pavement section both with and without tining or a curing compound. The model indicates that applying a curing compound increases core compressive strength by 45 psi (10% on average) and tining decreases core strength only by 5 psi (1% on average). Additionally, using LS in place of SRG increases strength by 107 psi (23% on average) and bottom cores are stronger than top cores by 72 psi (16% on average). It is clear that the increase in strength as a result of using LS and bottom specimens is much greater than the loss of strength as a result of tining and eliminating a curing compound. Data, p-values for variables, and r^2 values associated with this equation can be found in Appendices C-9 and C-10. These results are reflected in 5.15

$$f'_t = 0.4571 + cure + pos + agg \qquad \text{(Eq 5.8)}$$

where

f't	=	splitting tensile strength, ksi
cure	=	type of curing method applied to pavement at core location
	=	-0.0455 for untined cores with a curing compound
	=	-0.0050 for tined cores with a curing compound
	=	0 for untined cores without a curing compound
pos	=	vertical location of the sample in the slab
	=	0.0723 for cores from the bottom of a slab
	=	0 for cores from the top of a slab
agg	=	aggregate type used in sample
	=	0.1073 for LS specimens
	=	0 for SRG specimens

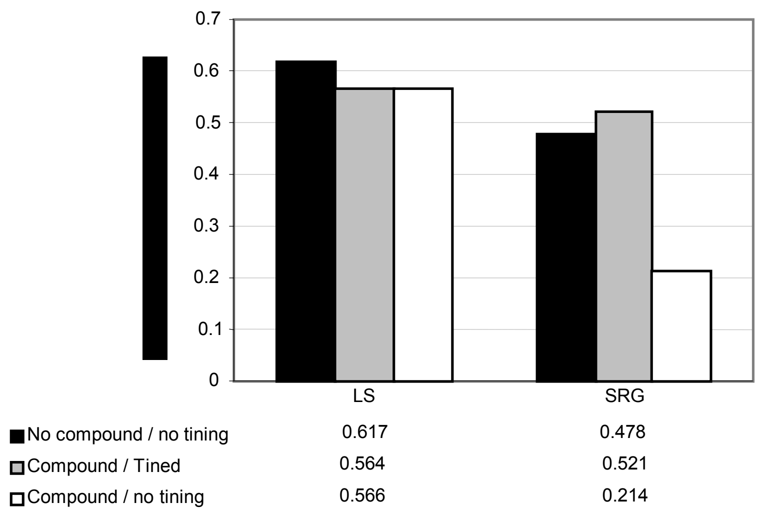

Figure 5.15 Average Tensile Strength of Cores from Slabs of Varying Surface Treatments

5.6 VERTICAL LOCATION OF SAMPLE IN SLAB

In this investigation, three analyses were performed to determine the effects of vertical position on compressive and tensile strength. The original analysis includes the effects of aggregate type, age at time of testing, and vertical location from representative top and bottom portions of the slab. The subsequent analyses considered environmental effects on strength, namely time-elapsed and evaporation rates, and water loss experienced by the concrete from time of placement to application of the curing compound (after the application moisture loss is assumed to be insignificant). The latter analyses were conducted to convert the developed model into more pertinent and applicable terms.

5.6.1 Original Analysis

Table 5.7 shows ANOVA results for the first analysis. It suggests that aggregate type is significant for tests on 4 in. cores. As is shown in Eq. 5.9, LS cores are significantly stronger than SRG cores. This is explained by the fact that the SRG aggregate was much larger than the LS aggregate, increasing its core diameter to nominal aggregate diameter ratio and decreasing strength.

Table 5.7 ANOVA Results of Vertical Position Data

Description	Compressive Tests		Tensile Tests	
	4 in. cores	6 in. cores	4 in. cores	6 in. cores
Aggregate type	✓		✓	
Age	-		✓	
Position	✓	✓		

The effects of position are better represented by running a separate analysis for LS and SRG specimens. Results shown in Table 5.8 suggest that only the LS batch experienced vertical strength differentials. This can be explained by the fact that, in general, the LS section was without a curing compound for 1 hour longer than the SRG section. These are the logical interpretations of the results and their causes. However, the sensitivity of the statistical analysis results, compounded with the small number of specimens available and discrepancies in compound placement time and aggregate sizes, make interpretations less reliable.

Table 5.8 ANOVA Results of Vertical Position Data Sorted by Aggregate Type

Aggregate	Variable	Limestone			
		Compressive Tests		Tensile Tests	
		4 in. cores	6 in. cores	4 in. cores	6 in. cores
LS	Age	-	✓	✓	✓
	Position	✓	✓	✓	
SRG	Age	-			
	Position	✓			

From the statistical analyses, Equation 5.9 was developed and can be used to estimate 7- through 28-day compressive and tensile strength of strength in 4 x 6 in. and 6 x 6 in. cores, LS, and SRG cores from the top and bottom of a 14 in. slab. The coefficients to be used in model M-9 are provided in Table 5.9. The model indicates that using LS aggregate in lieu of SRG aggregate significantly increases the strength of 4 in. cores by 17–27% for compressive and tensile strength, respectively. The effects of aggregate type on the compressive and tensile strength of 6 in. cores are very small, increasing strength only by 1–3% on average. Explanations for effects of aggregate type on the strength of 4 in. cores are provided in the discussion chapter. The model also indicates LS cores cut from the bottom exhibit 30% higher compressive strength, but not higher tensile strength on average. Recall, however, that the additional analysis revealed that top-bottom strength differentials were present only in the LS specimens, in general. SSII will readdress this effect with more precision through a more in-depth experimental plan as shown in Chapter 7. Data, p-values for variables, and r^2 values associated with this equation can be found in Appendices C-11 – C-13.

strength = int +agg + pos + A * age (Eq 5.9)

where

strength	=	tensile or compressive strength, ksi
int	=	the base strength value; intercept of the equation, ksi
agg	=	type of aggregate used in the sample, LS or SRG
position	=	vertical location of the sample in a 14-in. slab, top or bottom
age	=	age of concrete between 7 and 28 days, days

Table 5.9 Coefficients To Be Used with Equation 5.9

Variable	(description)	Compressive Tests		Tensile Tests	
		4 in.	6 in.	4 in.	6 in.
int	intercept	3.3323	3.093	0.377	0.4397
agg	LS	0.577	0.1353	0.1039	0.0069
	SRG	0	0	0	0
pos	bottom	1.2535	0.7921	0.0321	-0.0139
	top	0	0	0	0
A	age	-	0.026	0.0022	0.0013

5.6.2 Effects of Time Exposed, Evaporation Rate, and Water Loss

Because the vertical strength differential of LS cores is attributed to the higher evaporation rates experienced by the section, additional models are provided in terms of evaporation rate, time exposed without a curing compound, and water loss during the time without a compound. This is done because the significance in position was not caused by aggregate type, but presumably by these factors. Additionally, the model would be in terms of more commonly utilized variables, namely, water loss.

5.6.2.1 Background

Construction schedules show that the LS section of the slab was placed at 12:50 p.m. and the SRG section at 1:50 p.m., with the curing compound being applied at 3:50 p.m. (March 1, 1999: El Paso, Texas). Thus, the LS specimens were without a curing compound for an hour more than the SRG specimens, resulting in possible increased moisture loss from the surface of the slab and lowered strength.

To determine the evaporation rates experienced by the slab from placement time until application of the curing compound, climatic and concrete data for that time period was required. The weather station that was in place to provide this data began readings 24 hours after the placement of the concrete and thus could not provide data. Instead, required climatic data was obtained from the National Climatic Data Center (NCDC) database Web site for the appropriate time and date in El Paso, Texas (NCDC 1999). Because NCDC data was provided hourly, evaporation rates were calculated hourly (Table 5.10). The concrete temperatures for the LS and SRG batches at time of placement were recorded as 70 °F and 72 °F, respectively. To estimate the increase in concrete temperature for each batch until application of the curing compound, comparisons were made to a similar tining investigation in Austin, Texas, with comparable ambient temperature, relative humidity, and wind speed (Rochefort 2000). The italicized values in the Table 5.10 below represent these estimated temperatures. Evaporation rates were calculated using the following equations (Grater 1997):

$$E = 0.0638 *(e_c - RH * e_o /100) * (0.253 + 0.0960 * WS)$$

where

e_c = $0.611 * e^{\{9.694*(Tc-32) / [(Tc-32)/1.8+237.3]\}}$
e_0 = $0.611 * e^{\{9.694*(Ta-32) / [(Ta-32)/1.8+237.3]\}}$
E = Evaporation rate, $lb/ft^2/hr$
RH = Relative humidity, percent
WS = Wind speed, mph
T_c = Concrete temperature, °F
T_a = Ambient temperature, °F

Table 5.10 Parameters Used for Evaporation Rate Calculations

Climatic Parameters					Batch Parameters					
Hour index	Dry Bulb Temp (F)	Rel Humidity (%)	Wind Speed (KT)	e_o	Batch 1 Concrete Temp (F)	Batch 1 e_c	Batch 1 Evap. (psf/hr)	Batch 2 Concrete Temp (F)	Batch 2 e_c	Batch 2 Evap. (psf/hr)
0	73.9	17	12	2.86	70	2.50	0.203	-	-	-
1	75.9	16	9	3.05	***82***	3.73	0.258	72	2.68	0.113
2	79	14	21	3.38	***78.5***	3.33	0.469	***84***	3.98	0.157
3	80	13	11	3.50	***87.5***	4.45	0.374	***80.5***	3.55	0.168

Figure 5.16 shows evaporation rates for each batch as a function of time after concrete placement, ending at the time of curing compound application. Integrating under the curves indicates a water loss of 1.331 lb/ft^2 and 0.438 lb/ft^2 for the LS and SRG batches, respectively. Thus, the LS batch underwent approximately three times as much evaporation as the SRG. This supports the previous hypothesis that a vertical strength profile was present only in LS due to higher evaporation rates.

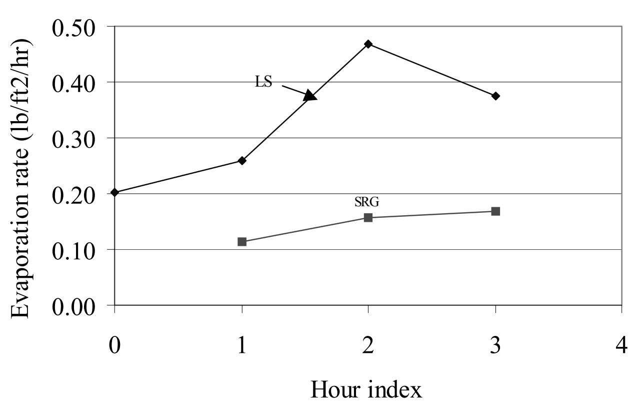

Figure 5.16 Evaporation Rates Prior to Placement of Curing Compound

5.6.2.2 Analysis Constraints

To obtain relevant ANOVA results concerning environmental effects, it was required that the aggregate variable be excluded. This is because the variance in aggregate type corresponds exactly with the variance in evaporation rate and/or variance in time exposed. In reality, each core has its own individual placement time. However, only one casting time was recorded for the placement of the entire LS batch and one time for the placement of the entire SRG batch. Therefore, variance in placement time corresponds exactly to variance in aggregate type. If the significance of aggregate type and time exposed are determined simultaneously, all significance is incorrectly attributed to only one variable. The exclusion of aggregate type is not only necessary, but can be justified from the standpoint that other parts of this investigation showed that aggregate type does not significantly affect strength.

5.6.2.3 Overall Results

As explained in Section 5.6.2.2, significance does not vary between aggregate type, time the slab was exposed without a curing compound, and evaporation rates the pavement was exposed to prior to compound application because no individual placement times for each core exists.

Equation 5.10 can be used to determine 7- through 28-day compressive or tensile strength of 4 in. and 6 in. cores located at the top or bottom of a 14 in. slab in terms of the selected effect (time exposed, evaporation rates, or water loss experienced by the slab from placement time until application of the curing compound). Coefficients for model Equation. 5.10 can be found in Table 5.11.

$$\text{strength} = \text{int} + A^{*}\,\text{age} + \text{eff} + \text{pos1} + \text{pos2} \qquad \text{(Eq. 5.10)}$$

where

strength	=	compressive or tensile strength, ksi
int	=	intercept of equation; base strength, ksi
A	=	coefficient for age
Age	=	time elapsed from placement to testing up to 28 days, days
eff	=	effect being considered: hours elapsed from time of placement to application of curing compound, cumulative evaporation rate until time curing compound application or cumulative water loss experienced by the core until time curing compound application
pos1	=	position of the sample in the slab, top or bottom
pos2	=	interaction between the position of the sample and selected effect

Table 5.11 Coefficients To Be Used with model Equation 5.10

Variable	Description	Effects of Time				Effects of Evaporation Rate				Effects of Water Loss			
		Compressive		Tensile		Compressive		Tensile		Compressive		Tensile	
		4"	6"	4"	6"	4"	6"	4"	6"	4"	6"	4"	6"
int	intercept	2.178	2.822	0.2642	0.426	3.0952	3.0373	0.3698	0.4369	3.0952	3.0373	0.3698	0.4369
A	age	-	0.0259	0.0022	0.0013	-	0.0259	0.0022	0.0013	-	0.0259	0.0022	0.0013
eff	effect	0.5770	0.1352	0.0665	0.0069	0.798	0.1873	0.0921	0.0096	0.798	0.1873	0.0921	0.0096
pos1	bottom	1.2535	0.7921	-0.1477	-0.0139	1.2535	0.7921	-0.0346	-0.0139	1.2535	0.7921	-0.0346	-0.0139
	top	0	0	0	0	0	0	0	0	0	0	0	0
pos2	bottom	0	0	0.0321	0	0	0	0.0986	0	0	0	0.0986	0
	top	0	0	0	0	0	0	0	0	0	0	0	0

5.7 AGGREGATE TYPE

Most analysis results indicate that neither compressive nor tensile strength are significantly affected by aggregate type. Analyses that showed otherwise indicated significance only in 4 in. cores. These results shall be discussed in greater detail in Chapter 7.

5.8 AGE

No tests showed strength to decrease significantly with age. Analyses either showed strength to be independent of age or to increase with age.

5.9 SUMMARY

For the ages, sizes, and other factors specified for each investigation, the following observations are made:

- The use of 4 in. diameter cores in lieu of 6 in. diameter cores increases both tensile and compressive strength. Compressive strength was found to be 6–10% higher for 4 in. cores than 6 in. cores, with length to diameter (L/D) held constant at 2.0. Tensile strength was found to be 10–15% stronger for the smaller cores. Additionally, at the same sampling rate, the use of 4 in. cores is unreliable because of the high variability of small specimens.
- Water-cured cylinders overestimate in situ compressive strength, but provide a good estimate of in situ tensile strength. Sand-cured cylinders underestimate in situ tensile strength, but provide good estimates of in situ compressive strength. Either curing method can be used to predict in situ compressive or tensile strength using the strength prediction equations included in the following section (*Strength Relationships*).
- The equations provided below have correlated closely with our data and are believed to be good estimates of strength.

$$f_r = 2.3\, f_c^{2/3}$$
$$f_t = 1.7\, f_c^{2/3}$$
$$f_t = 0.74\, f_r$$

where

f_r = tensile strength, psi
f_r = flexural strength, psi
f_t = compressive strength, psi

- The presence of steel in a sample has no effect on tensile strength so long as the steel is not in the plane of failure of the sample. Thus, reliable tensile strength can by obtained from cores containing reinforcement. However, reinforcement may significantly increase compressive strength.
- There is no significant difference in compressive or tensile strength between SRG and LS specimens so long as aggregates are chosen such that the core diameter to average aggregate diameter ratio, D/d, is greater than or equal to 3.

- The application of a curing compound significantly increased the compressive strength of specimens, but not tensile strength. Tining did not significantly affect either compressive or tensile strength.
- The effects of age are as expected, both tensile and compressive strength generally increased with age. If that was not the case, it may be because the analysis compares 7-day and 28-day strengths, where large strength differentials are not anticipated because of the high-early strength of the concrete.
- The strength of cores increases with depth when high evaporation was experienced by the pavement; i.e., the top was weaker. Where minimal evaporation was experienced, i.e., the SRG slab, no strength differential with depth was exhibited.

6. Small Slab I Nondestructive Results and Analyses

This chapter presents the results of the use of seismic equipment tests used to determine the influence of selected variables on Young's modulus. Results are compared to moduli obtained from mechanical tests and to strength results. In general, results from the nondestructive testing (NDT) produced more intuitive results than the results from the destructive tests (DT). Additionally, moduli from DT are lower than those estimated from seismic equipment. In this study, two seismic tests were used to estimate Young's modulus: the Free-Free Resonant Column method (RF) was used on molded specimens and cores, and the Portable Seismic Pavement Analyzer (PSPA) was used on the slab. The effects of aggregate type are not discussed as it is known that seismic tests are sensitive to aggregate type. When necessary, analyses are separated to account for this effect.

6.1 NONDESTRUCTIVE DETERMINATION OF SEISMIC MODULUS

If the development of Young's modulus determined that using seismic equipment is going to be included in specifications as an indirect way of estimating concrete strength gain, it is important to assess which effects of commonly occurring field conditions significantly affect measurements. The variables selected for NDT analyses correspond to those used in the DT analyses. Knowing the effects on moduli of the presence of reinforcement in a core and vertical position in a slab is beneficial for researchers to know which specimens should be used to calibrate seismic equipment to reflect in situ conditions. Ultimately, the use of seismic equipment should not involve cores, as this defeats the purpose of nondestructive testing. Thus, this section discusses results of variables that can affect modulus prediction, whether a core, cylinder, or slab.

6.1.1 Cylinder Curing Method Using Resonant Frequency

The first analysis was to compare moduli of cores, and water/sand-cured cylinders and water-cured beams. Because moduli were determined at 1, 3, 7, 14, and 28 days for the 4 in. cores, but only at 7 and 28 days for 6 in. cores, 4 in. cores were used for comparisons to cylinders rather than restricting the analysis only to 7- and 28-day specimens that would ensure geometric compatibility (6 x 12 in. versus 6 x 12 in., Table D.1). A separate analysis of variance (ANOVA) demonstrated that the difference in moduli between 4 in. and 6 in. diameter cores was not significant, warranting the use of 4 in. cores in this analysis (Table D.2). The use of 4 in. cores rather than 6 in. cores increased the sample size from twenty-four to sixty. Figure 6.1 shows that 4 in. and 6 in. samples of the same aggregate type have nearly identical moduli. A separate analysis also showed that the moduli of water-cured beams did not vary significantly from those of water-cured cylinders (r^2 = 0.9109, n = 87). Therefore, subsequent analyses to determine effects of curing on cylinders were run with moduli of cylinders and beams representing the water-cured samples (Table D.2). This showed that geometrical effects between beams and cylinders on RF tests were negligible and beams could be included in the subsequent analysis, increasing the sample size by twenty-eight specimens.

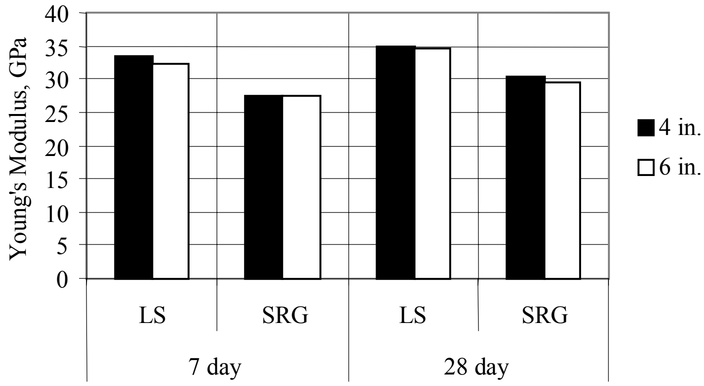

Figure 6.1 Average Moduli of 4 in. and 6 in. Diameter Cores

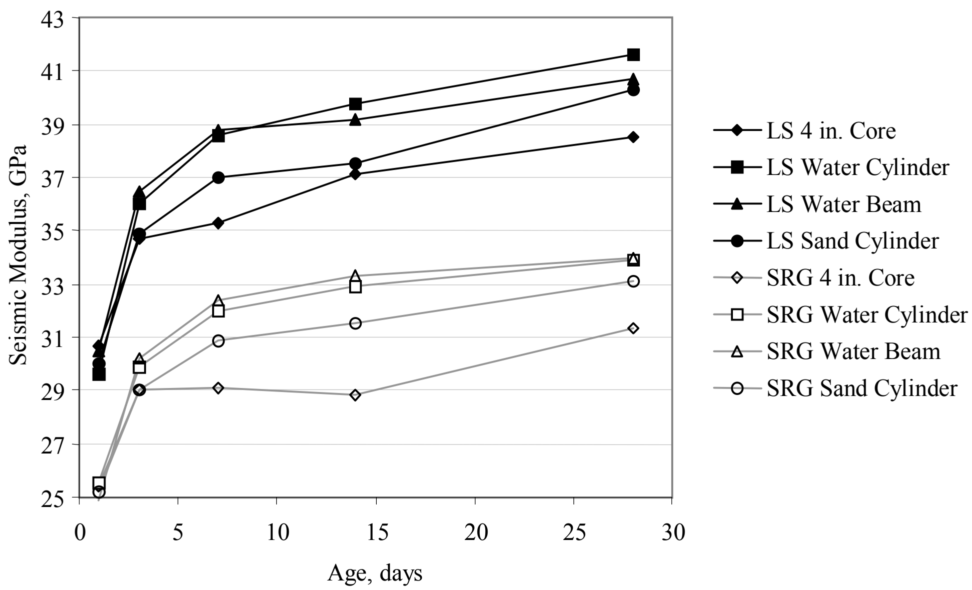

Figure 6.2 Average Moduli of Water-Cured Cylinders and Beams

Results of ANOVA comparing moduli of sand-cured cylinders, water-cured cylinders, water-cured beams, and 4 in. cores are provided in Table 6.1. Moduli are also plotted against age in Figure 6.2. Note that Figure 6.2 also shows that the moduli of water-cured cylinders and water-cured beams of the same aggregate type are nearly identical, as was discussed in the previous paragraph. Results indicate that moduli are significantly affected by all methods of curing. The water-cured specimens produced moduli that were higher by a statistically significant amount than those produced by both sand-cured cylinders and cores (Appendices D.3 and D.4). Additionally, sand-cured cylinders yielded moduli that were significantly higher than those of cores.

Equation 6.1 can be used to estimate the moduli of water-cured beams, water-cured cylinders, sand-cured cylinders and cores up to 28 days after casting for both LS and SRG samples. Resulting from the wide variety in ages available for data analysis, a logarithmic regression was developed. Comparisons of water-cured samples and cores show that water-curing produces moduli that are approximately 7% higher than those produced by cores, and moduli of sand-cured cylinders are 3% lower than cores.

Table 6.1 ANOVA NDT Results of Cylinder Curing Method Effects on Moduli

Variable	Significant?		
	wtr vs cor	snd vs. cor	snd vs. wtr
Curing Method	✔	✔	✔
Age	✔	✔	✔
Aggregate Type	✔	✔	✔

$$E = 26.87 * cur * agg * age^{0.078} \quad \text{(Eq 6.1)}$$

where

E	=	Young's modulus, GPa
Cur	=	curing method used on samples
	=	0.928 for cores
	=	0.969 for sand-curing
	=	1 for water-curing (either cylinder or beam)
agg	=	aggregate type used in sample
	=	1.20 for limestone samples
	=	1 for siliceous river gravel samples
age	=	days elapsed from time of placement until testing

[1 GPa = 145 ksi]

6.1.2 Reinforcement

Resonant frequency (RF) was used to determine the effects of the number of mats of steel in a slab and the presence of steel in a specimen on Young's modulus. Four-inch cores were from the reinforced limestone (LS) slab containing both single and double mats, with half of the cores containing steel and the other half from the unreinforced LS slab (Table D.5). Figure 6.3 plots the average modulus for each sample type. Table 6.2 shows that neither the presence or amount of steel in a specimen caused a statistically significant change in modulus, similar to the results of the reinforcement analysis on tensile strength (Table D.6).

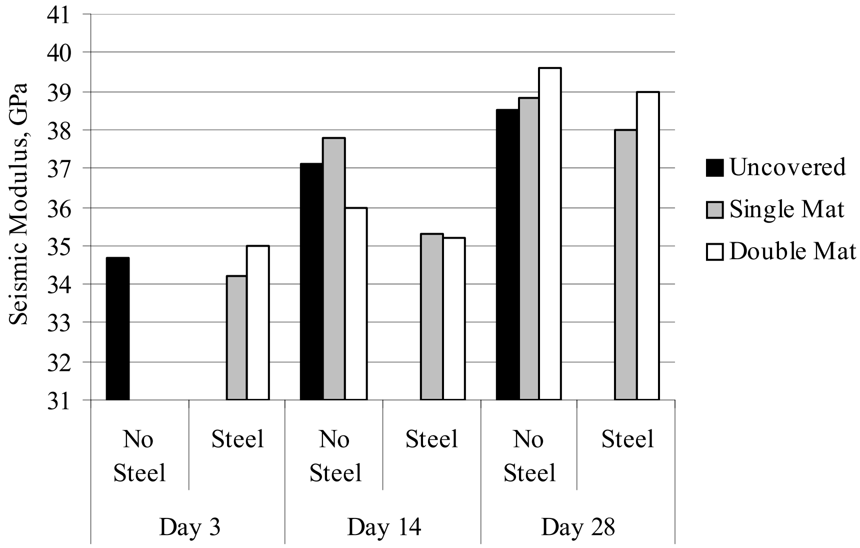

Figure 6.3 Average Moduli of Cores from Reinforced and Unreinforced Slabs

Equation 6.2 can be used to estimate the modulus of cores with steel using RF. Variables included in the analysis, except age, are nearly equal to unity. Thus, the model simply expresses the increase in modulus with age. For example, Eq. 6.2 would be multiplied by 1.0054 if double mats are used in the slab, and multiplied by 1 if no slabs are used.

Table 6.2 ANOVA NDT Results of Reinforcement Data

Variable	Significant?
Presence of steel	
Single or double mats	
Age	✓

$$E\ [\text{GPa}] = 32.4 * \text{age}^{.044} \qquad \text{(Eq 6.2)}$$

where

age = days elapsed from placement to time of testing

6.1.3 Tining and Elimination of Curing Compound

PSPA measurements were used to determine the effects of curing compound on the moduli of the LS and siliceous river gravel (SRG) slabs. Moduli were measured between 5 hours and 28 days from time of placement on slab sections with curing compound, or covered with cardboard (Table D.7). Figure 6.4 shows that LS moduli are consistently higher than SRG moduli, and analyses show this difference to be statistically significant (Table 6.3, Table D.8). Samples with a curing compound also show consistently higher moduli than samples without a compound, though the difference is statistically insignificant. Data was only obtained beginning

5 hours after placement, because the PSPA must be placed once the concrete begins hardening. Note in Figure 6.4 that like compressive strength, the modulus increases more slowly over time. Unlike compressive strength, however, research has shown that long-term modulus gain is smaller than compressive gain.

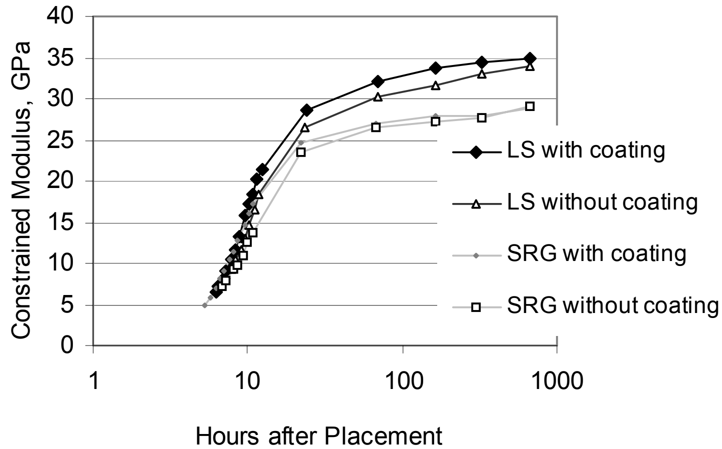

Figure 6.4 Development of In Situ Modulus from 5 Hours to 28 Days after Placement

Table 6.3 ANOVA NDT Results of Pavement Treatment Data

Variable	Significant?
Aggregate type	✓
Compound	
Age	✓

Figure 6.5 shows the average moduli of cores cut from the tined and "cardboard covered" slab sections. Figure 6.4 plotted PSPA measurements from the slab, whereas Figure 6.5 graphs actual core moduli. Figure 6.5 suggests that the modulus calculated using RF from cores is sensitive to pavement finish, though not by a statistically significant amount. Recall that PSPA measurements on the slab showed curing compound decreased compressive strength.

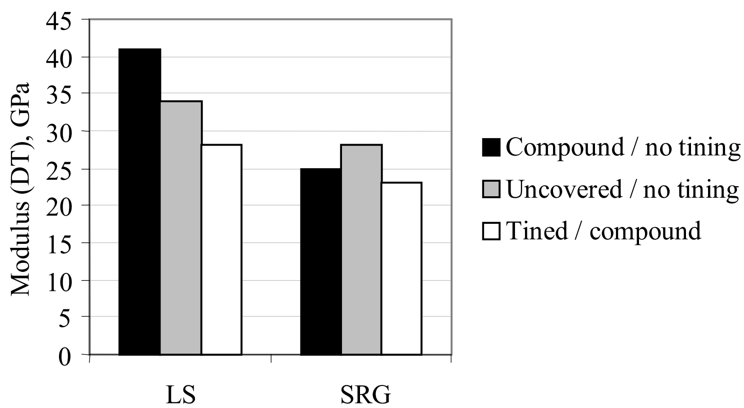

Figure 6.5 Destructive Testing Moduli of Cores from Various Slab Surface Conditions

Equation 6.3 can be used to estimate the modulus of LS and SRG concrete between 5 hours and 28 days after placement using PSPA testing. The model does not include a variable for a curing compound, as its value was unity for both presence and lack of a curing compound.

$$E\ [\text{GPa}] = 5.63 * agg * .2969 \qquad \text{(Eq 6.3)}$$

where

agg	=	type of aggregate used
	=	1.21 for LS samples
	=	1 for SRG sample
age	=	hours elapsed from time of placement to testing

[1 GPa = 145 ksi]

6.1.4 Vertical Position

To determine the effect of vertical location in the slab on cores' moduli, RF tests were conducted on 7-day, 4 in. cores (Table D.9). Results of ANOVA and a model that can be used to estimate moduli of these samples are provided in Table 6.4 and Equation 6.4 (model M.4 was derived from LS and SRG specimens analyzed simultaneously). The model is not logarithmic as specimens were only tested at one age, and thus no variable increases modulus values exponentially. Results show that cores obtained from the bottom of the LS slab exhibit significantly higher moduli than cores obtained from the top, but SRG specimens were not affected by vertical position. Those results are consistent with the results on strength and are explained by the increased evaporation rates and consequential water loss experienced by the LS (see Section 4.6.2). Again, LS cores were found to have significantly higher moduli than SRG cores. Figure 6.6 shows the increased moduli of bottom cores.

Table 6.4 ANOVA NDT Results of Position Data

Variable	Significant?		
	All	LS	SRG
Aggregate type	✓		
Position	✓	✓	

$$E\ [\text{GPa}] = 28.47 + agg + pos \qquad \text{(Eq 6.3)}$$

where

agg	=	6.84 for LS samples
		0 for SRG samples
pos	=	2.68 for samples from the bottom of the slab
		0 for samples from the top of the slab

[1 GPa = 145 ksi]

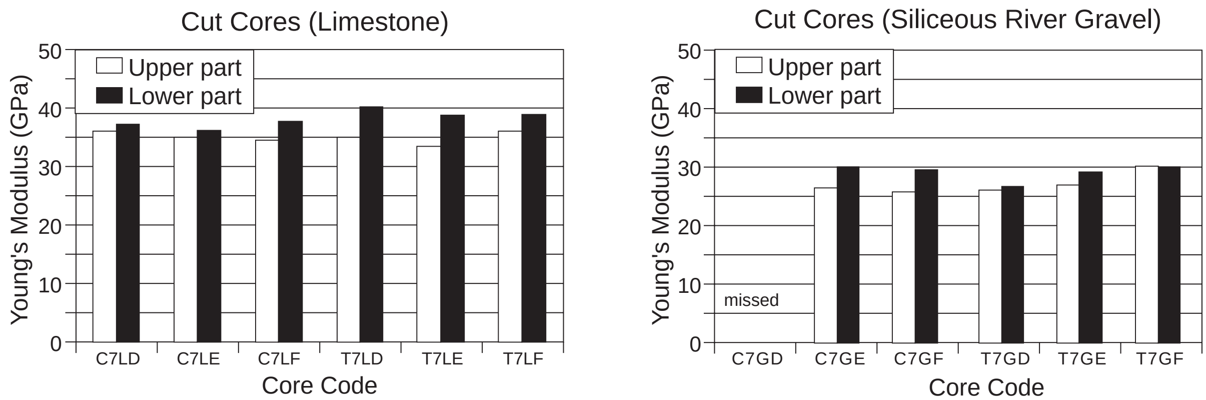

Figure 6.6 Moduli of 4 x 8 in. Cores

6.2 Seismic Test Comparison: Resonant Frequency Versus Portable Seismic Pavement Analyzer

This section compares Young's moduli obtained using the PSPA on the slab to core moduli obtained using RF. The cores tested with RF were cut from the same location where the PSPA was placed to determine if significant differences between the seismic testing methods of RF and PSPA exist. The PSPA calculations assumed a Poisson ratio of 0.2, typical for concrete, and a density of 145 pcf obtained from core averages.

Table 6.5 provides analysis results of 4 in. and 6 in. moduli determined using PSPA and RF. As shown, aggregate type, age, and testing method are all statistically significant. According to the analysis, moduli obtained from PSPA were approximately 6% lower than those obtained using RF. No statistically significant difference was exhibited between 4 in. and 6 in. cores (a 2% difference). Data and analysis results for this analysis can be found in Appendices D.10, D.11, and D.12.

Table 6.5 ANOVA Results of PSPA versus RF Testing Methods

Variable	Significant?
Aggregate	✓
Core Diameter	
Age	✓
Test Method	✓

These results do not agree with the current philosophy that the PSPA should provide higher modulus values than RF. A slab has many boundary conditions and provides an estimate of a constrained modulus, whereas the RF tests are on specimens that are freer to vibrate (unconstrained modulus), thereby decreasing modulus values. Tables 6.7 and 6.8 clearly show that moduli were higher for 4 in. and 6 in. cores (RF) than PSPA estimates were over the locations in the slab from which cores were cut. This result disagrees with the current philosophy. Figure 6.7 also included RF and PSPA comparisons of cores from the reinforced LS slab. Statistical analyses of this data show that no significant difference between moduli determined by PSPA and RF exists. However, the low $r^2 = 0.0417$ (n=24) value indicates that these results may contain errors. Figure 6.9 plots moduli determined using RF against those determined using the PSPA. Results show that nearly all RF moduli are higher than PSPA moduli.

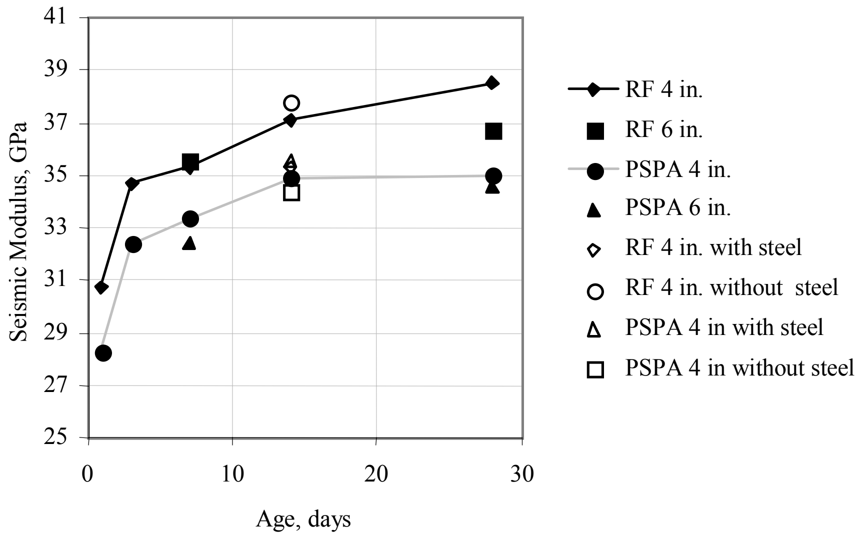

Figure 6. 7 Average Seismic Moduli of Limestone Aggregate

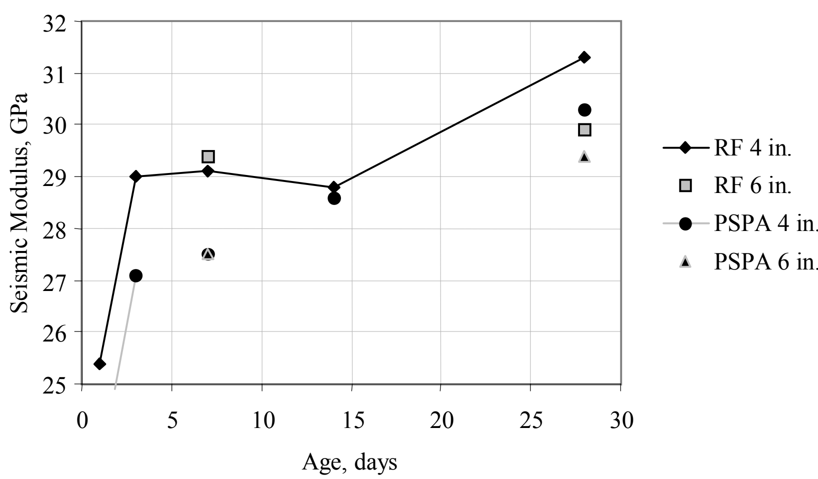

Figure 6.8 Average Seismic Moduli of Limestone Aggregate

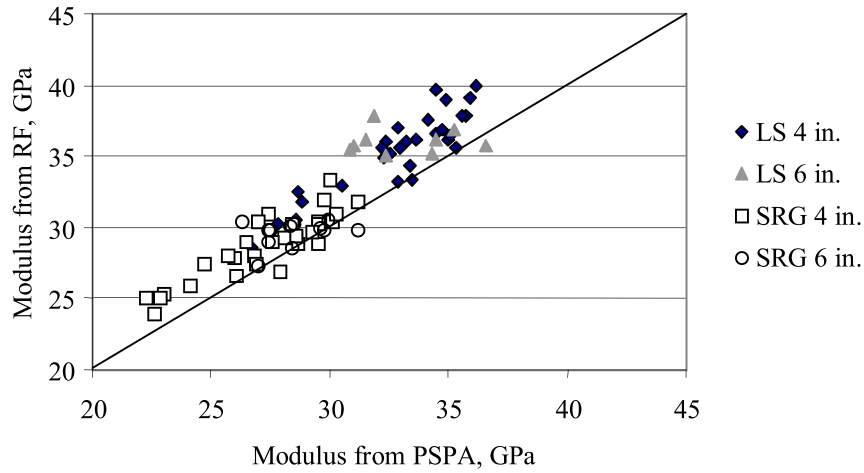

Figure 6.9 Comparison of RF and PSPA Moduli from 4 in. and 6 in. cores

6.3 SEISMIC MODULUS VERSUS MECHANICAL MODULUS

The moduli of cores and cylinders obtained using the standard mechanical elastic modulus test were consistently much lower than those moduli obtained from PSPA and RF tests. Figures 6.10 and 6.11 compare moduli obtained by NDT and DT methods of LS and SRG cylinders, respectively. Both figures clearly show that moduli obtained using RF are much higher than those using mechanical tests. This difference, however, does not preclude the use of seismic testing for future estimation of strength gain as this relationship is relative and only requires calibration. The intent of seismic equipment is ultimately for estimation of strength gain, not estimation of moduli. Figures 6.11 and 6.12 are similar to Figures 6.9 and 6.10, but compare core moduli. Again, moduli from seismic tests are greater than those predicted by mechanical tests. Figure 6.13 shows the same trend for tests of reinforced 4 in. cores.

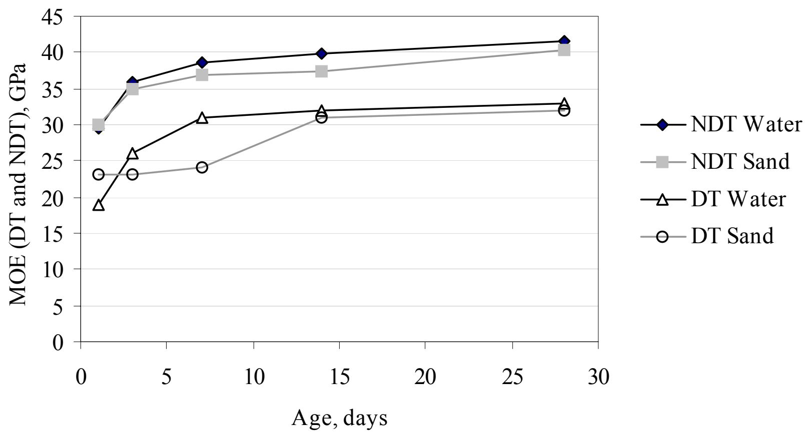

Figure 6.10 Comparison of RF and Mechanical Tests of Limestone Cylinders

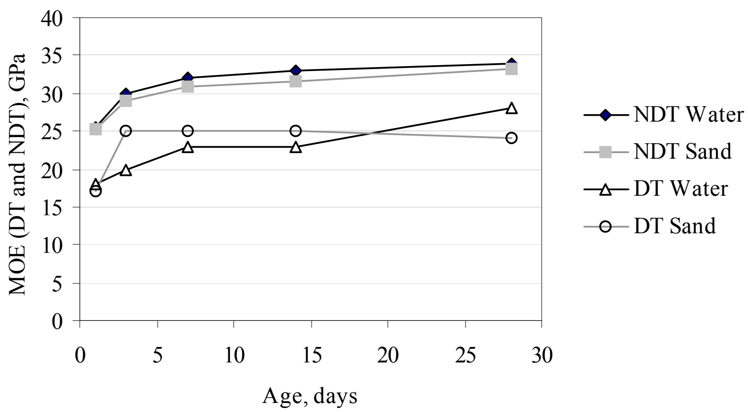

Figure 6.11 Comparison of RF and Mechanical Tests of SRG Cylinders

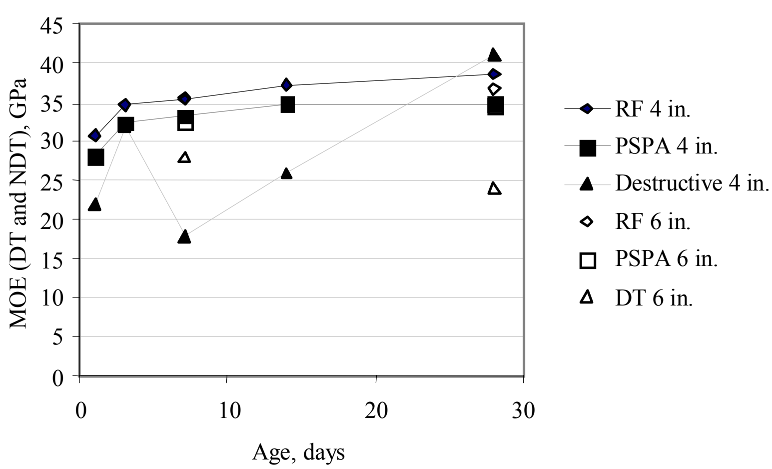

Figure 6.12 Comparison of RF, PSPA, and Mechanical Tests on LS Cores

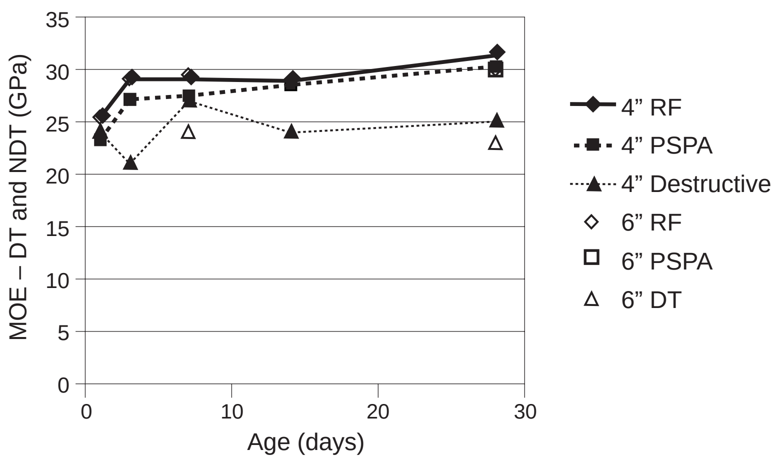

Figure 6.13 Comparison of RF, PSPA, and Mechanical Tests on SRG Cores

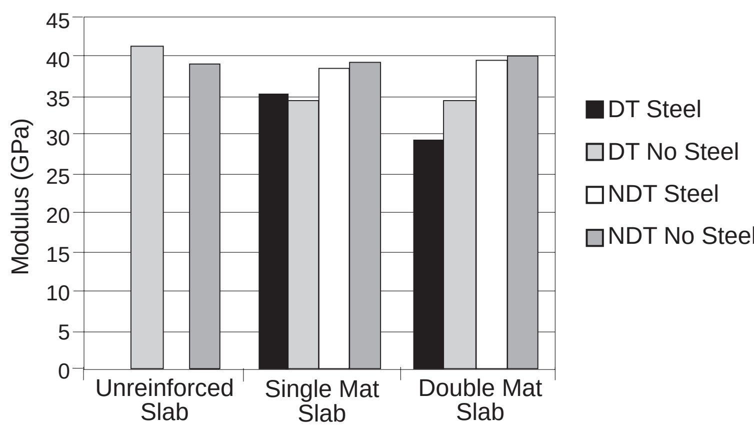

Figure 6.14 Comparison of RF and Mechanical Tests on 4 in. LS Cores w/ Steel

6.4 USE OF SEISMIC MODULUS FOR STRENGTH PREDICTION

Results from SSI demonstrate a strong correlation between strength and seismic modulus. Figures 6.15–6.21 plot the development of tensile strength and seismic modulus estimated by the PSPA for LS and SRG samples. These findings do not support the theory that early age moduli increases faster than early age strength. However, they do show that strength continues to increase at later ages and modulus does not. Both tensile and compressive strength increase more rapidly at early ages than the modulus, and continue to increase at the times when modulus development begins to level out. The figures also show that strength and modulus gain do not vary greatly between LS and SRG.

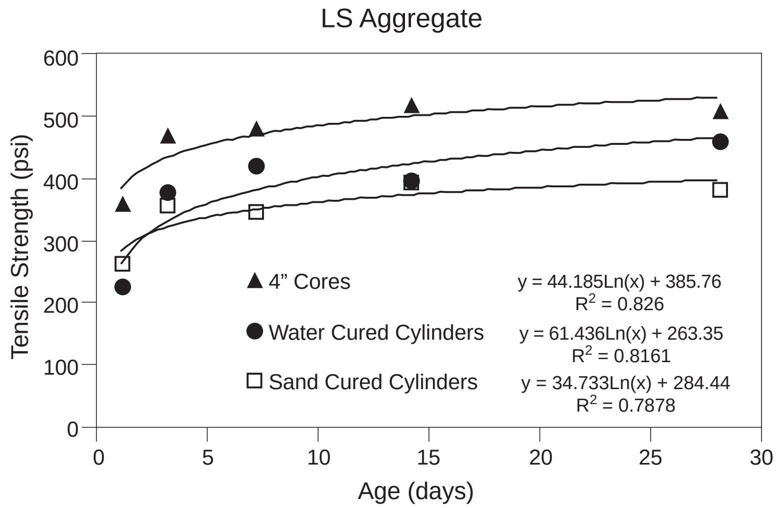

Figure 6.15 Average LS Tensile Strength Gain with Age (Yuan 2001)

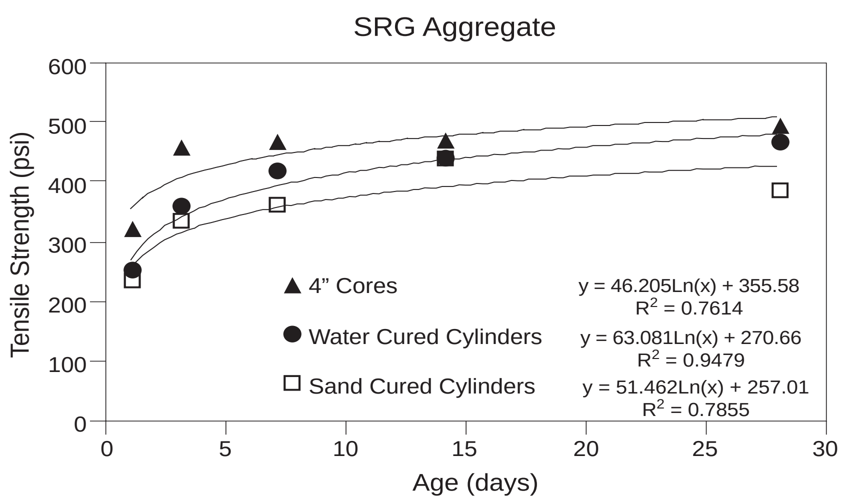

Figure 6.16 Average SRG Tensile Strength Gain with Age (Yuan 2001)

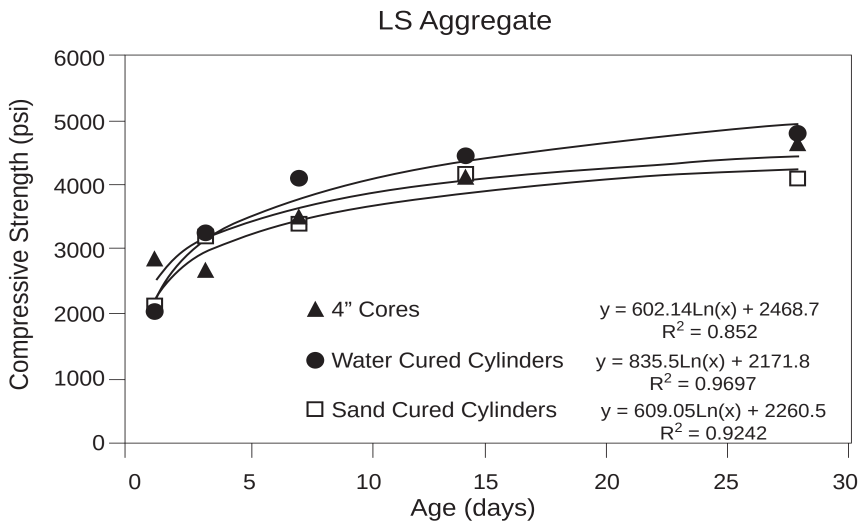

Figure 6.17 Average LS Compressive Strength Gain with Age (Yuan 2001)

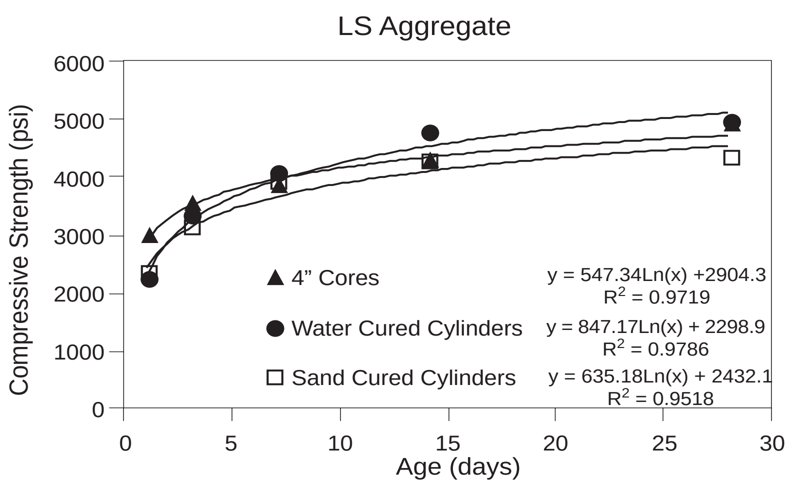

Figure 6.18 Average SRG Compressive Strength Gain with Age (Yuan 2001)

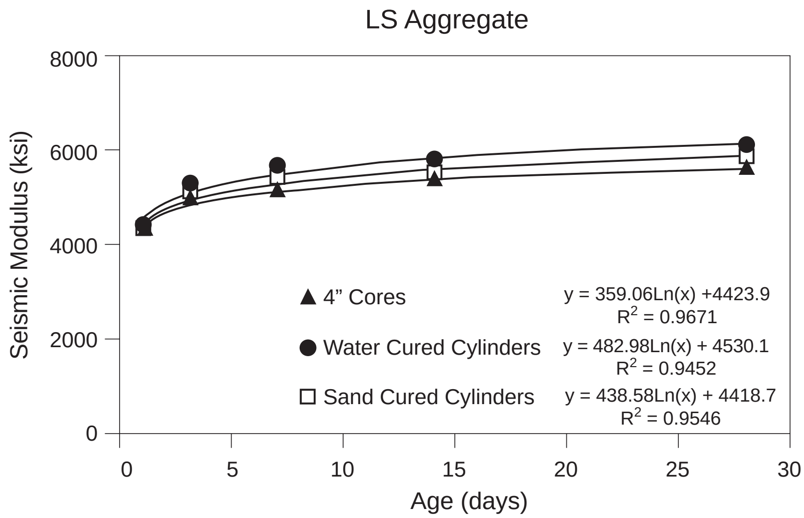

Figure 6.19 Average LS Modulus Strength Gain with Age (Yuan 2001)

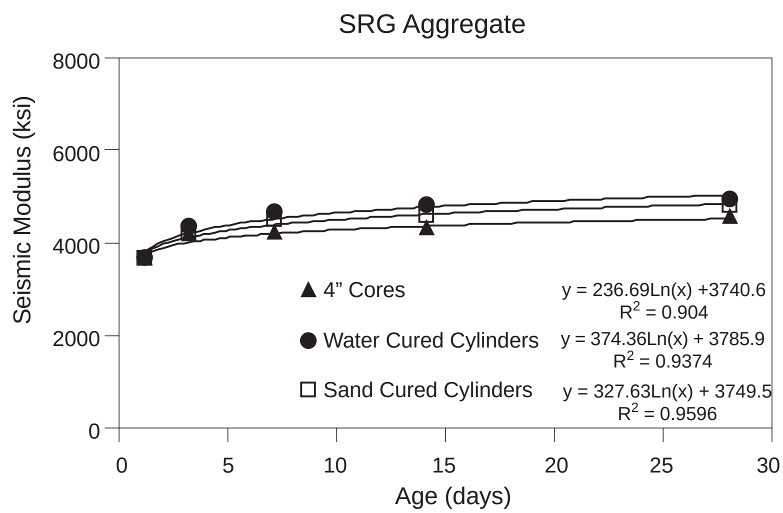

Figure 6.20 Average SRG Modulus Strength Gain with Age (Yuan 2001)

Figure 6.21–6.24 show regression lines that can be used to estimate tensile and compressive strength of LS and SRG concrete using seismic moduli obtained from PSPA. The figures show that there is a very high correlation between moduli and strength. When determining this correlation, LS and SRG samples were not be analyzed together, as concrete properties that differ between batches and may affect results (in this case density).

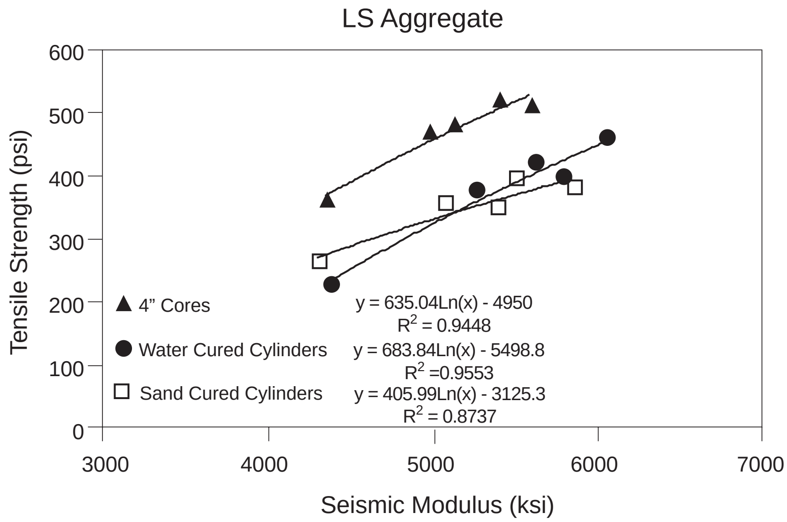

Figure 6.21 Average Tensile Strength versus Average Moduli of LS Specimens (Yuan 2001)

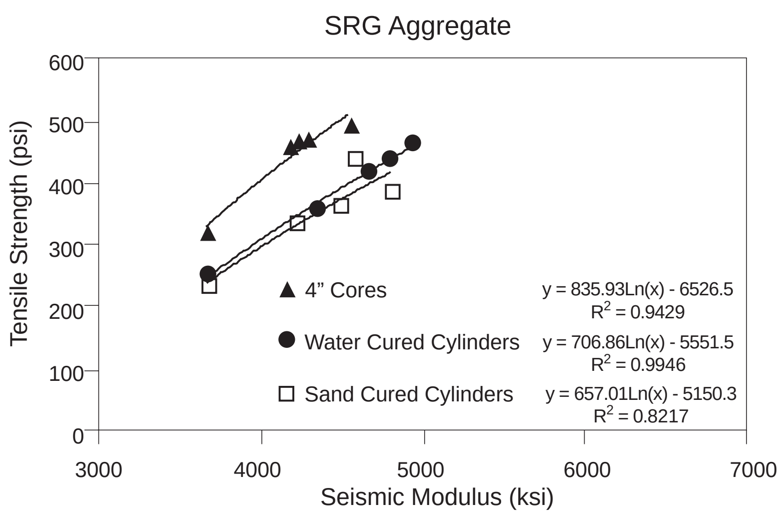

Figure 6.22 Average Tensile Strength versus Average Moduli of SRG Specimens (Yuan 2001)

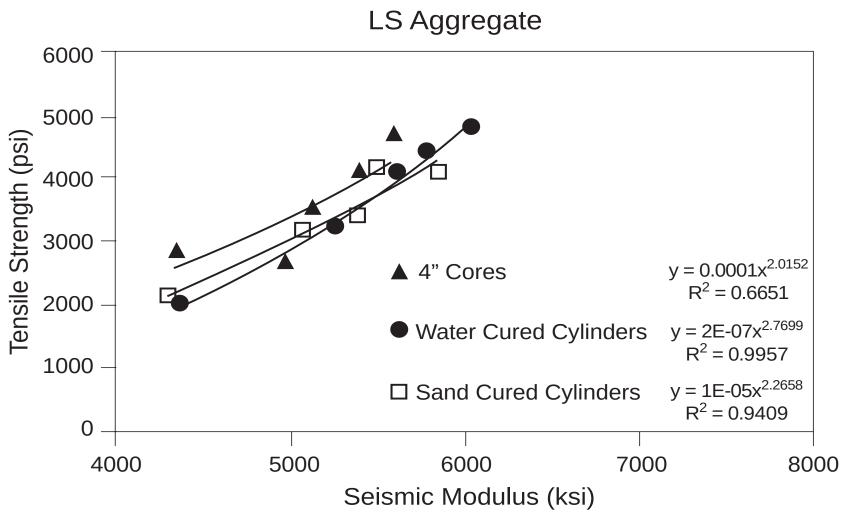

Figure 6.23 Average Compressive Strength versus Average Moduli of LS Specimens (Yuan 2001)

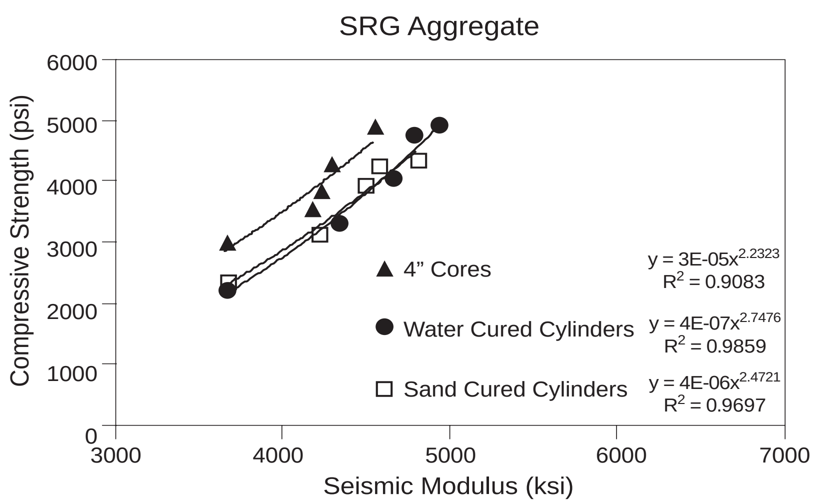

Figure 6.24 Average Compressive Strength versus Average Moduli of SRG Specimens (Yuan 2001)

Note that in all of the figures, the highest correlation between modulus and strength is always exhibited by water-cured samples. Figures 6.25 and 6.26 plot the coefficient of variation of LS and SRG cores and cylinders. These plots also show that 4 in. cores can be highly variable. Due to the destructive nature of the tests, compressive and tensile tests also exhibit high variability. However, this was significantly reduced by using water-cured samples.

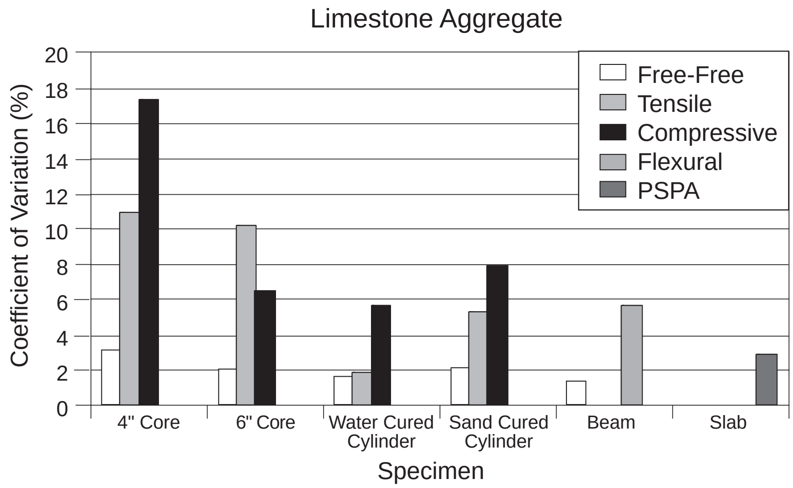

Figure 6.25 Coefficient of Variation of LS Specimen (Yuan 2001)

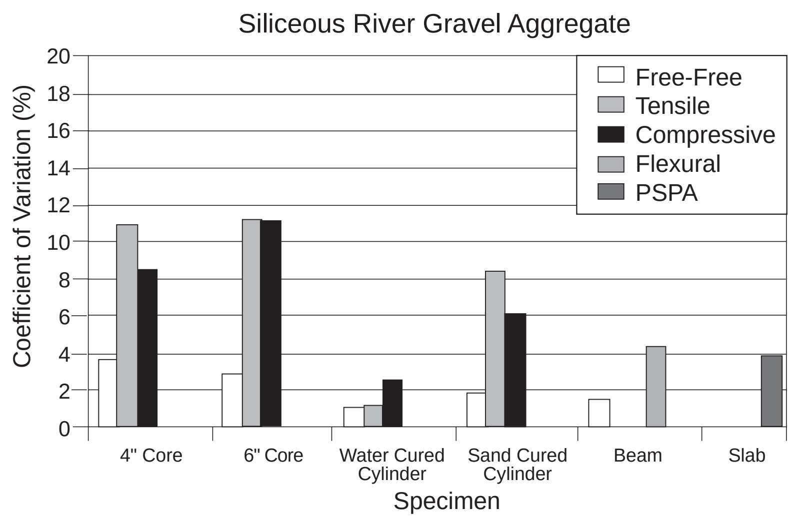

Figure 6.26 Coefficient of Variation of SRG Specimen (Yuan 2001)

7. Experimental Test Results of Small Slab Study II

In this chapter, the effects of pavement curing history on strength will be presented, in addition to the various means of obtaining temperature and moisture history in a slab.

7.1 Temperature

As discussed previously, two types of gauges were used in Small Slab Study II (SSII) to estimate maturity: the standard maturity meter utilizing a thermocouple, and the new Thermacron i-Button proposed as a possible replacement for conventional maturity meters. Prior to construction of SSII, a few tests were conducted to determine the variability and logistics of using the i-Buttons. The following two sections discuss the results of temperature data from both SSII and the earlier experiments. Chronology of the construction sequence can be found in Appendix E.

7.1.1 Small Slab II Temperature History

The data obtained from the i-Button probes was consistent with the readings obtained from the established maturity meter and yielded revealing results. As can be seen from Figures 7.1–7.3, the maturity probes, placed at mid-depth in the slab, read temperatures that were very nearly averages of the temperatures indicated by the top and bottom i-Buttons (contact with the probe in the *S* slab was lost during concrete placement). Results are very promising as the i-Buttons correlated very well with results yielded by the well-established maturity meter. As shown in Figures 7.1 and 7.2, thermocouple readings took approximately 2 to 3 days to steady, with early readings fluctuating greatly. Most likely, this is due to errors in their craftsmanship, as these fluctuations are not common. i-Buttons were not only accurate but also steady from onset of data collection.

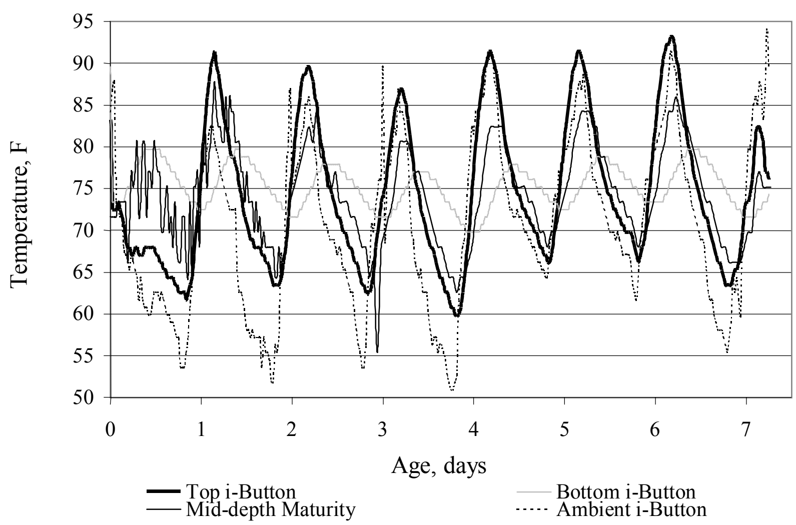

Figure 7.1 Recorded Temperatures in *No Compound* Slab

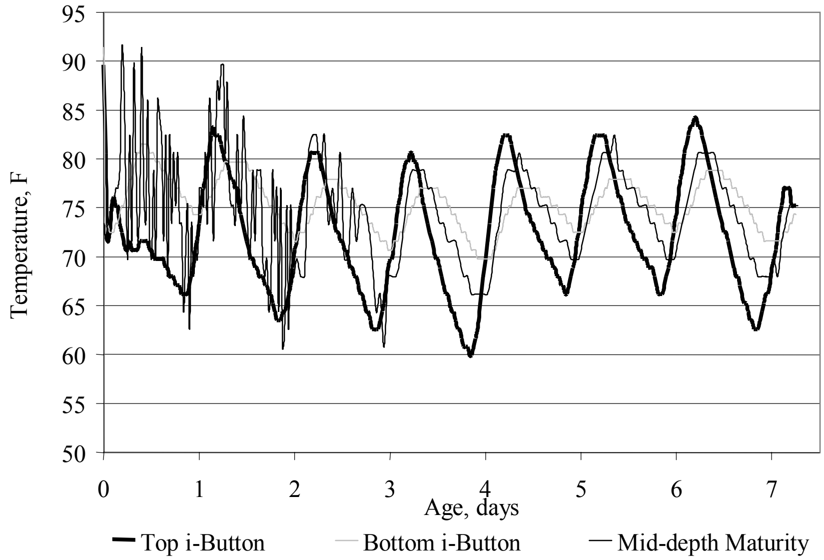

Figure 7.2 Recorded Temperatures in Slab *8*

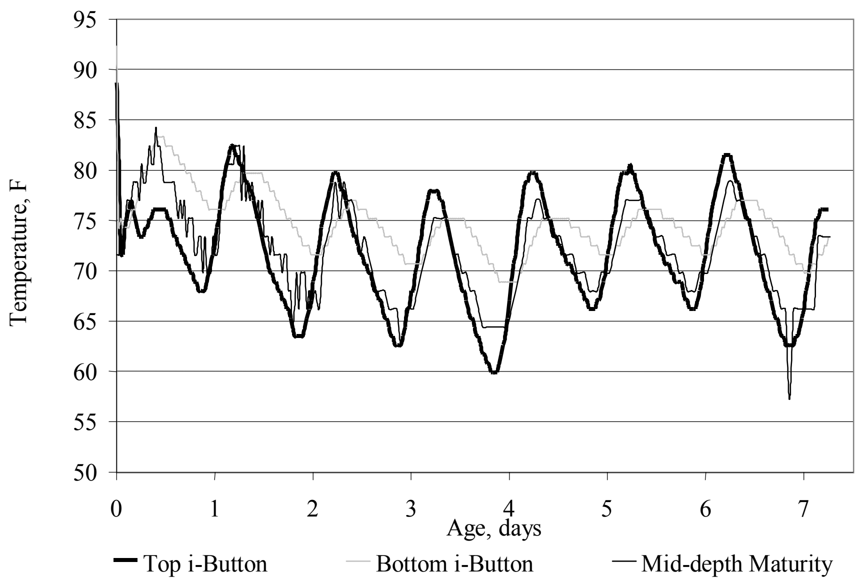

Figure 7.3 Recorded Temperatures in Slab *2*

Figure 7.1 also shows that the temperature at the top of slab *N* fluctuates much more than the temperature at the bottom. Where the bottom temperature varies between 70–80 °F (excluding day 1), the top i-Button varies between approximately 60 °F and 95 °F. Also, the temperature of the top button in slab *N* closely coincides with ambient temperatures, whereas the temperatures of the bottom buttons lag ambient temperatures. The top i-Button in slab *N* follows ambient temperatures because there is no curing compound to act as an insulator (Figure 7.4). The higher temperatures may be due to the dark gray color of the slab absorbing heat versus the white curing compound that served to reflect light. This absorption of solar heat by the top concrete causes the top i-Button to read higher daytime readings than the other slabs. Note that nighttime readings are identical between slabs. Thus, we can also see that heat absorbed from the sun is greater than the increased retention of hydration heat that the insulation of the curing compound provides. Figure 7.5 plots the temperature of the ambient i-Button against temperatures recorded by the on-site weather station and the National Climatic Data Center at the El Paso Airport. The ambient i-Button shows increased daytime temperatures, probably because of the effects of nearby light. Though the button was placed in the shade on a hollow plastic disc, the shaded area may not have been sufficient to prevent the effects of the warmer temperatures of the concrete.

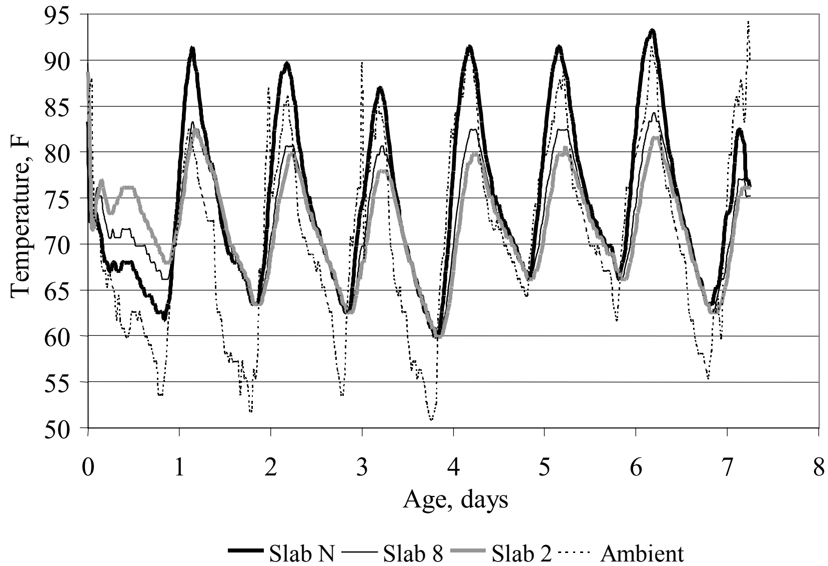

Figure 7.4 Temperatures Recorded by i-Buttons 1 Inch from Slab Surface

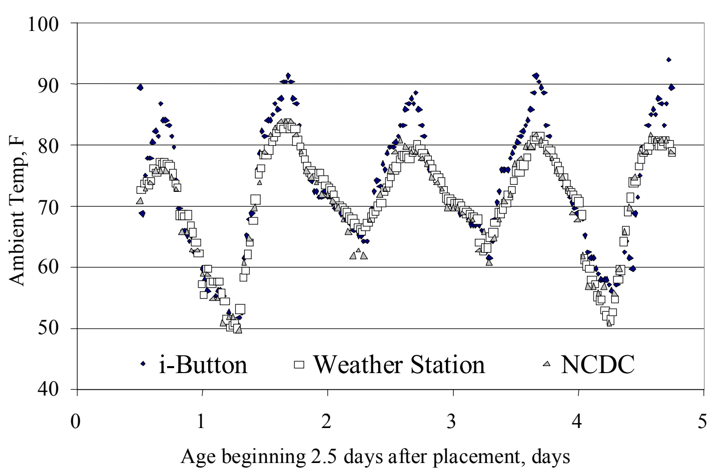

Figure 7.5 Ambient Temperatures Recorded by NCDC, Weather Station, and i-Button

Figure 7.7 shows that bottom temperatures are coolest in slab *8* during the first day from time of placement. This suggests that the cooling effects of evaporation are felt through the depth of the 14 in. slab. The figure shows that a curing compound can act as an insulator from solar heating as well as evaporation. In Figure 7.8, it can be seen that the slab with black plastic sheeting is much warmer than the other slabs. This is most likely due to the retention of increasing heat during hydration, prevention of evaporative cooling, and solar heat absorption.

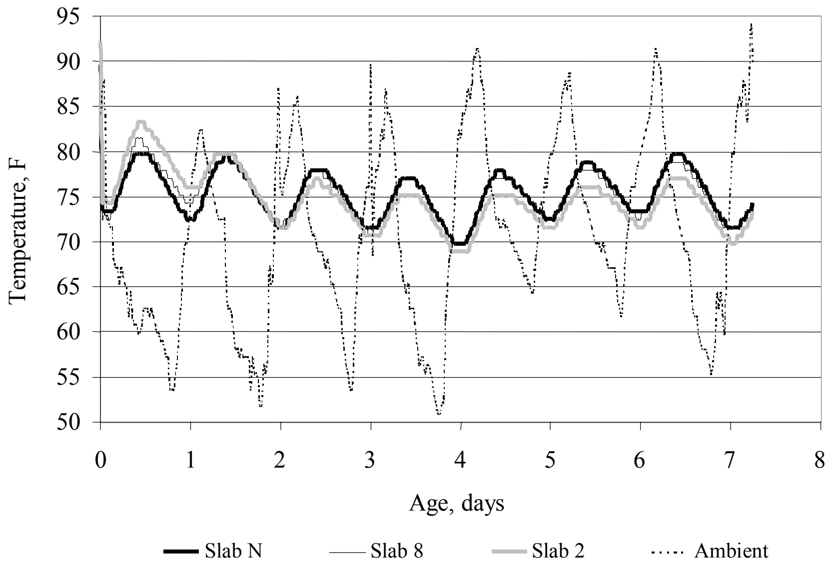

Figure 7.6 Temperatures Recorded by i-Buttons 1 Inch from Slab bottom

In Figure 7.7, we see the variability in temperature between all slabs as measured by the mid-depth maturity probes. The plot shows that the section covered by plastic was the hottest followed by sections *N*, *8*, *S*, *2,* and *O*. It is likely that the slab with plastic sheeting was hottest because the plastic retains heat from hydration, absorbs solar radiation rather than reflecting it as curing compound might, and shields the slab from wind thereby reducing evaporation and temperatures. The i-Buttons also show that the slabs with no curing compound is hotter than those with curing compound, probably due to its darker color and sensitivity to wind and evaporation.

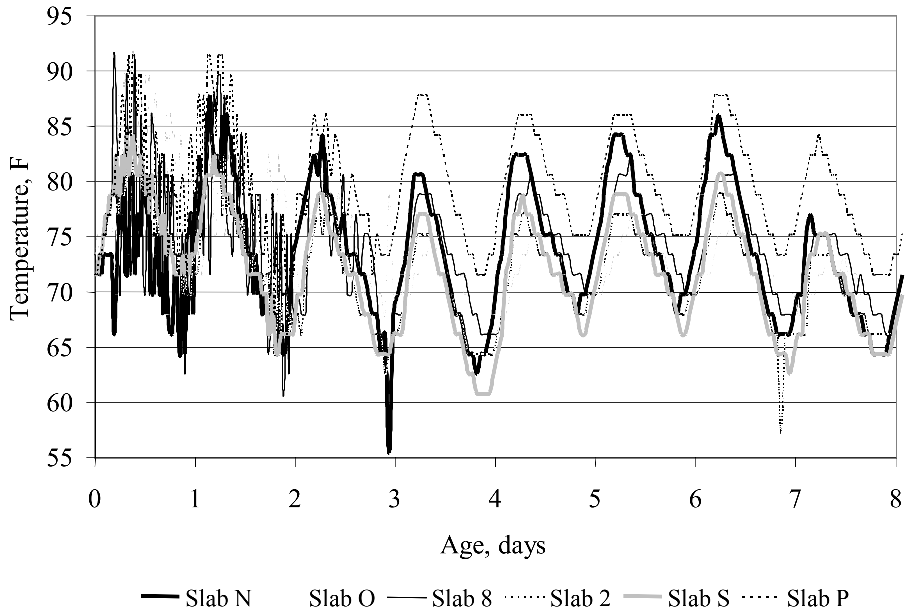

Figure 7.7 Temperatures Recorded by Thermocouples at Mid-Depth

7.1.2 Preparatory i-Button Lab Experiments

Results of the first test conducted to determine the variability between two i-Buttons are shown in Figure 7.8. Two i-Buttons were placed in a room and allowed to log continuously for 1 day. The figure shows that temperature varied by only 1 °F or less between the two buttons. The blocking seen in this and subsequent figures is due to the time increment selected for readings.

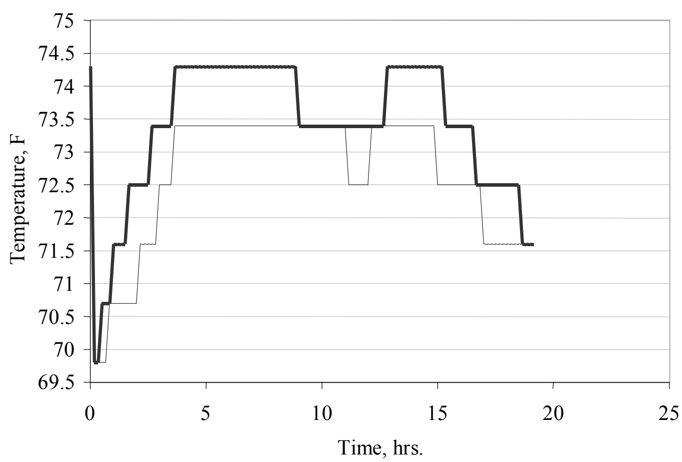

Figure 7.8 Temperatures of Two i-Buttons in Ambient Conditions

After a few unsuccessful trials, a material was found that did not deteriorate in the high-alkaline environment of concrete; epoxy. Next, it was necessary to determine the thermal effects of using epoxy. Figure 7.9 shows results of a 1 hour test in which a control button and an epoxy-coated button were moved back and forth between steam and ice-water baths. The plot shows that the epoxy button slightly exaggerates temperatures with a minimal lag time compared to the control. Again, variability in temperature between the controls was minimal. Accuracy was found to be acceptable for maturity calculations.

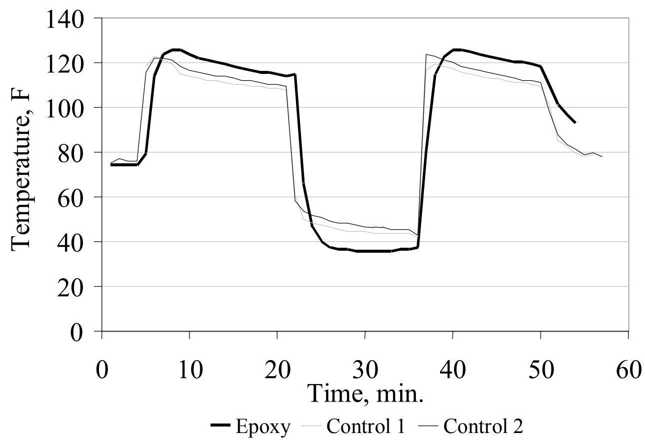

Figure 7.9 Variability in i-Buttons and Effect of Using Epoxy Casing

When testing encapsulating materials, it was also found that wax suitably protected the i-Button connection. Though it was not used in SSII because of its fragility, results comparing a control button to epoxy-covered and wax-covered i-Buttons are provided for future use. Again, only a 1 °F temperature difference was exhibited between the encased and control buttons, with the control i-Button cooling off faster, but heating up more slowly, than the encased buttons.

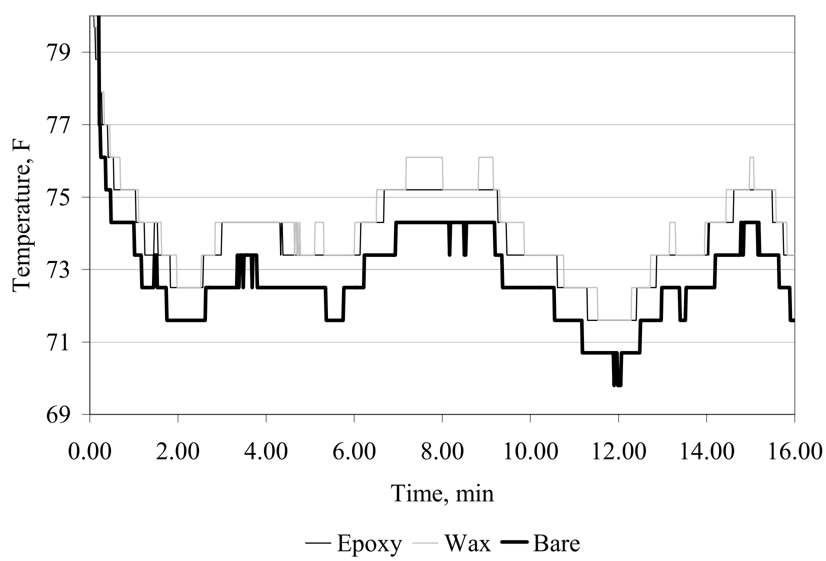

Figure 7.10 Temperature Comparisons Between Control, Waxed, and Epoxy-Encased i-Buttons

7.2 TENSILE STRENGTH RESULTS

In order to isolate the effects of a curing regime on strength, it was necessary to normalize strength data to account for temperature effects. The strength data cannot be normalized using simply the maturity index or equivalent age, because maturity continues to increase indefinitely with time though strength gain levels off. This is shown in Figure 7.11. Thus, data was normalized using strength predicted from each slab's equivalent age and the maturity curve.

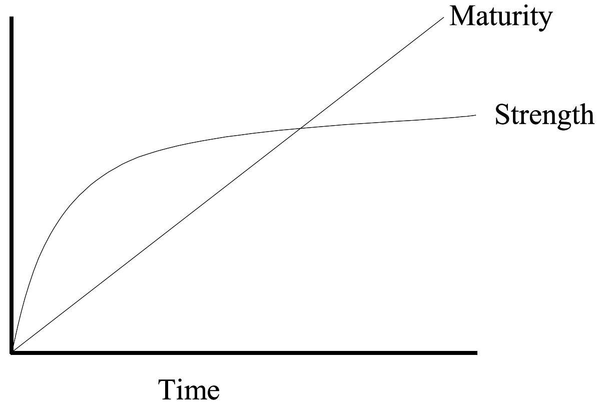

Figure 7.11 Comparison of Maturity Value to Strength Gain

Equivalent age was used for construction of the maturity curve as opposed to time-temperature factor (TTF) as this method is more precise. TTF is usually selected because of its simplicity and acceptable accuracy, though both have been adopted by the American Society for Testing and Materials. Equivalent age was determined for all i-Buttons and thermocouples so that top specimens could be normalized by equivalent age at the corresponding depth. Therefore, the tensile strength of the top and bottom disks tested in tensile strength were divided by the equivalent ages calculated by the top and bottom i-Buttons, when possible. The thermocouple values were used for normalization of mid-depth samples. Where temperature was missing because of thermocouple malfunction or no i-Button in certain locations, averages were taken. Both i-Button and thermocouple data were used for these normalizations, as measurements between the two were shown to be interchangeable.

Normalization of data for maturity is a way of analyzing strength data for the direct determination of the effects of moisture loss independent of the influence of temperature history. Figure 7.12 shows the tensile strength maturity curve calculated from water-cured cylinders along with the actual tensile strength of cores from all slabs (maturity was only calculated up to 7 days due to low 14-day strength results). The core strengths that fall above the curve have a normalized strength greater than unity, representing a specimen whose curing history has resulted in higher strengths than the water-cured beams. Most of these samples were from the bottom of the slab where moisture was presumably fairly constant. Data for construction of this curve can be found in Appendices F.1 through F.4.

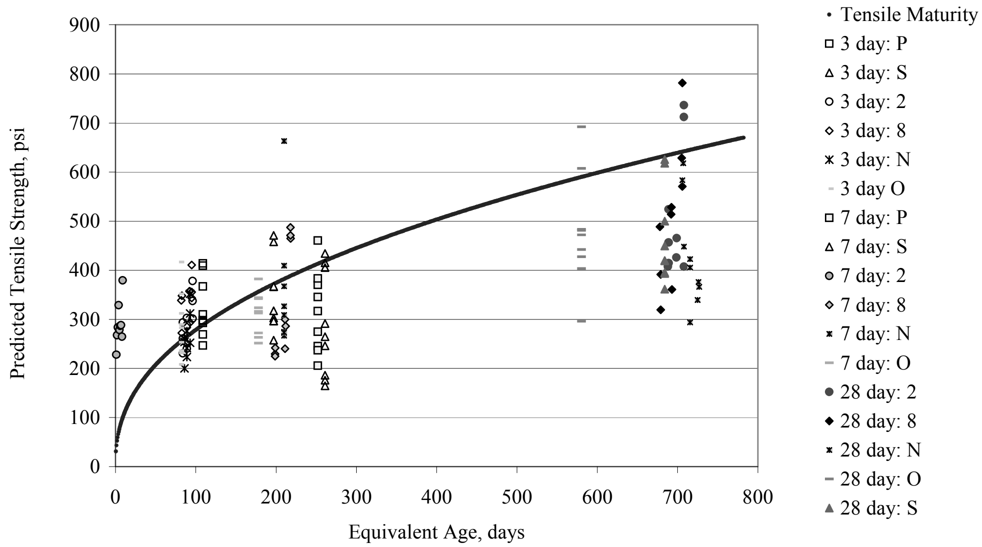

Figure 7.12 Comparison of Tensile Strength Maturity Curve to Actual Core Tensile Strength

Tensile strength results (normalized by equivalent age) show that the effects of different curing are most significant after 7 days. Figures 7.13–7.18 present the vertical tensile strength results of 7- and 28-day core tests. Comparisons are made to slab *S* in all cases, as this represents the standard cure as per the Texas Department of Transportation (TxDOT) standards. Figures 7.13 and 7.14 compare *best* case, *standard* case, and *worst* case curing scenarios from left to right. The black bars indicate normalized tensile strength of the top specimens, *w* for tests on three samples, *a*, *b,* and *c*. Most normalized values are less than unity indicating that strength was less than that exhibited by a water-cured specimen of equivalent age, which is the usual case. Comparison of normalized top strengths between sets *S* and *N* show that elimination of curing compound causes lowered strength. The low values for the plastic curing (P) are not understood due to missing 28-day data from thermocouple malfunction.

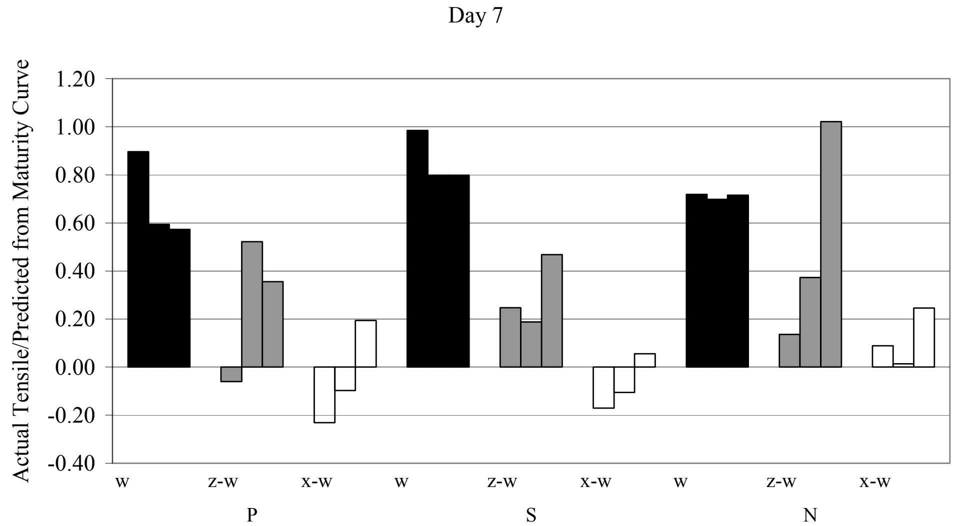

	P w	P z-w	P x-w	S w	S z-w	S x-w	N w	N z-w	N x-w
a	0.90	-0.06	-0.23	0.98	0.25	-0.17	0.72	0.14	0.09
b	0.59	0.52	-0.10	0.80	0.19	-0.11	0.70	0.37	0.01
c	0.57	0.36	0.19	0.80	0.47	0.06	0.72	1.02	0.25

(w = top, z-w = bottom – top, w – x = middle-top – top)

Figure 7.13 Normalized 7-Day Tensile Strength Comparison between Slabs *P*, *S*, and *N*

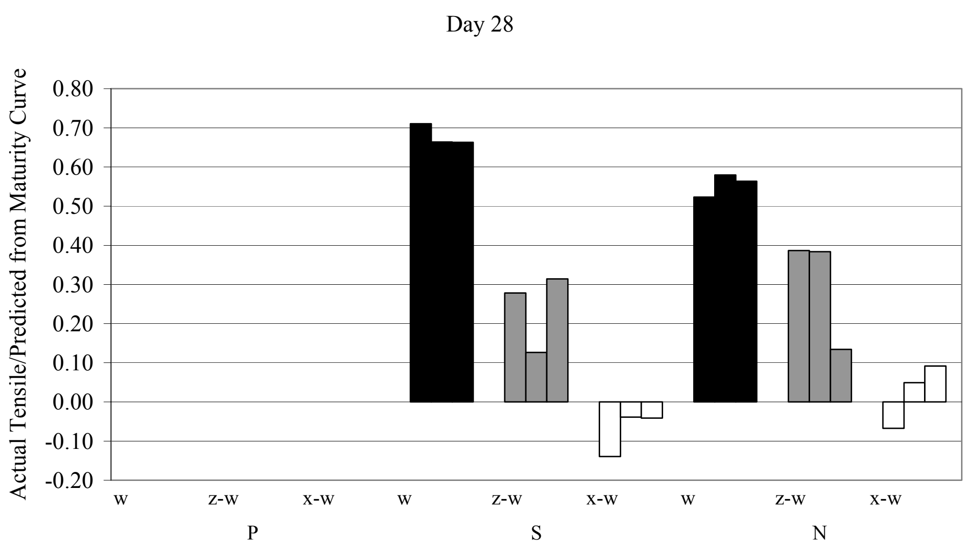

	P w	P z-w	P x-w	S w	S z-w	S x-w	N w	N z-w	N x-w
a	0.00	0.00	0.00	0.71	0.28	-0.14	0.52	0.39	-0.07
b	0.00	0.00	0.00	0.66	0.13	-0.04	0.58	0.38	0.05
c	0.00	0.00	0.00	0.66	0.31	-0.04	0.56	0.13	0.09

Figure 7.14 Normalized 28-Day Tensile Strength Comparison between Slabs *P*, *S*, and *N*

The gray plots the difference in normalized top and bottom strengths in each slab. Comparison of normalized top strengths between sets *S* and *N* show that the elimination of curing compound causes higher vertical strength differential. These results are exhibited in both 7-day and 28-day strength results.

The last set of bars, the white, plots the differences in normalized strength of the two top sections. Results indicate that strength does not vary greatly between samples and at times the top-most sample can be slightly stronger than the one just below it.

Figures 7.15 and 7.16 present the effects of delayed curing compound application on the vertical strength profile. They chart the 7- and 28-day normalized strength data of the standard slab where monomolecular film (MMF) has been applied to all slabs at sheen, and curing compound has been applied at sheen loss, and 2 and 8 hours thereafter. Results are similar to previous charts in that poor curing (delayed compound application in this case) results in lowered strength and increased vertical tensile strength differential.

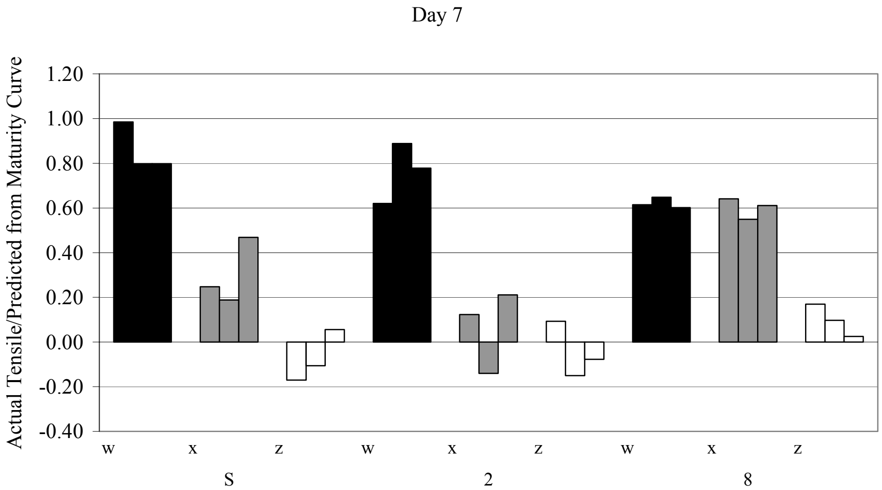

	S w	S x	S z	2 w	2 x	2 z	8 w	8 x	8 z
a	0.98	0.25	-0.17	0.62	0.12	0.09	0.61	0.64	0.17
b	0.80	0.19	-0.11	0.89	-0.14	-0.15	0.65	0.55	0.10
c	0.80	0.47	0.06	0.78	0.21	-0.08	0.60	0.61	0.02

Figure 7.15 Normalized 7-Day Tensile Strength Comparison between Slabs *S*, *2*, and *8*

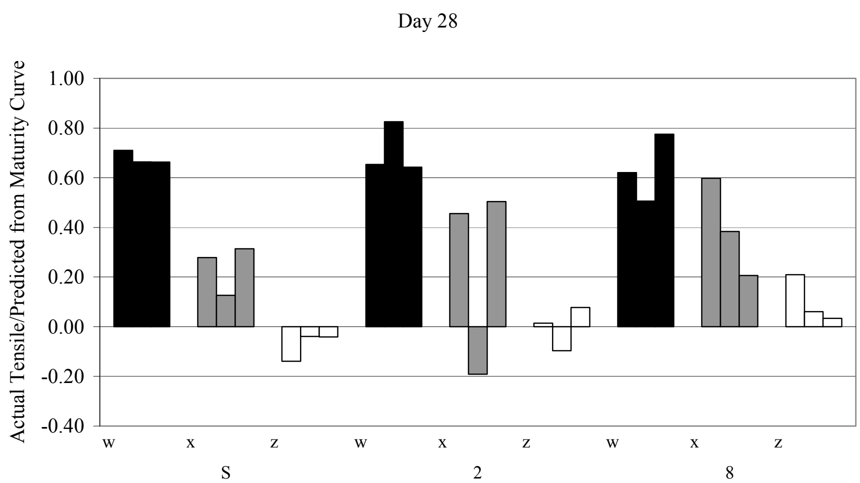

	S w	S x	S z	2 w	2 x	2 z	8 w	8 x	8 z
a	0.71	0.28	-0.14	0.65	0.46	0.01	0.62	0.60	0.21
b	0.66	0.13	-0.04	0.83	-0.19	-0.10	0.51	0.38	0.06
c	0.66	0.31	-0.04	0.64	0.50	0.08	0.78	0.21	0.03

Figure 7.16 Normalized 28-Day Tensile Strength Comparison between Slabs *S*, *2*, and *8*

The previous charts all show that after 7 days, *poor* curing leads to decreased strength and increased vertical strength differentials. The results of the 3-day tensile strength tests exhibit nearly opposite trends. As shown in Figures 7.17 and 7.18, normalized strength is higher and strength differentials are lower when no curing compound is applied, or if its application is delayed, the effects increase with delay (except for results from slab *P*). Possible explanations for these results are provided in the discussion.

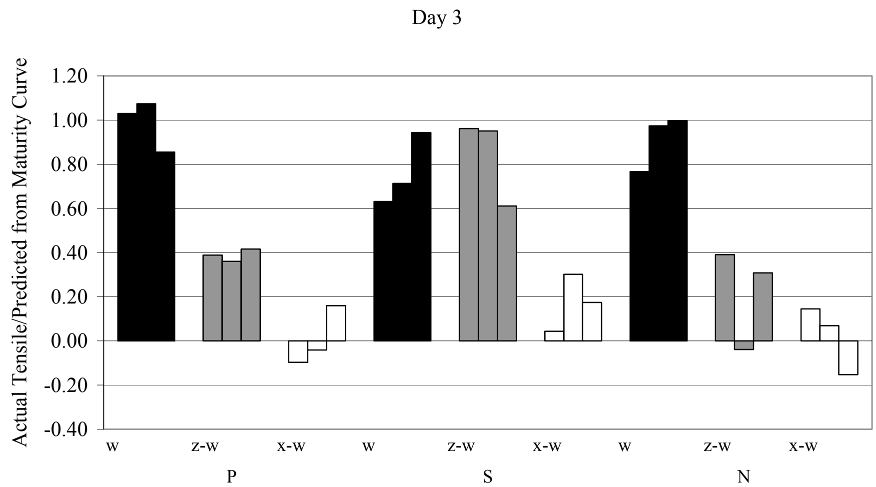

	P w	P z-w	P x-w	S w	S z-w	S x-w	N w	N z-w	N x-w
a	1.03	0.39	-0.10	0.63	0.96	0.04	0.77	0.39	0.15
b	1.07	0.36	-0.04	0.71	0.95	0.30	0.97	-0.04	0.07
c	0.85	0.42	0.16	0.94	0.61	0.17	1.00	0.31	-0.15

Figure 7.17 Normalized 3-Day Tensile Strength Comparison between Slabs *P*, *S*, and *N*

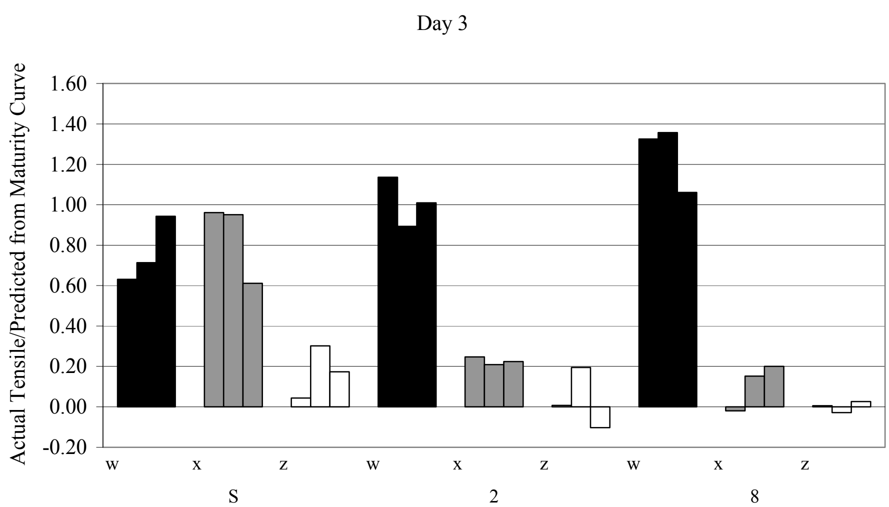

	S w	S x	S z	2 w	2 x	2 z	8 w	8 x	8 z
a	0.63	0.96	0.04	1.14	0.25	0.01	1.33	-0.02	0.01
b	0.71	0.95	0.30	0.89	0.21	0.19	1.36	0.15	-0.03
c	0.94	0.61	0.17	1.01	0.22	-0.10	1.06	0.20	0.03

Figure 7.18 Normalized 3-Day Tensile Strength Comparison between Slabs *S*, *2*, and *8*

The effects of MMF were investigated by placing curing compound at sheen loss on two slabs, one with and one without curing compound. It should be noted in interpreting results that the application of the curing compound was 1 hour after placement on the slab without MMF and 2 hours after placement for the slab with MMF. Figures 7.19–7.21 graph the normalized 3-, 7-, and 28-day tensile strength results. As no large difference is indicated between cores of each slab for 7- and 28-day results, the effects of MMF do not appear to be great. It is worth noting, however, that at early ages the vertical strength differential is very high in the slab with both MMF and curing compound.

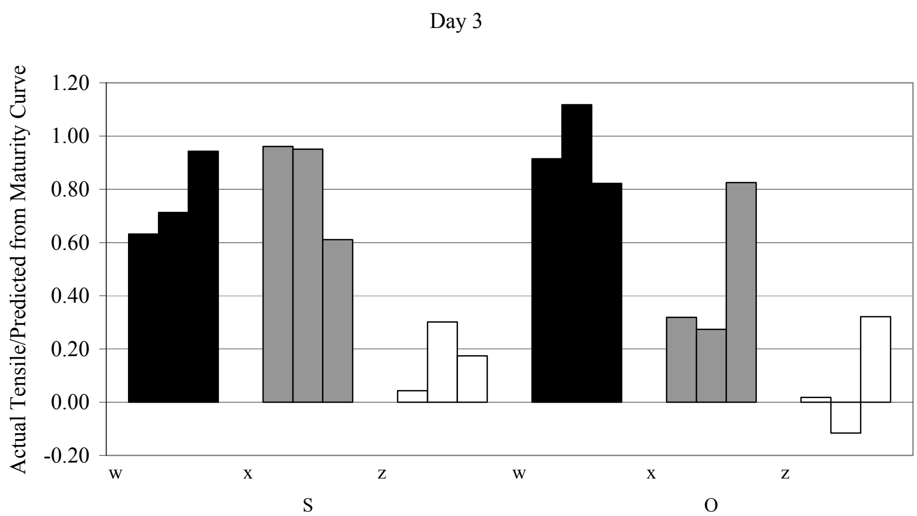

a	0.63	0.96	0.04	0.91	0.32	0.02
b	0.71	0.95	0.30	1.12	0.27	-0.12
c	0.94	0.61	0.17	0.82	0.83	0.32

Figure 7.19 Normalized 3-Day Tensile Strength Comparison between Slabs *S* and *O*

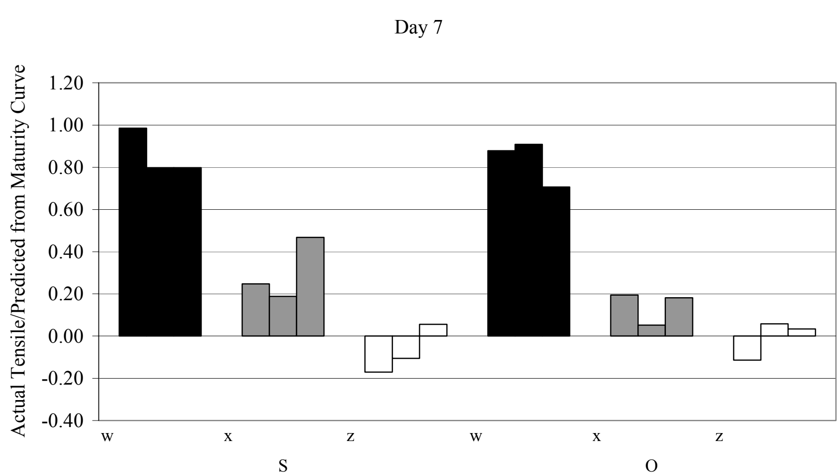

a	0.98	0.25	-0.17	0.88	0.19	-0.11
b	0.80	0.19	-0.11	0.91	0.05	0.06
c	0.80	0.47	0.06	0.71	0.18	0.03

Figure 7.20 Normalized 7-Day Tensile Strength Comparison between Slabs *S* and *O*

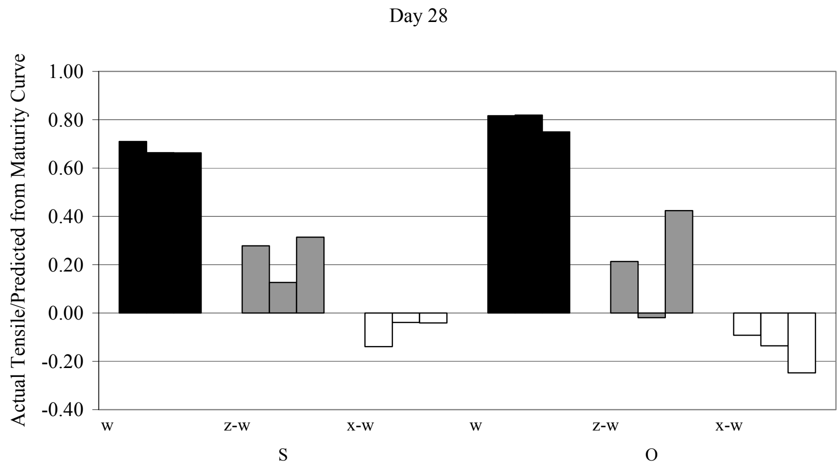

a	0.71	0.28	-0.14	0.82	0.21	-0.09
b	0.66	0.13	-0.04	0.82	-0.02	-0.14
c	0.66	0.31	-0.04	0.75	0.42	-0.25

Figure 7.21 Normalized 28-Day Tensile Strength Comparison between Slabs *S* and *O*

7.3 AQUAMETER

For additional moisture comparisons, data was obtained using the James Instruments Aquameter. The meter has been calibrated by James Instruments to predict moisture content from capacitance readings. Results from this study show that if the Aquameter is to be used accurately, strict guidelines must be followed. Results of SSII were highly variable and counter intuitive. Only when a very controlled test was conducted in the laboratory did the Aquameter perform satisfactorily. Accurate results can be obtained, but only if surfaces are very smooth and readings are taken in a consistent location; even a small amount of air or dust will affect readings. Concrete surfaces where readings are to be taken should be troweled smooth and readings should be taken in the same location for every test.

7.3.1 Small Slab Study II Results

Before SSII data could be analyzed, raw Aquameter sensor readings had to be calibrated for the design mix used. The internal calibration (*concrete mode*) built into the Aquameter was used for comparisons. To calibrate the meter, two concrete pans were weighed hourly to compare actual moisture content curves with raw Aquameter sensor readings taken on both pans at the same time. Both were 1 foot in diameter and 6 in. deep, with the empty mold weighing 6 kg (13.23 lb). Figure 7.22 shows the moisture content of the pans both open to wind and sheltered from wind calculated from scale measurements. The figure shows that, as expected, the pan sheltered from the wind experienced less water loss than the pan open to the wind.

Figure 7.23 plots these same values along with values obtained using the Aquameter. One set of readings was taken in the concrete mode where moisture content is provided based off the Aquameter's internal calibration curve. The other set of readings was taken in the calibration mode where raw sensor readings are provided and can be used to create a moisture content estimation curve calibrated for specific concrete mixes. The raw sensor readings are divided by ten so that they fit on the chart (data can be found in Table F.5). Though these raw readings are not quantitative, their inclusion shows the trend of data to increase with time. Moisture content in these charts is calculated by wet weight: weight of water divided by weight of water and weight of materials. The initial amount of water in each pan is estimated as the percent of water in the batch by weight multiplied by the weight of the sample.

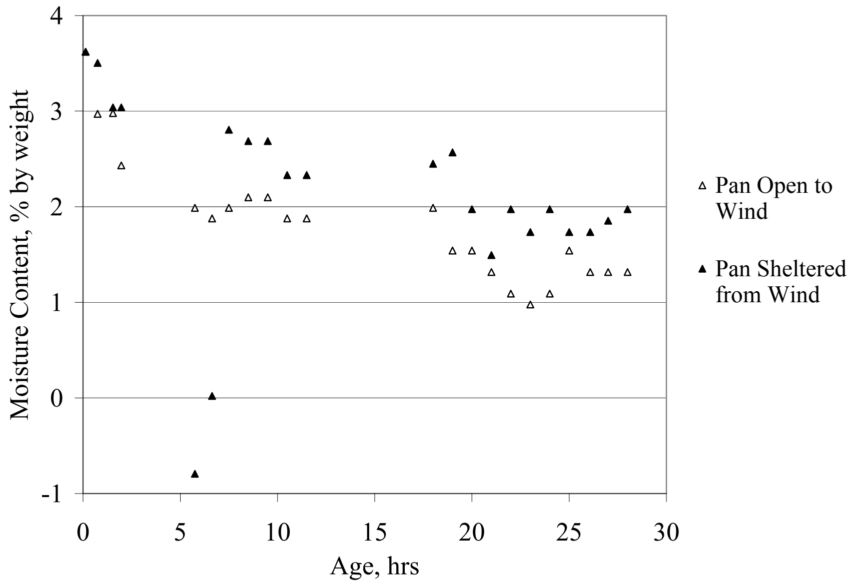

Figure 7.22 SSI Pan Wet Weight Moisture Content from Scale Measurements

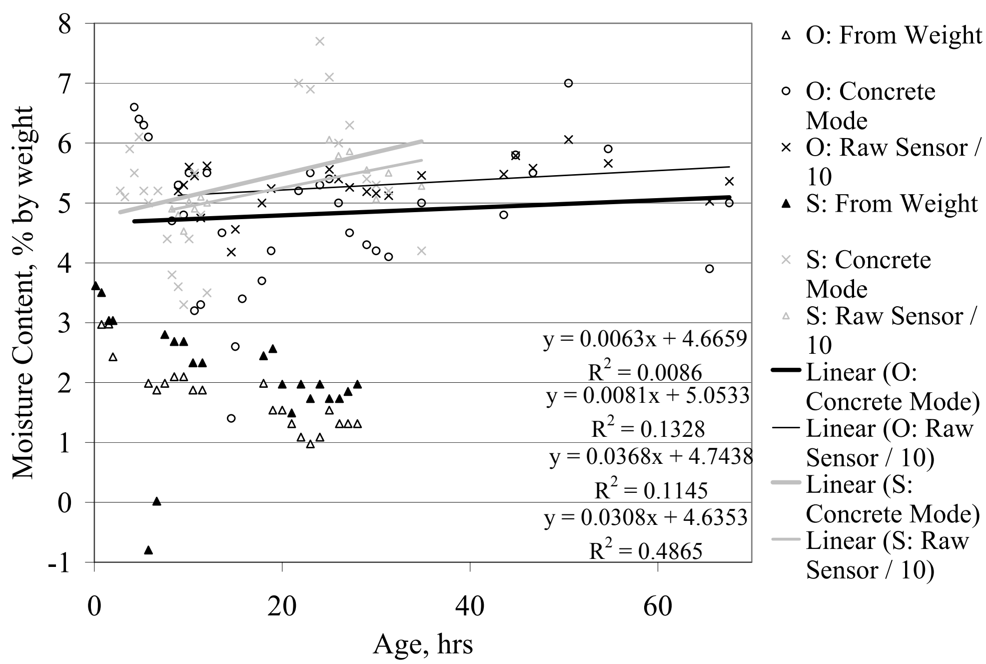

Figure 7.23 SSII Pan Moisture Content by Weight and Aquameter

In Figure 7.22, we see that the weighed moisture content of these pans decreases with time. However, Aquameter readings in both the concrete and calibration modes increase with time. As these results are not reasonable, it appears the Aquameter did not accurately represent moisture loss. In these pans, the data cannot be used to calibrate slab data. According to this data, Aquameter readings taken in the concrete mode on the slab will provide only a relative idea of moisture content, possibly overestimating moisture content by 5%.

Aquameter results from all slabs are plotted in Figure 7.24. Data can be found in Table F.6. Results indicate that moisture content was highest in the slab with a curing compound with no MMF followed by the slab with plastic sheeting. The slab with both a curing compound and MMF has the lowest moisture content. All other slabs lay in between these at a moisture content of approximately 5%.

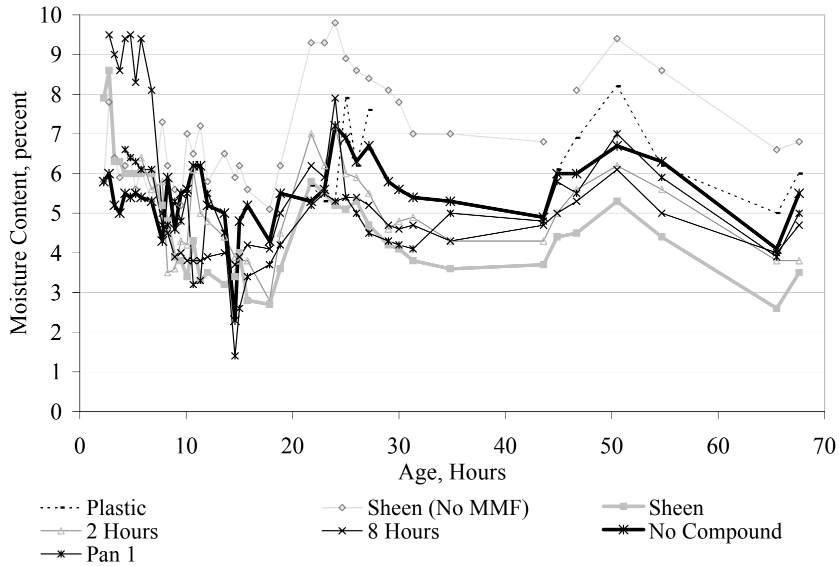

Figure 7.24 Concrete Mode Aquameter Readings for All SSII Slabs and Pans

7.3.2 Lab Tests to Determine Aquameter Sensitivity

Prior to SSII, an additional test was conducted to determine the accuracy of the Aquameter. A 2 x 15 x 6 in. concrete specimen was constructed in a pan and troweled to a smooth finish. In this test, the moisture read by the Aquameter decreased with time as it should, but still overestimated moisture content (Figure 7.25). Unlike SSII results, these results follow the anticipated trend that Aquameter readings should decrease as moisture content decreases. However, again the Aquameter readings overestimated actual moisture content as determined by weight.

Since the Aquameter should not be placed directly on a wet concrete surface, readings were taken in various locations: on plastic wrap, on the wet surface, on the side of the air-insulated box (¼ in. separation), and 1/8 in. above the concrete surface. Because of the sensitivity of the instrument to air, only readings taken on the plastic wrap were comparable to those taken on the surface. Results are shown in Figure 7.26.

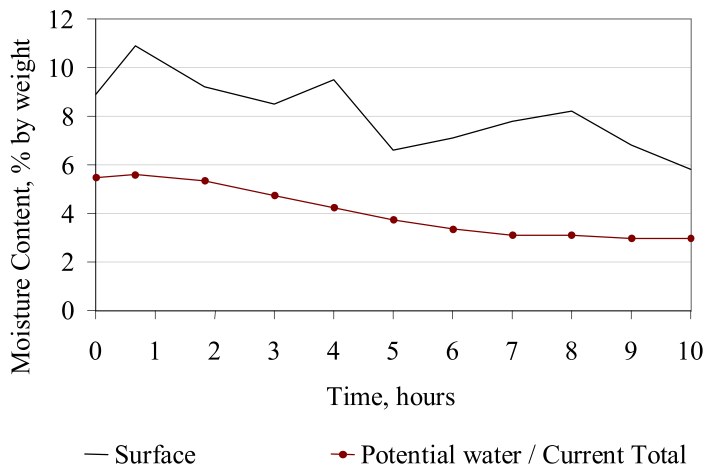

Figure 7.25 Concrete Mode Aquameter Results of Lab Test on Small Pan

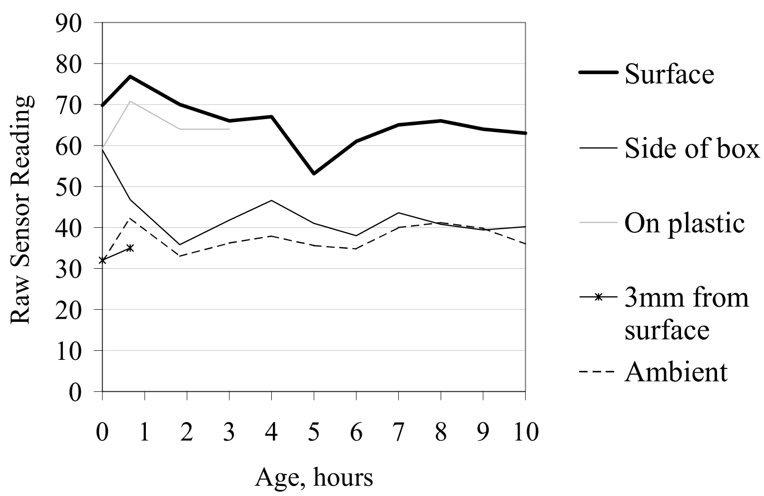

Figure 7.26 Effects of Interface on Aquameter Readings

7.4 Humidity and Dew Point Sensors

Humidity sensors were obtained from the same supplier as the i-Buttons a few weeks prior to construction of SSII. Because they were inexpensive but highly sensitive to changes in humidity, it was decided that they would be evaluated in SSII. The following section discusses tests conducted in preparation for their use along with results from SSII.

7.4.1 Preparatory Humidity Sensor Tests

Tests were conducted prior to construction to determine the best manner in which to use the sensors. Before any tests in concrete were conducted, tests to determine the sensitivity and logistics of the use of sensors were run. In the first test, the sensor was placed in a small container covered by a wet cloth. The sensor would change from ambient humidity (~50 %) and stabilize to the saturated air relative humidity in the cup (~100%) within approximately 30 seconds. This showed the sensor could reflect humidity changes in real time. In fact, simply holding the sensor by the wire while transferring it into the 100% humidity chamber increased readings due to the moisture of the researchers' hands, though they were not noticeably wet. The success of the sensors in these initial tests showed promise for their use in concrete.

In order to read concrete moisture, a method had to be developed for the sensors to obtain readings while not in actual contact with the concrete (the alkalinity of bleed water was observed to cause sensor malfunction), but still reflecting the concrete's internal moisture conditions. Initially, orange plastic capsules were used for sensor barrels. To allow moisture to permeate the capsule, a series of tests were conducted to determine the number and size of holes that would allow rapid changes in moisture, but prevent infiltration of water. Short intervals are desired so the sensor can capture immediate changes in moisture. Capsules were tested with small needle holes and larger pinholes, varying from five to eighty in number. Results of this test are shown in Figure 7.27 and indicate that only the size, not the number of holes, significantly affects the rate at which moisture stability is established. For example, there is no significant difference between using twenty-five or forty small holes or in using forty, sixty, or eighty large holes. But a rate change occurs when using forty large holes rather than forty small holes. A capsule with forty large holes only requires approximately 5 minutes to stabilize in the 100% humidity environment, whereas it takes approximately 25 minutes with forty small holes.

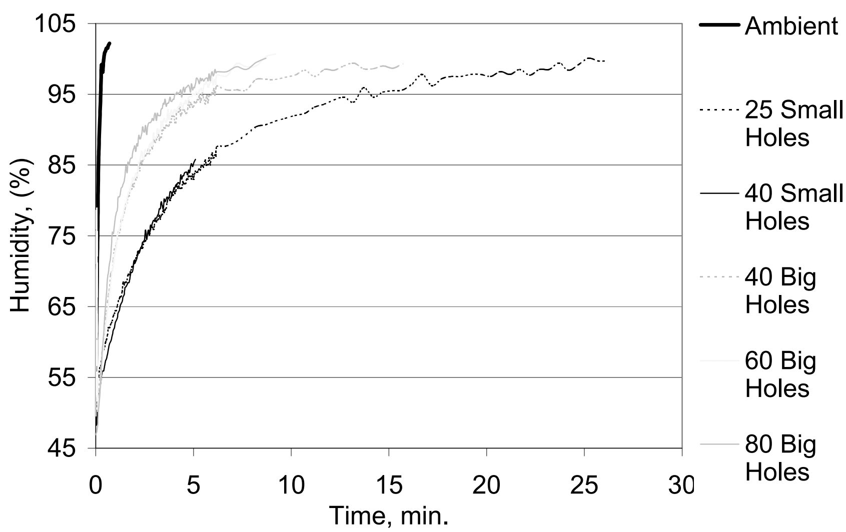

Figure 7.27 Effect of Perforation Parameters on Humidity Permeability of Capsule

After this next point, a capsule with forty large holes was embedded ¾ in. into a small concrete specimen. It was found that only a few drops of mortar would seep through the holes, not reaching the sensor. Thus, a perforated capsule can be placed in concrete without damage to the sensor. However, if the entire capsule is embedded so that humidity can be obtained at various depths within the concrete, additional tests should be conducted to verify the capsule's functionality at increasing depths/pressures. These tests were needed as capsules used in these tests were only embedded approximately ¾ in. Because only surface moisture was to be measured in SSII, capsules did not need to be completely embedded. Thus, pinholes were not required and capsules with their bottoms cut out were used. Prior to SSII, it was determined that the concrete would rise to a level equal to the level of surrounding concrete, and it was necessary to ensure that the humidity sensor remained above the concrete area. The humidity sensor is soldered to wires and the wires run through the capsule cap so that the cap can be placed on the capsule with the sensor suspended inside. A series of tests were conducted on these specimens with the following results observed: 1) Humidity readings quickly reached a maximum, then changed slowly, with nearly no observable changes during the first day, with readings falling slowly during the second through sixth days; and 2) simply cutting off the bottom of the capsule did not produce noticeable changes in readings or accuracy from the perforated barrels.

7.4.2 Small Slab II Humidity Sensor Results

Results of SSII proved very educational in the logistics of using the sensors. The first and most dramatic effect was that of direct sunlight on sensor readings. SSII was placed at noon. The humidity readings during this time were relatively low, beginning at 69% at noon and increasing to 95% by sunset. During the night, readings were near 100% and only began decreasing once the sun rose again. Thereafter, readings dropped to approximately 68% until approximately 3:00 p.m. Until this point, all readings were as expected. The initial rise in surface moisture can be explained by water rising to the top of the slab as bleed water, with readings stable overnight because of lack of wind and sun. When the sun re-emerged, it was logical that surface moisture would begin decreasing due to increased evaporation and solar heat. However, the fact that humidity rose significantly on the second night indicated problems. Additionally, when the sensors were covered with plastic during the day, they provided the same readings as those of the previous night, possibly indicating that readings were influenced by light. Though some moisture gain is to be expected, it should not significantly surpass that of the previous night. From Figure 7.28 one can see that the readings vary with sunset and sunrise (Appendices F.7 – F.12). The typical application of these sensors is in a weather station. Thus, they are not usually required to function in direct sunlight. In future experiments, it is therefore suggested that humidity sensors be placed in black capsules such as plastic film capsules, which do not allow light to permeate,.

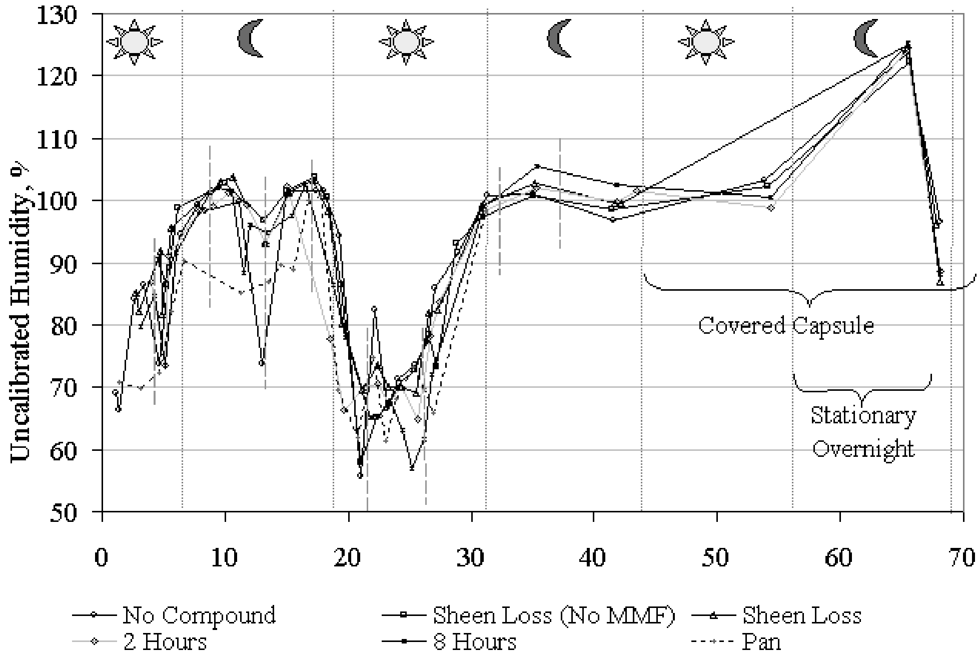

Figure 7.28 Humidity Sensor 1 Readings from Five Slabs and Open Pan

On the third night, the capsules were allowed to stay in a slab for over 5 hours. Previously, two sensors had been rotated from chamber to chamber and stored between uses. On the third night, the two sensors were placed in two capsules overnight while covered with plastic. This appeared to increase readings significantly, indicating that sensors should not be rotated, but should remain in situ during and in between all readings.

7.5 Moisture Sensor Comparisons

Though additional calibrations will be required for the humidity sensor, its relative sensitivity to moisture was still demonstrated. This is shown in Figure 7.29 where humidity in slab *N* from the dew point sensors and humidity sensors is plotted against time. In this figure, one can see that except for two skewed points, behavior in moisture was compatible between the two sensors. The drop in humidity during the day, which was previously assumed to be caused by only sunlight infiltration, is also exhibited by the dew point sensors though their sensors are protected from light; the mirror used for sensing is in an enclosed black plastic chamber. These results indicate that the daytime drops of the humidity sensors are due to both the presence of incident light and actual moisture loss.

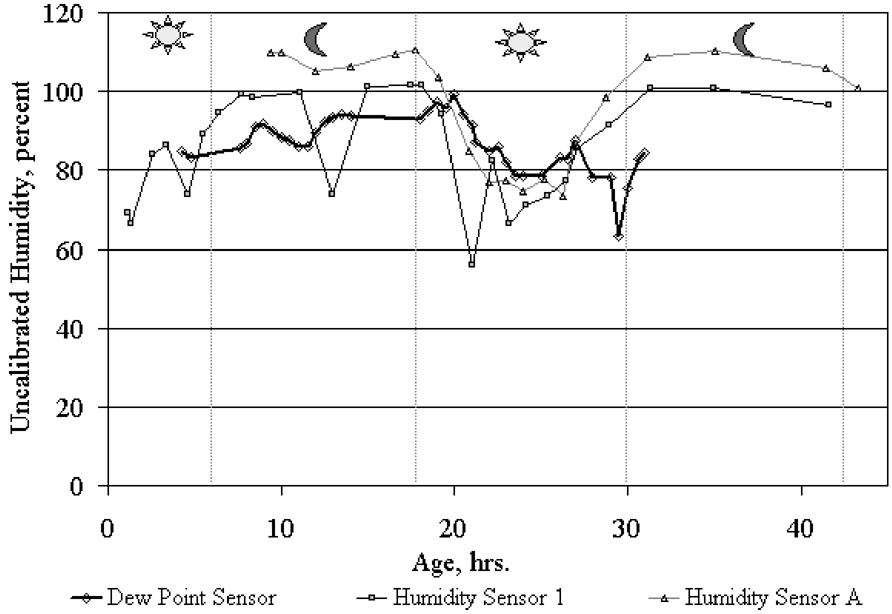

Figure 7.29 Humidity and Dew Point Sensor Measurements up to 42 Hours

Though the humidity sensors required calibration for sunlight, attempts to determine relative moisture loss between slabs were made. To do this, the area under the curve shown in Figure 7.28 was calculated. This was repeated for Aquameter readings shown in Figure 7.24. The cumulative Humidity-hr and Moisture Content-hr are plotted in Figure 7.30. In addition to these measurements, water *loss* was estimated using a model developed in a tining study for the Texas Department of Transportation (Rochefort 2000). The equation takes into account the effects of the number of curing compound coats applied and if the application is delayed. The equation does not specifically account for the difference between application at 2 and 8 hours and the application of MMF or plastic sheeting. Thus, coefficients were fit to suit this study as much as possible and give only a rough comparison. Note that the first two graphs plot moisture content in each slab, whereas the third plot water loss. In order for all plots to fit on one graph, humidity sensor values were divided by 1,000 and Aquameter values by 100.

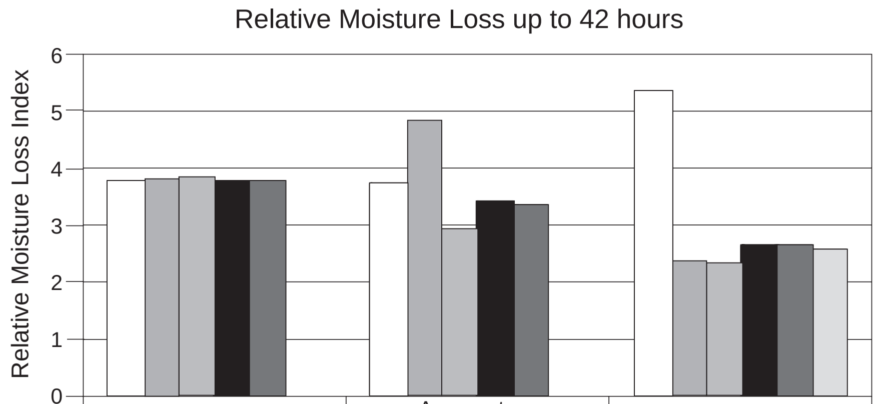

	Humidity (hr. / 1000)	Aquameter: Moisture Content (hr / 100)	Roche: WL*3 (lb)
N	3.733	3.71	5.34
O	3.813	4.82	2.37
S	3.849	2.92	2.34
2	3.758	3.38	2.61
8	3.735	3.32	2.61
P			2.55

Figure 7.30 Comparison of Relative Moisture Content and Moisture Loss between Slabs up to 42 Hours

The plots show that though humidity measurements obtained by the humidity sensor agreed with those from the dew point sensor, no significant variation in humidity between slabs was captured. Measurements from the Aquameter yield counterintuitive results as slab *N* has one of the highest moisture contents, followed by slabs *2* and *8*, with slab *S* exhibiting the lowest moisture. No readings were taken on the slab with plastic as the sheeting could not be removed without affecting results. The third graph shows the expected moisture loss predicted. This graph appears to agree with that next to it, but because it graphs moisture loss and not moisture content, it shows discrepancy between expected values and those obtained by the Aquameter.

8. Discussion

Possible causes and interpretations of the results of Small Slab Studiy I (SSI) and Small Slab Study II (SSII) are discussed below.

8.1 Core Diameter

SSI results show the use of 4 in. diameter cores in lieu of 6 in. cores significantly increases both compressive and tensile strength. This is in agreement with Wright's findings, which also found that tensile strength is increased by 10% when 4 x 4 in. cores were used in place of 6 x 6 in. cores (Wright 1955). Literature review findings revealed that most researchers also found compressive strength to increase with diameter, but not by a significant amount (with diameters greater than 1.5 in.) (Concrete Society 1987). Thus, if small-diameter cores are used, increased tensile strength and possibly increased compressive strength should be anticipated and accounted for.

Apart from increased strength, the use of smaller cores is also discouraged by many because of their increased variability. Equivalent accuracy in samples is usually based on equivalency in the net-bearing cross section of all specimens tested. For example, it takes five 4 in. diameter specimens (20 in.^{2}) to obtain the same accuracy as three 6 in. specimens (18 in.^{2}), the standard established by most codes. Therefore, the advantages of using small-diameter cores, such as decreased damage to a pavement and easier cutting, are negated by the fact that more specimens are required to obtain acceptable accuracy. Small diameter cores are still useful, however, when larger cores cannot be cut due to reinforcement congestion, pavement dimensions, or cutting equipment. This has been addressed in codes by allowing for 4 in. cores, if necessary, so long as specified guidelines are followed.

8.2 Cylinder Curing Method

SSI results show water-cured cylinders overestimate the strength of sand-cured cylinders and cores. This is logical as more water is available for hydration of the cementitious particles. Sand-cured cylinders exhibited comparable compressive strength as to cores, suggesting sand-cured cylinders may indeed reflect in situ moisture loss and provide more accurate predictions of in situ compressive strength. This is beneficial for two reasons: 1) in situ strength can be predicted more accurately—that is, moisture loss is accounted for—and 2) sand-curing is economical and easily implemented in the field.

The results of SSI showed that the tensile strength of sand-cured cylinders was much lower than that of the water-cured cylinders and cores. This is why water-curing decreased strength when it appears that it should produce opposite trends.

8.3 Strength Relationships

The strength results obtained from SSI data were compared to strength regressions developed by Raphael, which were based on the results of over 1,500 specimens and are accepted by many. The relationships used in the American and Canadian codes for computing flexural strength from compressive strength significantly underestimate flexural strength. The equations continue to be used, however, as they provide codes with a built-in factor of safety and the added benefit that the 0.5 exponential relationship is easier to utilize in a calculator than the more accurate 2/3 power suggested by Raphael. Data from this investigation has a high correlation with Raphael's equations, suggesting that his equations are reliable for strength relationships.

Of significance are findings that SSI results agreed with Raphael's compressive-tensile relationship. As discussed in the introduction, in the design of pavements it is best to test specimens for strength in the same manner as the expected failure mode, tensile strength. Because of the initial difficulties in conducting a direct tensile test, flexural tests were developed and evolved into the norm. Now, most codes provide relationships for computing flexural strength from compressive strength. However, the correlation between flexural and compressive strength testing is often low when compared to that of compressive and tensile tests. In this study, 85% of SSI data, within one standard deviation, crossed Raphael's compressive-tensile regression whereas only 61% crossed his compressive-flexural relationship. The fact that the compressive-tensile relationship showed to be more reliable than compressive-flexural relationships, that flexural strength is used more because of chance than actual applicability, and that pavements fail in tension, suggests that current codes should strongly consider incorporating tensile strength specifications and relationships.

8.4 REINFORCEMENT IN SPECIMENS

Results of SSI show that the presence of reinforcement in a core significantly increases compressive strength. This is contrary to literature review results that stated compressive strength will decrease by 0-10% when steel is present in a core due to stress concentration's aggregate-mortar bond (Concrete Society 1987). Thus, a possible explanation for the conflicting results of SSI may be that the steel-mortar bond was sufficiently strong to allow the higher strength of the steel to contribute to the sample's composite strength. Using this logic, however, the presence of two reinforcement bars rather than one should have increased compressive strength. These conflicting results indicate that the presence of reinforcement in a sample makes compressive strength estimates unreliable. That is, reinforcement may either significantly increase or decrease strength possibly depending on the concrete used, steel-mortar bond, etc.

No literature was found that addressed the effects of reinforcement on tensile strength. The only statement was that specimens used for tensile tests should not contain reinforcement. Results of this study suggest that the presence of steel does not affect tensile strength so long as the reinforcement does not cross the failure plane. This is different than compressive tests where it is not possible to position steel so that it does not intersect the failure zones (See Figure 8.1).

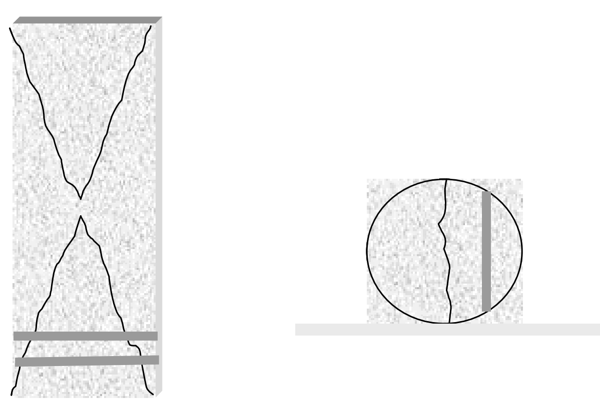

Figure 8.1 Locations of Reinforcement in Specimens

8.5 Effects of Curing Regime and/or Surface Finish

The effects of varied curing on strength derived from results of SSI and SSII are provided below. Effects on strength and the vertical strength profile are presented along with causes because of variation in temperature, slab surface, and evaporation.

8.5.1 SSII Temperature and Evaporation Effects

Results of SSII exhibit that both the i-Buttons and thermocouple provided accurate and comparable data. Temperatures in the top of the slabs were highest and decreased with depth. The mid-depth temperatures were nearly an average of top and bottom i-Buttons. During the night, all slabs exhibited the same surface temperatures, indicating that the variation in daytime temperatures is due to differences in solar heat absorbed. This is supported by the fact that the slabs with the curing compound (white) were coolest, followed by the uncovered slab (gray), and then the slab covered by plastic (black).

Results of SSII support the use of i-Buttons for long-term use. They are inexpensive (~$9), have a battery life of 10 years, and can be re-missioned or have data downloaded at any time. This is a significant advantage as thermocouples require a meter to be left at a site to log readings preventing their use at other sites. In the event that connection is lost with an i-Button, its sturdy casing allows it to be cored out at any time without data loss. There is also great versatility in its logging capabilities, such as delayed start, a roll-over option, instant graphing capabilities, and temperature alarms. i-Buttons make long-term temperature monitoring feasible at an economical and practical level. Additionally, as shown previously, the i-Buttons also log data consistently from onset of data collection. The thermocouple requires approximately 3 days for readings to stabilize. These initial fluctuations were on the order of 20 °F in SSII, possibly, caused by poor construction/welding of thermocouples or the presence of moisture at connections.

Results of SSII also indicate that the presence of a curing compound serves as an insulator from ambient temperatures as shown by the lowered differential between top and bottom temperatures of slabs with a curing compound. The compound also kept temperatures low by reducing evaporation and reflecting light. The increases in temperatures due to retained heat of hydration retention when using a white curing compound was surpassed by the increase in temperature in slab *N* due to its darker color.

During the first day after casting, the slab with no curing compound demonstrated lower temperatures throughout the depth of the slab compared to those with curing agents. This suggests that the slab underwent higher evaporation than the other slabs, which affected the entire depth of the slab. By the second day, this slab was consistently the hottest as less water was available for evaporation, and its relatively dark color absorbed solar heat.

8.5.2 Strength and Tensile Strength Vertical Profile

Cores from SSI showed that the elimination of a curing compound significantly reduced compressive strength, but did not affect tensile strength. It was expected that both tensile and compressive strength would be affected similarly, increasing with the use of a compound. However, results of the pavement curing analyses are skewed due to the inconsistencies in specimens used. All specimens used for tensile tests were 4 x 6 in. However, the specimens used for compressive strength analyses were 4 x 6 in. and 4 x 8 in. Thus, inconsistencies in cores used for compressive strength existed in the specimen's L/D ratio and core diameter to nominal aggregate diameter ratio. These inconsistencies may have made the results unreliable. SSII readdresses this issue in greater detail.

Analysis results of SSI data sorted by aggregate type showed that position generally affected only the limestone (LS) specimens. This strongly suggests that the vertical compressive and tensile profile is dependent on the curing history of the concrete. That is, the LS slab was without a curing compound for 1 hour more than the siliceous river gravel (SRG) slab. It is possible that this extra hour (during a high evaporation period) provided the time required for water evaporation from the surface of the pavement to affect strength. Therefore, the fact that only LS and not SRG specimens exhibited top-bottom strength differentials suggests that evaporation effects may significantly decrease the strength of concrete near a surface when a curing compound is not applied in a timely manner.

Strength data from SSII was normalized using equivalent age of each specimen at testing time to account for varying degrees of hydration to determine effects of moisture loss due to curing. Nearly all normalized tensile strength comparisons indicate that after 7-day strength tests, elimination of curing compound or delaying its application will decrease the strength of top concrete and increase the vertical strength differential. However, prior to 7-day strength test, nearly opposite trends are exhibited in all comparisons. Results of 3-day tests show that *poor* curing yields higher strength and lower strength differentials. The cause of this discrepancy is not well understood. If the data are correct for these early tests, the differences may be due to the effects of hydration. Some of the literature concerning moisture in concrete indicates that moisture content and hydration level off 3 days after placement. Also, research simulating pavements under high winds (similar to those experienced in this study) show moisture loss leveling off after 1 to 2 days (Rochefort 2000). As mentioned in the literature review, the research of Aïtcin showed that the difference in strength between water-cured and sand-cured cylinders was identical before 7 days, with strengths decreasing by up to 20% thereafter (Aïtcin 1994). It is possible that a strong relationship exists between the effects of the curing regime and time of hydration cessation. In any case, this study seems to confirm previous experience that inadequate control of moisture loss may result in faster strength gain at early age (due to maturity effects) but will ultimately result in weaker pavements and poorer vertical strength profile. More research is recommended on this critically important finding.

Normalized tensile strength comparisons between slabs, where curing compound is applied at sheen loss both with and without MMF showed that elimination of MMF does not significantly affect strength. Results vary slightly between ages.

The effects of tining were tested as a secondary objective in SSI, though no significant strength differentials were expected. As long as a curing compound is applied, as in SSI, the additional surface area introduced by tining should not affect either compressive or tensile strength. This was supported by SSI results. If no compound had been applied, it is possible that the tined area would have produced slightly lower strengths than the untined area.

8.6 AGGREGATE TYPE

Nearly all analyses in SSI showed that aggregate type did not significantly affect either compressive or tensile strength. This is intuitive as the specifications required a specific strength that mix designs were required to provide. Tests that showed otherwise were all from results of analyses on 4 in. cores, indicating that the problem was due to differences in aggregate size. Though both batches were designed to reach the same strength, ¾ in. and 1 in. LS and 1 ½ in. SRG aggregate was used. Current codes require that the core diameter to aggregate diameter ratio (D/d) be at least 3:1 to prevent reductions in strength resulting from large aggregates. The

SRG did not satisfy this requirement (D/d = 2.66) and, thus, SRG reductions in strength are most likely because of this effect. Reductions are not assumed to be caused by differences in curing between the batches because the LS was placed first and thus should exhibit lower strength due to increased surface water loss. Additionally, according to Bloem's investigations, concrete cores made from lightweight aggregate (i.e., LS) produced slightly higher strengths than those made from normal weight aggregate (i.e,. SRG). This is due to the excess moisture absorbed by porous lightweight aggregates (Bloem 1965). The fact that significance in aggregate type was demonstrated only by 4 in. cores and not 6 in. cores suggests that higher LS strengths were due to discrepancies in aggregate size and not aggregate type

8.7 AGE

No tests in SSI showed strength to decrease significantly with age. Analyses either showed strength to be independent of age or increase with age. The latter result is expected and no additional comments will be made regarding the cause. The former can be explained by the high early age strength of the concrete mix due to the fine grind of the cement. That is, this insignificance in age was seen only in specimens tested between 7 and 28 days, where a majority of the strength was already reached by 7 days.

8.8 SSI NONDESTRUCTIVE TESTS

When determining the modulus of concrete pavements by seismic methods, there are factors that can affect either the measured or actual value of the modulus. In this study, the factors investigated that affect the measurement of the modulus include the presence of reinforcement, specimen shape, specimen geometry, and testing equipment used. Factors investigated that affect the actual value of modulus include curing method and position of a core in a slab.

The value of the modulus measured with resonant frequency (RF) procedures was not affected by the size or shape of the specimen, i.e., between 4 in. and 6 in. cores or between water-cured cylinders and water-cured beams. This is beneficial, because it imposes fewer restrictions on the requirements necessary for obtaining accurate measurements. Other research, however, has shown that specimen size and geometry can affect values (Malhotra 1994). One possibility is that fluctuations in the relative homogeneity of specimens in regards to the specimen-constituent material size ratio (Malhotra 1994). Because the modulus measured from seismic tests is influenced by resonant frequency, it is inherently a function of specimen size, slenderness, and size of constituent materials. In SSI, the relative ratios of specimen size and geometry to constituent material size/geometry were such that no statistically significant difference in moduli between cores of varying diameter or shape were exhibited.

Similarly, the presence of steel in cores did not significantly affect moduli. Again, this is most likely because steel did not significantly affect the relative homogeneity in regard to specimen-to-constituent material size.

The effects of increased water available for curing are exhibited in all modulus tests: moduli of water-cured cylinders were significantly higher than those of sand-cured cylinders, which were significantly higher than those of cores, moduli of concrete from the slab sections with curing compound were significantly higher than moduli from the areas without a curing compound; and the moduli of cores cut from the bottom of the pavement were higher than moduli cut from the top. These are the expected results from the corresponding destructive tests; results from destructive tests were counterintuitive as variables known to increase strength instead weakened the concrete. As in the destructive tests, however, only the LS moduli were significantly higher in the bottom of the slab. Again, this is attributed to the higher evaporation rates experienced by the LS slab due to its earlier placement. The results of the nondestructive tests of SSI show that seismic methods accurately captured the increase in moduli expected from procedures designed to enhance curing.

Moduli determined using resonant frequency (RF) should, theoretically, yield lower values than Portable Seismic Pavement Analyzer (PSPA) tests on the same sample. This is because the PSPA test is conducted over a specimen, i.e., a slab, with many boundary conditions that constrain movement, increasing modulus values. Results of tests in this study exhibited opposite trends. Tests using RF yielded moduli approximately 6% higher than those using PSPA. Usually, PSPA values are approximately **7**–8% lower than values obtained using RF.

Tests on cylinders and cores consistently show that moduli estimate from destructive tests are lower than those obtained from RF tests on the same specimen.

Regressions of strength versus seismic moduli determined using PSPA yielded high correlations. This is expected as strength should increase as modulus increases. The American Society for Testing and Materials (ASTM) currently allows the use of seismic equipment for estimation of concrete degradation. Similarly, the method may be used to measure concrete hardening. Though ASTM currently discourages this practice, results of this study indicate that with further research the modulus may provide an accurate and truly nondestructive method of estimating strength.

8.9 AQUAMETER

Aquameter readings from SSII were problematic; it is possible that errors were introduced in several ways. First, four people were in charge of taking readings. Considering the sensitivity of the device, small differences in technique can significantly alter results. For example, applying light pressure aids in closing the air gap between the sensor and concrete surface, increasing sensor accuracy. Also, initial readings were taken in arbitrary locations to obtain an average moisture content in each slab section. Though this has potential benefits, in practice, it is best to record the highest readings obtained as this most likely represents a good interface (readings are lowered by air gaps). By the end of the first day of readings, locations on each slab and pan had been designated for readings. Even if readings are taken in exactly the same way every time, even dust brought in by wind can skew readings. These variables are all the likely factors contributing to the counterintuitive results of the Aquameter readings.

One point of concern is that in the real world it may not be possible to have a perfectly smooth finish. For example, most pavements have a rough finish to prevent skidding. Measurements cannot be taken on these surfaces. Designated areas must be set where concrete can be finished to a smooth surface.

8.10 HUMIDITY SENSOR

The humidity sensor data obtained from SSII must be calibrated to reflect the amount of sunlight reaching the sensor, or a dark environment must be maintained. Though manufacturers warned that the sensor should not be used in direct sunlight, the degree of sensitivity was understated. Since some readings were taken during sunlight with plastic sheeting, it is possible that all data can be made compatible if calibrations are made that adjust data for ambient light levels. Tests conducted in concrete prior to SSII were done under fluorescent light, with readings at approximately 102% during the first day after casting and decreasing to 70% humidity after 7 days. As these numbers were near the expected values, after minimal calibration to reflect use in concrete, no light problems were anticipated for SSII.

The capsules used in SSII were a dark, clear plastic. Combined with the facts that the sensors were shielded from direct sunlight by the caps, throughout nearly the entire humidity data collection period the sky was overcast, and that most capsules were nearly covered by the opaque, white curing compound, researchers were led to assume that no direct sunlight could reach the sensor. When humidity readings shot up on the second night, however, researchers realized another factor was in play.

Thus, on the third day of testing, readings were taken with a small piece of opaque black plastic sheeting fastened over the capsule. From Figure 7.28 one can see that with the plastic, moisture did not drop as it had the day before when no plastic was used. On the third night, two sensors were left undisturbed in the slab for 5 hours rather than being rotated for readings. Figure 7.28 shows that readings shot up again. These results indicated that a sensor should not be exposed to **any** light and should not be handled or moved during readings. A suggested capsule that would prevent light effects is a black plastic film capsule.

To verify that the observed effects were due to differences in light intensity and not moisture, a small test was conducted outdoors. A sensor was placed in a new capsule in which a small amount of water (~ ¼ in. in height) was added to create a saturated environment. The capsule was then rotated from an exposed condition in the sun to a covered condition by placing the capsule under black plastic in the shade. (Note: at the time of this test, the sky was no longer overcast and no curing compound was on the capsule. This test, thus, maximizes the effects of light). The results are plotted in Figure 8.2. In this 2 hour period, readings varied between 65% and 110% moisture though moisture content truly did not vary.

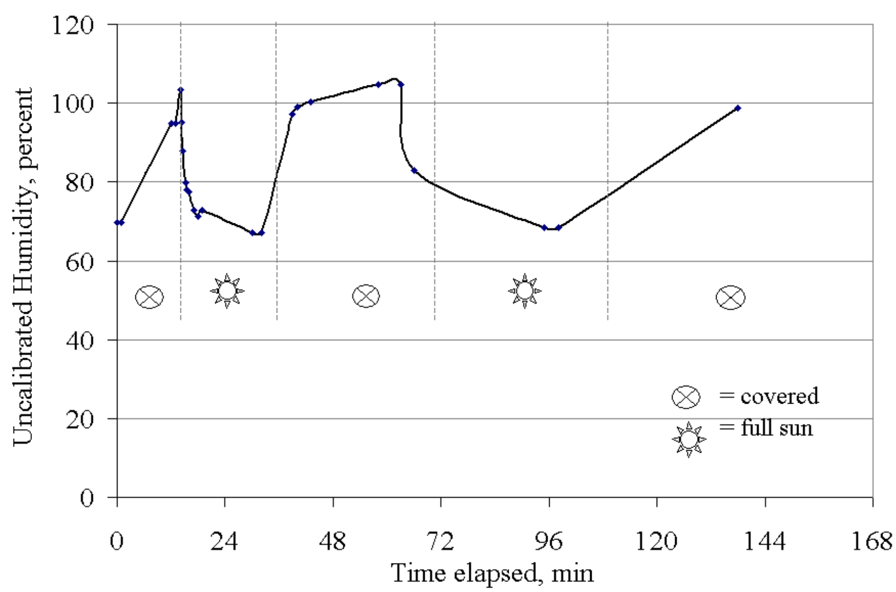

Figure 8.2 Effects of Sunlight on Humidity Sensor Readings of Water-Saturated Air

The manufacturers of this product are aware of the problem introduced by the sensitivity of these sensors to light and have already developed a sensor that adjusts for light. The new sensor, with a built-in power supply, is currently used for agricultural purposes and provides humidity as a function of voltage supply, voltage output, incident light, and temperature. The model used for this device can also be applied to SSII data to account for incident light. Discussions are underway with the manufacturer to tailor the button for concrete applications.

8.11 MOISTURE SENSOR COMPARISONS

Though multiple dew point sensors were not available for use in each slab, results did indicate that the daytime temperatures exhibited by the humidity sensors were not entirely due to sunlight but also due to actual moisture loss. Both sensors predict relatively the same behavior in humidity, though the humidity sensors read slightly higher during the night. The comparisons of the humidity sensors to the dew point sensors show promise that the humidity sensors may be serviceable after some further developments and calibration.

9. Implementation

Project 3925, introduced in Chapter 1, lists recommendations for increased performance of high performance concrete (HPC) pavement design resulting from 20 years of field experience on continuously reinforced concrete (CRC) pavements in Texas. The recommendations developed constitute an implementation plan to be used for future pavement specification and design considerations. Small Slab Studies I and II (SSI and SSII) investigate many of the implementation recommendations developed, as well as new issues that have surfaced since the publication of Report 3925. This chapter provides results and recommendations developed from SSI and SSII, most representing continued research concerning recommendations from Report 3925. The reader is invited to refer to the publications cited (principally, McCullough 1998 and McCullough 1999) for a thorough presentation of the analyses leading to the recommendations of Project 3925.

As introduced in Chapter 1, Project 1700 continues investigations for improvements on HPC pavements. Figure 9.1 illustrates an overview of the research and associated implementation areas for the project. Results and recommendations from SSI and SSII are listed below. Most recommendations of SSI and SSII are directly related to the major implementation items of Project 1700.

Implementation →

Research Area ↓

AREA	DESIGN	SPECS	CONST.
Temperature	Target PCC set temp.	Placement Limits	QC Mix Design QA Monitor set temp and maturity
Moisture	Design for Strength Profile	Method	QC In Situ QA Strength Profile
Aggregate	Design for COTE range	Set Limits/ Range	QC During Const. QA In Situ
Programs	Evaluate PCC design	Establish Limits limits	Evaluate as-built sections
Acceptance / Opening	Eval. Effect of early opening	Set limits for early opening	QA combine items for quality pavements

Figure 9.1 Research Areas and Implementation Items of Project 1700

9.1 EFFECTIVENESS OF CURING COMPOUND AND MONOMOLECULAR FILM

Report 3925 identifies that evaporation should be monitored and managed to maintain stress at acceptable levels, with critical situations of excessive evaporation minimized using special procedures such as application of a curing compound, use of monomolecular film (MMF), expedited application of a curing compound, etc. Experience has shown that large amounts of water loss may occur quickly in hot, windy, and/or sunny conditions. These conditions may lead to undesired effects such as cracking and spalling. Wet burlap, ponding, wet cotton, and plastic sheeting have been shown to provide the best control of water loss.

SSI and SSII (principally SSII) addressed the effects of delayed curing compound application, elimination of curing compound, and elimination of MMF on the *strength* of the concrete slabs. Results are discussed in the following two chapters, stating that in general MMF did not increase strength significantly. The effects of varying the curing regime implemented were insightful, however. The expected results that plastic sheeting would yield the highest strengths, followed by ideal curing compound application times, and, lastly, delayed and no curing compound application would produce decreasing strengths was only exhibited 7 days after placement. Three-day strength tests showed opposite trends, with "best-case curing" leading to lower strength. Other researchers have observed these strange early age strength trends as well. It is hypothesized that these unintuitive trends are due to interaction between the effects of heat of hydration and evaporation present during the hydration phase. However, strength results after the 3-day time period do agree with common theory that poor curing (whether from delayed curing compound application, not using plastic sheeting, or leaving concrete uncovered) will significantly decrease long-term strength.

Specific Recommendations:

- Monomolecular film did not increase strength gain and should not be used for this purpose. Its use for crack and delamination prevention may still be possible though more research is required.
- Specifications should emphasize application of curing compound as soon as possible to avoid detrimental long-term strength loss under high evaporation.
- The relationship between heat of hydration and curing regime should be investigated further. Strength tests during heat of hydration showed unintuitive results, (i.e., in order of decreasing strength: no compound, delayed application of a curing compound, the Texas Department of Transportation (TxDOT) standards, and plastic sheeting).

9.2 TESTING TECHNIQUES FOR MEASURING CONCRETE TEMPERATURE

Report 3925 indicates that high set temperatures in concrete cause large tensile stresses as the concrete cools, resulting in cracking as the early-age strength is exceeded. Though SSII did not develop techniques of decreasing concrete temperatures or continue investigations on the effects of high set temperatures, a reliable technique for determining in situ concrete temperatures was developed. As described in many sections of this report, Thermacron i-Buttons were successfully placed in many locations of the slab in SSII. The buttons successfully captured the vertical temperature profile in the 14 in. slabs, and the RJ-11 telephone jacks proved sturdier than originally anticipated, surviving encrusted mud, cleaning by a steel brush, embedment in sand, and encrusted concrete truck wash debris. Considering the life, versatility, sturdiness, and applicability of these sensors, their incorporation into pavements is highly recommended.

Specific Recommendations

- Conduct further developments on the use of the Thermacron i-Button for concrete applications. These improvements should include design improvements (i.e., at soldered connections) and developments on parallel usage.

- Establish parameters to determine critical spacing and distribution of i-Buttons.

9.3 ESTIMATION OF EVAPORATION

As mentioned previously, minimizing surface evaporation plays a significant role in reducing delamination and cracking in pavements. Evaporation rates for the pavements analyzed in Project 3925 were monitored using on-site weather stations. Part of SSII focused on the estimation of surface evaporation for comparisons with curing regime and resulting strength. Though a weather station was used to determine evaporation rates in each slab, output only reflects differences in each slab's temperature as the only difference in input between each slab was its temperature. Thus, it was not possible to separate the effects of temperature and evaporation using data from the weather station.

Two separate devices were used to monitor the moisture content at the surfaces of each slab. Both devices show promise, but require additional research before being adopted into specifications.

Specific Recommendations:

- Investigate further the use of humidity sensors. They show potential but must be better engineered for applicability in concrete. Continued discussions with manufacturer are recommended.

- Investigate further the use of the Aquameter for surface concrete moisture estimation. Establish specifications on the interface, testing locations, and use for the sensor in concrete.

9.4 OPENING TO TRAFFIC / IN SITU STRENGTH ESTIMATION

Many aspects of SSII contribute to better estimations of the in situ strength of concrete, and thus more accurate estimation times for opening pavements to traffic. The primary means of estimating in situ strength is from the maturity method. However, the temperature experienced by concrete is affected by surface evaporation, which is affected by the curing regime of the concrete. Though temperature and evaporation are interrelated, results of this investigation showed concrete surface color dictated temperatures rather than curing regime. That is, the slab covered with black plastic sheeting was hottest, followed by the uncovered slab, and lastly by the slabs with white curing compound. If evaporation was the controlling variable in temperature, the uncovered (gray) slab would have been the coolest because of increased evaporative cooling.

Differences in evaporation rates/surface moisture between each slab could not be determined using the standard equation because the only changing input variable was each slab's temperature. Thus, resulting evaporations only reflected changes in temperatures, making comparisons between slab temperature and evaporation rates unrevealing. The trial equipment, the Aquameter and humidity sensors, though demonstrating potential, did not provide useful data for the experiment.

The Thermacron i-Buttons proved very accurate and reliable, yielding maturity values nearly identical to those from the thermocouples. However, their versatility, applicability, sturdiness, and 10-year life provide strong arguments for their incorporation into pavement construction and monitoring.

Specific Recommendations:

- Develop specifications for integration of i-Buttons for use in strength prediction using the maturity method.
- Continue developments of humidity sensors and specifications of the Aquameter for use in evaporation and moisture content monitoring of concrete pavements.
- Use developments of humidity sensors and the Aquameter for investigations of the relationship between temperature build-up and moisture loss (evaporation) in terms of strength predictions using maturity calculations.

9.5 Confirmation of NDT Strength Estimations

The most important relationship in estimating in situ strength using nondestructive testing (NDT) methods is that of NDT versus actual in situ strength. Recommendations are provided below as developed from SSI and SSII findings.

Specific Recommendations:

- Specify use of tensile tests for confirmation of in situ strength, as this is the primary mode of failure for pavements.
- Develop an acceptable level of vertical strength variation that minimizes the vertical strength differential for future Q/A.
- Sand-cured cylinders can be used to estimate in situ compressive strength as curing conditions reflect field conditions.

9.6 Forensics: Coring Strength Tests

- 6 in. cores should be used for all tests. The use of 4 in. cores is unreliable and should be done only when restrictions apply and more 4 in. samples can be cut to account for their increased variability.
- Cores with reinforcement can be used for tensile strength tests so long as reinforcement is not in and is aligned with the plane of failure of the specimen.
- Tensile strengths obtained from cores can be converted with sufficient accuracy to flexural strengths using Raphael's strength equations for compatibility with code terms. Tensile

strength should still be utilized for in situ strength estimates as this is the primary failure mode for pavements.

9.7 AGGREGATE TYPE

The selection of aggregate type is of great significance in the performance of pavements. The type of aggregate used is a major factor in the resulting width of transverse cracks developed in a pavement, load transfer properties, and stress development. These characteristics ultimately determine the amount of spalling (delamination) and thus potential pavement life. The effects of the aggregate used are dependent on bond strength, coefficient of thermal expansion, curing practices, ambient temperature, and steel design.

In SSI siliceous river gravel (SRG) and limestone (LS) aggregate were used. The performance of LS and SRG pavements in Project 3925 was evaluated by spalling, crack distribution, crack width, crack randomness, delamination spalling, and vertical distribution of tensile strength in pavements subject to heavy traffic. In SSI, only the effect of aggregate type on strength was investigated (with no traffic loads). The result of aggregate type on strength showed that LS and SRG concrete designed for the same strength yielded similar strengths.

Specific Recommendations:

- Investigations on the effects of aggregate type on strength may be eliminated from the implementation plan.
- Investigations on the effects of aggregate type on performance should be continued as per Project 3925. This includes, but is not limited to, investigations for thermal coefficient of concrete and aggregates and aggregate bond strength.

10. Conclusions

The following conclusions can be made according to results of the Small Slab Study I (SSI) and Small Slab Study II (SSII). The conclusions address the original objectives of the studies as outlined in Section 1.2.

10.1 SMALL SLAB STUDY I

Conclusions regarding variables tested in SSI are listed below:

10.1.1 Factors Affecting Mechanical Tests: Core Size and Reinforcement

The use of small-diameter cores increases compressive and tensile strength by approximately 10%. It is possible, as found by other researchers, that the effects on compressive strength may be much smaller, and insignificant in some cases. Of greater concern is the fact that at the same sampling rate, variability of small-diameter will be increased and can only be compensated for by increasing the number of small-diameter test specimens. This increase, however, negates the benefits of reductions in damage to the pavement and easier cutting resulting from using small diameter cores.

Tensile tests can be conducted on specimens containing reinforcement with no significant effects on strength as long as steel is not present in the plane of failure of the specimen. In the case of compressive strength, SSI results show that the presence of steel increases compressive strength whereas most research states the opposite. These conflicting results suggest that the presence of reinforcement in specimens used for compressive strength makes results unreliable.

10.1.2 Factors Affecting Strength: Curing, Vertical Location, and Aggregate Type

Sand-curing can be used to accurately predict in situ compressive strength but will underestimate tensile strength. Though results of this study show that water-curing can be used to accurately predict in situ tensile strength but underestimate compressive strength, these results do not agree with current theories and should be used with caution. More research is needed to investigate and quantify the sources of variability in these comparisons.

Results of SSI indicate that if a curing compound is applied in a timely manner, no vertical strength differential will exist. However, if the slab/pavement experiences significant evaporation, bottom specimens will be significantly stronger than top specimens.

Results of SSI data analysis indicate that the presence of tining on a pavement in which a curing compound has been applied has negligible effects on both compressive and tensile strength. The presence of a curing compound will increase compressive strength significantly. The effects of a curing compound on tensile strength could not be determined.

No significant strength differentials are caused by using SRG in lieu of LS aggregate. However, the size of aggregate can have significant effects if the core diameter to nominal aggregate diameter is less than 3:1. When such is the case, strength may be significantly reduced.

10.1.3 Evaluation of Accuracy of Strength Relationships

Findings from this study indicate that Raphael's strength relationships can be used for accurate conversions among compressive, tensile, and flexural strength. Code relationships tend to underestimate strength, providing for a built-in factor of safety.

SSI data suggests that there is a higher correlation of compressive strength to tensile strength than to flexural strength. This and the fact that pavements fail in tension suggest that the flexural strength estimated from compressive strength specimens should not be used for estimates of pavement strength. Incorporation of tensile strength specifications and relationships into codes should be strongly considered.

10.1.4 Nondestructive Tests for In Situ Strength and Modulus Estimations

Specimen shape and presence of reinforcement in a core do not significantly affect seismic modulus values obtained from resonant frequency (RF) tests as determined from 4 in. cores, 6 in. cores, 6 in. cylinders, and 6 x 6 x 20 in. beams.

Seismic tests accurately capture the increase in modulus due to increased water available during hydration. This was demonstrated by the higher moduli of water-cured cylinders compared to sand-cured cylinders; pavement covered with compound compared instead of cardboard; and core sections from the bottom of a slab rather than the top of a slab.

More research is necessary on the use of Portable Seismic Pavement Analyzer (PSPA) versus RF. Contrary to the rationale that moduli obtained using PSPA should yield higher moduli than those obtained using RF, results of SSI NDT tests show higher moduli are obtained using RF. Additionally, moduli estimated from seismic tests significantly overpredict the actual moduli obtained through destructive mechanical tests.

Seismic tests can be used to accurately predict in situ concrete strength, so long as precise prediction equations are used that account for the specific material properties. Molded specimens of the same concrete should be utilized along with seismic tests for calibration of measurements.

10.2 SMALL SLAB STUDY II

Conclusions regarding variables tested in SSII are listed below:

10.2.1 Effects of Curing History on Strength and Vertical Strength Differential

Eliminating or delaying the application of curing compound will lower concrete strengths and increase the vertical strength differential in a slab 7 days after placement, but may increase early age strength and decrease the early age vertical strength differential, depending on environmental conditions. The difference in trends is believed to be caused by the significant effects of hydration at early ages.

10.2.2 Temperature and Maturity Calculations

Widespread use of i-Buttons for long-term pavement study and maturity calculations is suggested. Results of their use were consistent, accurate, economical, and practical.

Temperatures were highly affected by the curing regime. The curing compound reflected light in the day and decreased temperatures, whereas the black plastic absorbed light and increased temperatures. Concrete not covered by any material will be more affected by ambient conditions, cooling off during hydration (10 °F in this study) if winds are high and heating up (10 °F in this study) if the sun is bright. The effects of heat from the sun on a slab with no curing compound may be greater than the effects of hydration heat retention from slabs with a curing compound, depending on the mix design and climatic conditions.

10.2.3 Evaluation of Moisture Sensors

Conclusions regarding the feasibility, accuracy, and use of the moisture sensors employed in SSII are provided below.

10.2.3.1 Aquameter Use

Because of the high variability of the Aquameter, additional research is suggested. The following guidelines are recommended for its use:

(1) Readings must be taken in the same way and at the same locations.

(2) Dust, grooves, and any other objects affecting the interface must not be present; a smooth surface is ideal.

(3) To obtain readings while the concrete is still wet, thin plastic such as Saran Wrap can be placed on the concrete where readings will be taken without significantly affecting results.

(4) Aquameter results in the lab were more satisfactory than in the field. More research is needed to resolve this disparity.

10.2.3.2 Humidity Sensor Use

The original humidity sensor was intended for use in a weather station. When it is used externally, readings must be calibrated for incident light. The new Hygro-button sensor, unavailable at the time of the experiment, or one specifically designed for concrete, should be researched to account for or prevent incident light. If the Hygro-button performs as well as the i-Buttons, accurate and cheap humidity readings in concrete may be feasible. Because conventional maturity methods assume adequate moisture for hydration, development of a device such as the Hygro-button that continuously monitors both temperature and humidity in situ may eventually replace the maturity meter as the preferred, more accurate device for quality control by the contractor and quality assurance by the agency. If so, the impact of this development on pavement (and bridge) construction will be substantial.

Appendices

Appendix A. Construction Specifics for Small Slab Study I

Table A.1 Mix Design Small Slab Study I Batches

Description	Amount		Inconsistencies
	LS	SRG	
Type I-II Cement (lb)	564	564	
Sand (lb)	1031	1040	✓
3/4" Aggregate (lb)	1700		✓
1" Aggregate (lb)	423		✓
1 1/2" Aggregate (lb)		1946	✓
Water (g)	29	29	
Air Entraining Agent (oz)	9.5	9.5	
Water Reducer (oz)	5.6	5.6	

Table A.2 Construction Sequence for Small Slab Study I Activities from March 1–3, 1999

Date	Time	Activity
March 1, 1999	12:50	LS placement (Batch 1)
	12:58	LS placement (Batch 2), Truck 1123
	13:10	LS placement (Batch 3), Truck 1137
	13:32	LS placement (Batch 4), Truck 1123
	13:35	Beams covered with plastic
	13:40	Four cylinders tested using maturity meters
	13:45	SRG placement (Batch 5), Truck 1137
	13:55	LS placement (Batch 6), Trcuk 1123
	14:10	SRG placement (Batch 7), Truck 1137
	14:25	Remove reinforcement from wood joint
	14:43	Pouring of concrete complete
	14:50	Tining and non-cured sections located by TxDOT
	15:50	Application of curing compound
March 2, 1999	8:30	CTR staff labels slab with location of day 1 cores
	9:30	Dr. Moon Won begin Vmeter measurements
	11:00	48 cylinders placed in sand curing conditions
		12 cylinders transported to lab (6 LS, 6 SRG)
	13:15	Day 1 cores drilled until 14:06 (6 LS, 6 SRG)
	14:20	Day 1 cylinders tested in compression (no water or sand curing)
	14:40	Day 1 cylinders tested in tension (no water or sand curing)
March 4, 1999	8:30	UT El Paso begins PSPA measurements
	10:20	Day 3 cores drilled until 11:26 (6 LS, 6 SRG)
	11:52	Day 3 reinforced 4 in. cores drilled (3 single, 3 double)
	12:35	Day 3 reinforced 4 in. cores drilled (3 no mat, 3 double)

Table A.3 Properties of Concrete Batches Used in Small Slab Study I

Batch	Slump (in.)	Air Content (%)	Conc. Temp. (F)	Unit Weight (pcf)	Beams made	Cylinders made
2	3	5.4	70.3	170.55	30	60
7	3	5	73.2	165.35	30	60
5			72			

Table A.4 Distribution of Concrete Batches for Small Slab Study I

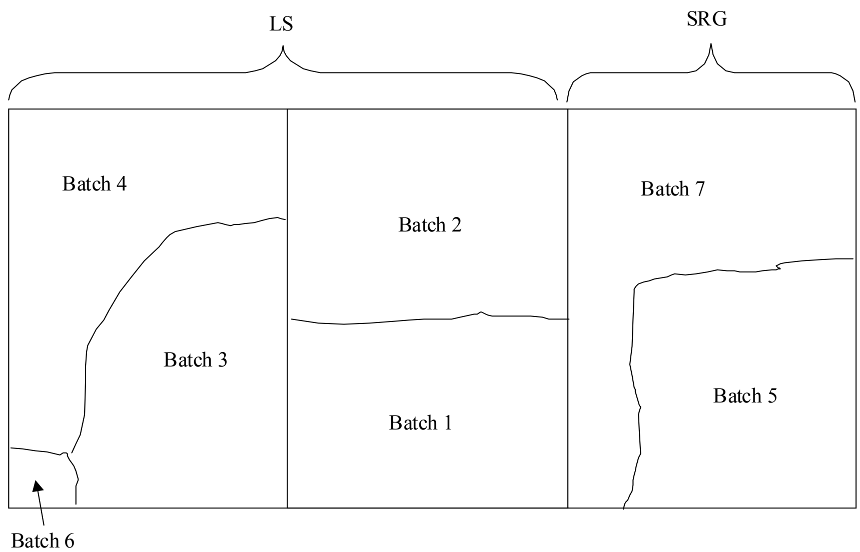

Appendix B. Detailed Coring Layouts for Small Slab Study I

Table B.1 Typical Coring Layout for Small Slab Study I Sections

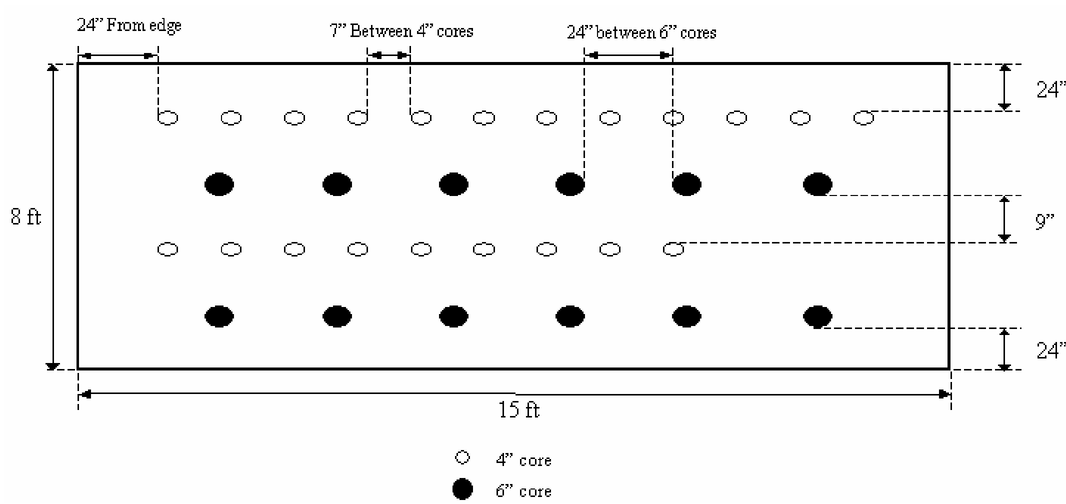

Table B.2 Core Identification Layout for Unreinforced LS Slabs

(Batch 2 used for upper LS section and Batch 1 used for lower LS section)

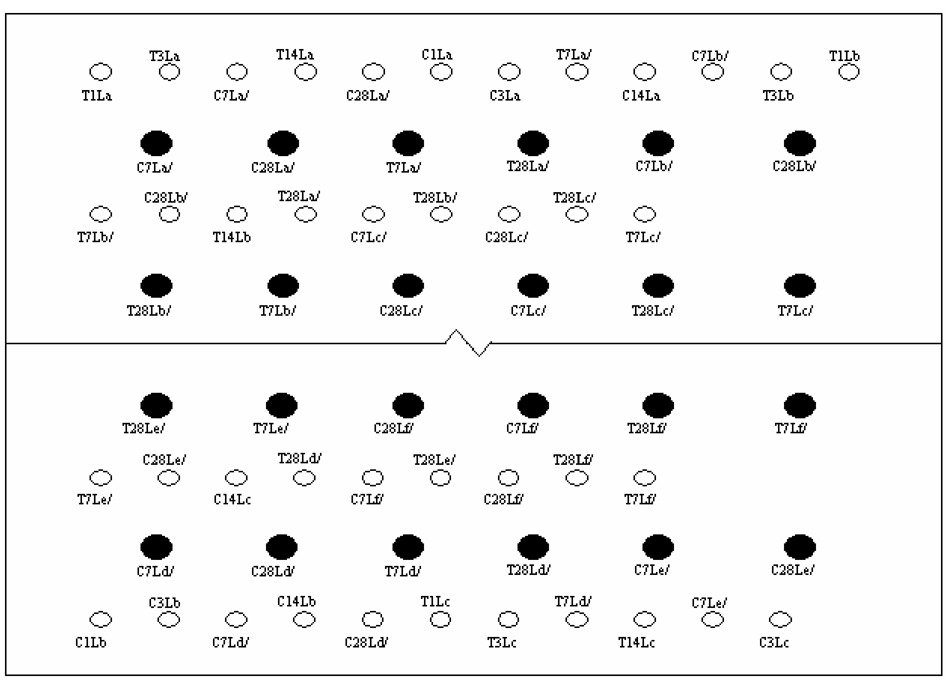

Table B.3 Core Identification Layout for SRG Sections
(Batches 5 and 7 were used as indicated for the upper and lower batches)

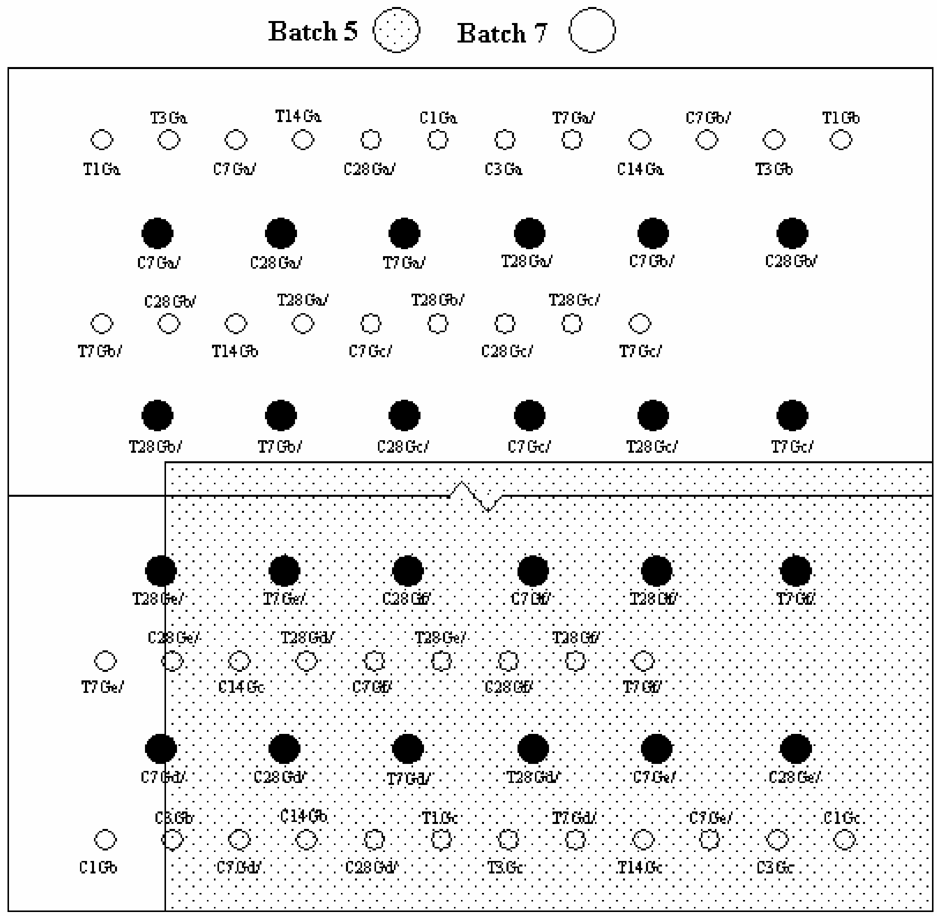

Table B.4 Core Labels with Associated Strengths

Aggregate	Age (days)	Tensile Strength (psi)				Compressive Strength (psi)			
		4 in. cores	Label	6 in. cores	Label	4 in. cores	Label	6 in. cores	Label
LS	1	362	T1LA			2308	C1LA		
		296	T1LB			2984	C1LB		
		416	T1LC			3223	C1LC		
	3	537	T3LA			2944	C3LA		
		438	T3LB			2387	C3LB		
		497	T3LC			2626	C3LC		
	7	537	T7LA	477	T7LA	3979	C7LA	2918	C7LA
		458	T7LB	464	T7LB	3024	C7LB	2829	C7LB
		438	T7LC	380	T7LC			3138	C7LC
	14	517	T14LA			3422	C14LA		
		517	T14LB			4337	C14LB		
		587	T14LC			4536	C14LC		
	28	477	T28LA	442	T28LA	5411	C28LA	4580	C28LA
		557	T28LB	495	T28LB	3342	C28LB	3979	C28LB
		487	T28LC	424	T28LC	5292	C28LC	4456	C28LC
SRG	1	371	T1GA			2666	C1GA		
		311	T1GB			3302	C1GB		
		271	T1GC			2944	C1GC		
	3	477	T3GA			3422	C3GA		
		438	T3GB			3342	C3GB		
		448	T3GC			3820	C3GC		
	7	468	T7GA	433	T7GA	3979	C7GA	3784	C7GA
		517	T7GB	376	T7GB	3740	C7GB	3678	C7GB
		408	T7GC	345	T7GC	3740	C7GC	2617	C7GC
	14	497	T14GA			4377	C14GA		
		438	T14GB			4496	C14GB		
		358	T14GC			3899	C14GC		
	28	468	T28GA	393	T28GA	4377	C28GA	4067	C28GA
		527	T28GB	486	T28GB	4655	C28GB	4067	C28GB
		477	T28GC	460	T28GC	5610	C28GC	4280	C28GC

Table B.5 Cut Cores Labels with Associated Top/Bottom Strengths

Strength (ksi)	Age (days)	Agg.	Pos	4 in.			6 in.		
				Strength	ID	Batch	Strength	ID	Batch
Compressive	7	LS	top	3.979	C7LD	1	3.289	T7LD(C)	1
				4.098	C7LE	1	3.148	C7LD	1
				3.342	C7LF	1	3.218	T7LE(C)	1
							3.077	C7LF	1
							3.431	T7LF(C)	1
			bott	3.74	C7LD	1	4.739	T7LD(C)	1
				5.093	C7LE	1	4.492	C7LD	1
				4.974	C7LF	1	4.173	T7LE(C)	1
							4.209	C7LF	1
							4.368	T7LF(C)	1
		SRG	top	3.024	C7GE	5	2.794	T7GD(C)	5
				3.382	C7GF	5	4.987	C7GE	5
			bott	4.974	C7GE	5	3.997	T7GD(C)	5
				4.456	C7GF	5	3.36	C7GE	5
	28	LS	top				4.492	C28LD	1
							3.714	C28LE	1
							3.784	CS8LF	1
			bott				5.164	C28LD	1
							5.553	C28LE	1
							5.199	CS8LF	1
		SRG	top				0		
							3.183	C28GE	5
							4.527	G28GF	5
			bott				0		
							5.164	C28GE	5
							3.537	G28GF	5
Tensile	7	LS	top	0.504	T7LD	1	0.424	C7LE(T)	1
				0.464	T7LE	1	0.389	T7LF	1
				0.345	T7LF	1			
			bott	0.504	T7LD	1	0.389	C7LE(T)	1
				0.517	T7LE	1	0.424	T7LF	1
				0.438	T7LF	1			
		SRG	top	0.345	T7GD	5	0.389	T7GF	5
				0.424	T7GE	7	0.495	C7GF(T)	5
				0.411	T7GB*	7	0.513	T7GE	5
			bott	0.424	T7GD	5	0.301	T7GF	5
				0.438	T7GE	7	0.504	C7GF(T)	5
				0.477	T7GB*	7	0.424	T7GE	5
	28	LS	top	0.519	C28LD(T)	1	0.513	T28LD	1
				0.519	C28LE(T)	1	0.522	T28LE	1
				0.637	C28LF(T)	1	0.539	T28LF	1
			bott	0.566	C28LD(T)	1	0.575	T28LD	1
				0.613	C28LE(T)	1	0.486	T28LE	1
				0.66	C28LF(T)	1	0.495	T28LF	1
		SRG	top	0.377	C28GD(T)	5	0.407	T28GD	5
				0.433	C28GE(T)	5	0.424	T28GE	5 OR 7
				0.472	C28GF(T)	5	0.407	T28GF	5
			bott	0.424	C28GD(T)	5	0.433	T28GD	5
				0.433	C28GE(T)	5	0.513	T28GE	5 OR 7
				0.566	C28GF(T)	5	0.46	T28GF	5

Appendix C. Small Slab Study I Destructive Test Raw Data and p-Values from Statistical Analysis Results

**Note: Statistical analysis of "corrected" denotes no crossed-out data was included in analysis. Bold text in results tables indicates significance of variables.*

Table C.1 Standard 4 in. and 6 in. Core Strengths

Age (days)	Aggregate	Compressive Strength (ksi)				Tensile Strength (ksi)			
		Core Diameter (in.)				Core Diameter (in.)			
		4		6		4		6	
		Value	Avg.	Value	Avg.	Value	Avg.	Value	Avg.
7	LS	3.979	3.502	2.918	2.977	0.537	0.478	0.477	0.440
		3.024		2.829		0.458		0.464	
				3.183		0.438		0.380	
	SRG	3.979	3.820	3.784	3.731	0.468	0.464	0.433	0.385
		3.740		3.678		0.517		0.376	
		3.740		2.617		0.408		0.345	
28	LS	5.411	5.352	4.580	4.338	0.477	0.507	0.442	0.454
		5.292		3.979		0.557		0.495	
		3.342		4.456		0.487		0.424	
	SRG	4.377	4.516	4.067	4.138	0.468	0.491	0.393	0.446
		4.655		4.067		0.527		0.486	
		5.610		4.280		0.477		0.460	

Table C.2 Statistical Analysis Results of Data in Table C.1

Variable	Compressive Tests		Tensile Tests
	Original Data	Corrected Data	All Data
Aggregate Type	0.5362	0.9260	0.1980
Age at Testing	**0.0001**	**0.0001**	0.0755
Core Diameter	0.0300	**0.0070**	**0.0059**
n	23	20	24
r^2	0.6163	0.7312	0.425

Table C.3 Water-Cured and Sand-Cured Cylinder Strengths

Age (days)	Description	Aggregate	Compressive strength (ksi)		Tensile strength (ksi)	
7	6 in. Cylinder: Sand-cured	SRG	3.890	3.902	0.396	0.360
			3.678		0.360	
			4.138		0.324	
		LS	2.936	3.360	0.382	0.346
			3.608		0.330	
			3.537		0.327	
	6 in. Cylinder: Water-cured	SRG	3.997	4.020	0.425	0.416
			4.067		0.416	
			3.997		0.407	
		LS	4.032	4.044	0.442	0.419
			4.014		0.399	
			4.085		0.415	
	6 in. Core	SRG	3.784	3.360	0.433	0.385
			3.678		0.376	
			2.617		0.345	
		LS	2.918	2.977	0.477	0.440
			2.829		0.464	
			3.183		0.380	
28	6 in. Cylinder: Sand-cured	SRG	4.138	4.315	0.376	0.385
			4.527		0.389	
			4.280		0.389	
		LS	4.138	4.056	0.367	0.380
			4.209		0.376	
			3.820		0.398	
	6 in. Cylinder: Water-cured	SRG	4.916	4.904	0.469	0.463
			4.881		0.451	
			4.916		0.469	
		LS	4.739	4.757	0.433	0.457
			4.651		0.460	
			4.881		0.477	
	6 in. Core	SRG	4.067	4.138	0.393	0.446
			4.067		0.486	
			4.280		0.460	
		LS	4.580	4.338	0.442	0.454
			3.979		0.495	
			4.456		0.424	

Table C.4 Statistical Analysis Results of Data in Table C.3

Variable	Compressive Tests			Tensile Tests		
	all samples	water vs. core	sand vs. core	all samples	water vs. core	sand vs. core
Curing method	**0.0001**	**0.0001**	0.1733	**0.0001**	0.5974	**0.0004**
Age	**0.0001**	**0.0001**	**0.0001**	**0.0012**	**0.0086**	**0.0355**
Aggregate type	0.067	0.5083	0.106	0.5082	0.2953	0.4567
n	36	24	24	16	10	4
r^2	0.783	0.845	0.644	0.625	0.332	0.545

Table C.5 Data Selected for Development of Strength Regressions

Aggrega	Age (days	Tensile Strength (psi				Compressive Strength (psi				Flexural (psi
		4 in. cores	6 in. cores	Water cured cylinder	Sand cured cylinder	4 in. cores	6 in. cores	Water cured cylinder	Sand cured cylinder	Water-beam
LS	1	362		*238*	265	230		167	206	
		296		212	274	298		213	193	
		416		225	247	322		215	229	
	3	537		406	355	294		290	304	595
		438		358	367	238		346	348	560
		497		362	342	262		325	290	575
	7	537	477	442	382	397	291	403	293	650
		458	464	399	330	302	282	401	360	590
		438	380	415	327		313	408	353	580
	14	517		429	393	342		431	435	700
		517		380	407	433		443	403	660
		587		376	376	453		443	403	710
	28	477	442	433	367	541	458	473	413	670
		557	495	460	376	334	397	465	420	720
		487	424	477	398	529	445	488	382	800
SR	1	371		248	234	266		225	232	
		311		252	217	330		216	225	
		271		252	248	294		215	237	
	3	477		392	383	342		302	343	525
		438		329	271	334		346	279	515
		448		347	347	382		336	311	530
	7	468	433	425	396	397	378	399	389	600
		517	376	416	360	374	367	406	367	570
		408	345	407	324	374	261	399	413	560
	14	497		433	424	437		468	447	600
		438		469	420	449		482	389	610
		358		407	469	389		468	435	540
	28	468	393	469	376	437	406	491	413	740
		527	486	451	389	465	406	488	452	670
		477	460	469	389	561	428	491	428	750

Table C.6 Statistical Analysis Results of Strength Relationship Models from Data in

Variable	Compressive vs. Tensile	Compressive vs. Flexural	Tensile vs. Flexural
	Corrected Data	Corrected Data	Corrected Data
n	101	78	83
r^2	0.9840	0.9938	0.9781

Table C.7 Strength of Cores from Reinforced LS Section Regressions

Age (days)	Description	Compressive Strength (ksi)			Tensile Strength (ksi)		
		Steel Present?	Strength	Avg.	Steel Present?	Strength	Avg.
3	Double				yes	0.517	0.4575
					yes	0.398	
					no	0.318	0.318
	Single				yes	0.458	0.4675
					yes	0.477	
					no	0.438	0.438
	No Steel				no	0.537	0.491
					no	0.438	
					no	0.497	
14	Double	yes	5.411	5.411	no	0.577	0.567
		yes	5.411		no	0.557	
		yes	~~4.178~~		no	0.567	
	Single	yes	~~3.263~~	4.775	no	0.517	0.532
		yes	5.173		no	0.547	
		yes	4.377		no	~~0.438~~	
	No Steel	no	~~3.422~~	4.437	no	0.517	0.540
		no	4.337		no	0.517	
		no	4.536		no	0.587	
27	Double	yes	4.974	4.934			
		yes	4.894				
		yes	4.934				
		no	4.615	4.469			
		no	4.496				
		no	4.297				
	Single	yes	~~4.098~~	5.192			
		yes	5.371				
		yes	5.013				
		no	4.695	4.801			
		no	4.974				
		no	4.735				
	No Steel	no	5.411	5.352			
		no	~~3.342~~				
		no	5.292				

Table C.8 Statistical Analysis Results of Data in Table C.7

Variable	Compressive Tests		Tensile Tests
	Original Data	Corrected Data	Original Data
No. of mats	0.8530	0.9890	0.223
Presence of Steel	0.4160	**0.0390**	0.151
Age	0.2610	0.2310	-
n	24	19	8
r^2	0.1319	0.3255	0.6557

Table C.9 Strengths of 4 x 6 in. Cores from Tined and Uncured Slab Sections (* denotes 4 x 8 in. specimens)

Aggregate	Surface Treatment	Compressive Strength (ksi)			Tensile Strength (ksi)		
		Strength	Avg.		Position	Strength	Avg.
LS	No compound/	~~4.934~~	3.741	*	top	0.557	0.517
	No tining	3.820				0.477	
		3.661			bott	0.743	0.717
						0.690	
	Compound/	~~4.814 *~~	4.079		top	0.491	0.524
	Tined	4.138				0.557	
		4.019			bott	0.637	0.604
						0.570	
	Compound/	5.411	5.352		top	0.519	0.519
	No tining	~~3.342~~				~~0.637~~	
		5.292				0.519	
					bott	0.566	0.613
						0.613	
						0.660	
SRG	No compound/	~~5.173~~	4.019	*	top	0.451	0.471
	No tining	3.820				0.491	
		4.218			bott	0.504	0.484
						0.464	
	Compound/	4.735	5.000		top	0.464	0.498
	Tined	5.013				0.531	
		5.252			bott	0.517	0.544
						0.570	
	Compound/	4.377	4.516	*	top	0.377	0.427
	No tining	4.655				0.433	
		~~5.610~~				0.472	
					bott	0.424	0.429
						0.433	
						~~0.566~~	

* See Section

Table C.10 Statistical Analysis Results of Data in Table C.9

Samples Used	Variable	Compressive Tests		Tensile Tests	
		Original Data	Corrected Data	Original Data	Corrected Data
All samples	Aggregate Type	0.2402	0.5223	**0.0010**	**0.0001**
	Curing and/or Tining	0.4021	**0.0308**	0.5047	0.1690
	Position	-	-	**0.0044**	**0.0028**
	n	18	13	28	23
	r^2	0.1977	0.5514	0.6090	0.6735
No tine: Uncured vs. Cured	Aggregate Type	0.6398	0.2557	**0.0010**	**0.0001**
	Curing and/or Tining	0.2755	**0.0054**	0.3100	0.1001
	Position	-	-	**0.0156**	**0.0126**
	n	13	9	20	18
	r^2	0.1418	0.7579	0.6803	0.7528
Cured: Tine vs. No tine	Aggregate Type	0.3041	0.8390	**0.0012**	**0.0010**
	Curing and/or Tining	0.8605	0.5035	0.3625	0.0988
	Position	-	-	**0.0406**	**0.0218**
	n	13	9	20	18
	r^2	0.1103	0.0718	0.5714	0.6785

Table C.11 Strengths of Cores from the Top and Bottom of Slab (4 x 6 in. and 6 x 6 in.)

Core Size (in)	Age (days)	Aggregate	Position	Compressive strength (ksi)		Tensile strength (ksi)	
				Data	Avg.	Data	Avg.
4	7	LS	top	3.979	4.039	0.504	0.484
				4.098		0.464	
				~~3.342~~		~~0.345~~	
			bott	~~3.74~~	5.034	0.504	0.511
				5.093		0.517	
				4.974		~~0.438~~	
		SRG	top	3.024	3.203	~~0.345~~	0.418
				3.382		0.424	
						0.411	
			bott	4.974	4.715	0.424	0.431
				4.456		0.438	
						~~0.477~~	
	28	LS	top			0.519	0.519
						0.519	
						~~0.637~~	
			bott			0.566	0.613
						0.613	
						0.66	
		SRG	top			~~0.377~~	0.453
						0.433	
						0.472	
			bott			0.424	0.429
						0.433	
						~~0.566~~	
6	7	LS	top	3.289	3.233	0.424	0.407
				3.148		0.389	
				3.218			
				3.077			
				3.431			
			bott	~~4.739~~	4.311	0.389	0.407
				4.492		0.424	
				4.173			
				4.209			
				4.368			
		SRG	top	2.794	3.891	~~0.389~~	0.504
				4.987		0.495	
						0.513	
			bott	3.997	3.679	~~0.301~~	0.464
				3.36		0.504	
						0.424	
	28	LS	top	~~4.492~~	3.749	0.513	0.525
				3.714		0.522	
				3.784		0.539	
			bott	5.164	5.182	~~0.575~~	0.491
				~~5.553~~		0.486	
				5.199		0.495	
		SRG	top	*0*	3.855	0.407	0.413
				3.183		0.424	
				4.527		0.407	
			bott	*0*	4.351	0.433	0.447
				5.164		~~0.513~~	
				3.537		0.46	

cores)

Table C.12 Statistical Analysis Results of Data in Table C.11

	Description	Compressive Tests		Tensile Tests	
		4 in. cores	6 in. cores	4 in. cores	6 in. cores
Original Data	Aggregate	0.4957	0.338	**0.0012**	**0.0576**
	Age	-	**0.02**	**0.003**	0.247
	Position	**0.0143**	**0.003**	**0.0043**	0.9502
	n	10	24	24	22
	r^2	0.6107	0.4777	0.5977	0.2529
Corrected Data	Aggregate	**0.0268**	0.9990	**0.0000**	0.7930
	Age	-	0.0650	**0.0180**	0.3130
	Position	**0.0011**	**0.0110**	0.1000	0.6000
	n	8	21	17	17
	r^2	0.9167	0.4134	0.7804	0.1084

Table C.13 Statistical Analysis Results of Data in Table C.11 Separated by Aggregate Type

Aggregate	Data used in analysis	Description	Compressive Tests		Tensile Tests	
			4 in. cores	6 in. cores	4 in. cores	6 in. cores
Limestone	Original data	Age	-	**0.0001**	**0.0053**	**0.0006**
		Position	0.1811	**0.0001**	0.1616	0.8560
		n	6	16	12	10
		r^2	0.3955	0.9175	0.6348	0.8328
	Corrected data	Age	-	**0.0001**	**0.0211**	**0.0002**
		Position	**0.0071**	**0.0001**	**0.0371**	0.2034
		n	4	13	9	9
		r^2	0.9859	0.9639	0.7912	0.9175
SRG	Original data	Age	-	0.6740	0.3091	0.9416
		Position	**0.0407**	0.8503	0.1161	1.0000
		n	4	8	12	12
		r^2	0.9202	0.0456	0.3174	0.0006
	Corrected data	Age	-	0.6740	0.2662	0.0810
		Position	**0.0407**	0.8503	0.7027	0.9928
		n	4	8	8	8
		r^2	0.9202	0.0456	0.2570	0.4871

Appendix D. Small Slab Study I NonDestructive Test Raw Data and p-Values from Statistical Analysis Results

Table D.1 Moduli of Molded Specimens and Standard Cores from Resonant Frequency Tests

Description		Modulus, Gpa									
		Day 1		Day 3		Day 7		Day 14		Day 28	
		Data	Avg.	Data	Avg.	Data	Avg.	Data	Avg.	Data	Avg.
Sand-cured	LS	30.6	30.0	34.6	34.9	38.8	37.0	37.9	37.5	40.1	40.3
Cylinders		28.6		35.1		36		36.8		38.6	
		30.6				36.2		37.8		40.1	
		30.6				37.6				41.5	
		29.0				36.3				40.9	
		30.4				37.3				40.4	
	SRG	23.9	25.2	29	29	31	30.9	31.7	31.5	32.9	33.1
		25.7		29		30.4		32.2		33.4	
		26.3				31.3		30.5		33.1	
		25.2				31.3				32.9	
		25.8				30.3				32.9	
		24.5				31.2				33.4	
Water-cured	LS	29.8	29.6	35.9	36.0	38.5	38.6	40.2	39.8	41.1	41.6
Cylinders		29.2		35.9		38.8		39.5		41.7	
		29.4		35.6		38		39.7		42	
		27.6		35.6		39		40.4		41.4	
		31.4		36.3		38.7		38.9		42.6	
		30		36.4		38.8		40		40.5	
	SRG	25.4	25.5	30.5	29.9	32.2	32.0	32.7	32.9	33.7	33.9
		25.3		30.1		32.3		32.9		34.3	
		25.7		29.2		32		32.9		33.7	
		25.6		29.7		32.2		33.1		33.5	
		25.7		29.6		31.3		32.2		34.5	
		25.5		30		32		33.6		33.7	
Water-cured	LS	30.7	30.5	36.3	36.5	39.3	38.8	39.9	39.2	41.4	40.7
Beams		30.2		36.8		38.8		39.3		40.4	
				36.3		38.3		38.3		40.4	
	SRG	24.7	24.9	30.9	30.2	32.8	32.4	33.7	33.3	34.2	34.0
		25.1		30		31.9		33.3		34.2	
				29.6		32.4		32.8		33.5	
4 in. Cores	LS	30.2	30.7	34.9	34.7	36.2	35.3	35.6	37.1	36.8	38.5
		28.5		32.9		35.6		37		39	
		30.5		35.6		34.3		39.1		37.8	
		31.8		33.4		36.2		36.6		37.6	
		32.5		36		33.2		37.9		39.6	
				35.1		36		36.4		39.9	
	SRG	23.9	25.4	28	29.0	28	29.1	28.9	28.8	32	31.3
		25.3		30.4		27.5		29		31.8	
		25.9		31		29.3		29.2		30.4	
		25		27.8		29		28.9		30.9	
		25.1		26.6		30.3		29.7		29.4	
		27.4		30.4		30.2		26.9		33.3	
6 in. Cores	LS					35.2	35.6			36.8	36.7
						35.4				37.9	
						36.1				35.8	
						35.7				36.7	
						36.2				37.4	
						35				35.4	
	SRG					29.9	29.4			29.9	29.9
						30.2				30.1	
						28.5				29	
						29.8				30	
						30.4				29.8	
						27.3				30.5	

Table D.2 Statistical Analysis Results of 4 in. versus 6 in. Core Moduli from RF

Variable	
Aggregate	**0.0001**
Age	**0.0001**
Mold	0.4749
n	87
r^2	0.9109

Table D.3 Statistical Analysis Results of Water-Cured Cylinder and Beam Moduli from RF

Variable	
Age	**0.0001**
Aggregate type	**0.0001**
Diameter	0.0859
n	82
r^2	0.904

Table D.4 Statistical Analysis Results of Cylinder Curing Moduli Comparisons from RF

Variable	All samples	Water-cured Cylinders vs. Cores	Sand-cured Cylinders vs. Cores	Sand-cured Cylinders vs. Water-cured Cylinders
Curing Method	**0.0001**	-	-	-
Age	**0.0001**	**0.0001**	**0.0001**	**0.0001**
Aggregate type	**0.0001**	**0.0001**	**0.0001**	**0.0001**
Sample Type	0.7349	**0.0001**	**0.0038**	**0.0001**
n	192	146	104	133
r^2	0.8688	0.8537	0.8511	0.9259

Table D.5 Moduli of Reinforced Slab and Cores

Test	Description	Moduli (GPa) Resonant Frequency								
		Day 3			Day 14			Day 28		
		Steel Present		Avg.	Steel Present		Avg.	Steel Present		Av.g
RF	Single Mat	✓	35.8	34.2		37.7	37.8		38	38.8
		✓	31.9			37.7			40.3	
		✓	31.8			37.9			38.1	
		✓	33.1		✓	33.7	35.3	✓	33.5	38.0
		✓	35.1		✓	40.5		✓	37.5	
		✓	37.1		✓	31.7		✓	43	
		✓	35.3							
		✓	33.7							
	Double Mat	✓	32.7	35.0		33.6	36.0		40.9	39.6
		✓	33.8			36.7			38.2	
		✓	37.3			37.7			39.7	
		✓	36.3		✓	37.4	35.2	✓	39.8	39.0
					✓	37		✓	39.2	
					✓	31.3		✓	38.1	
PSPA						32.8	34.4			
						34.2				
						36.2				
					✓	33.1	35.6			
					✓	35.6				
					✓	38.1				
						32.3	33.9			
						34.1				
						35.3				
					✓	38.1	36.5			
					✓	33.8				
					✓	37.6				

Table D.6 Seismic Moduli of Reinforced Slab and Cores

Variable	RF testing
Presence of steel	0.2876
Single or double mats	0.53378
Age	**0.0001**
n	54
r^2	0.4033

Table D.7 Seismic Moduli of Slabs With and Without Curing Compound from PSPA

Coated				Uncoated			
LS		SRG		LS		SRG	
Age, hrs.	Moduli, Gpa	Age, hrs.	Moduli, Gpa	Age, hrs.	Moduli, Gpa	Age, hrs.	Moduli, Gpa
6.25	6.5	5.25	5	7.8	9.2	6.75	7.1
6.45	7.1	5.7	5.9	8.35	10.4	7.25	8
7	8.2	6.25	7	9.13	11.7	8	9.2
7.33	9.1	6.6	8.1	9.62	13.1	8.5	9.8
7.83	10.4	6.98	9.1	10.33	14.7	9.25	10.9
8.25	11.7	7.55	10.4	11.05	16.5	10	12.6
8.92	13.3	8.2	11.3	11.9	18.3	10.75	13.8
9.58	15.7	8.7	12.9	23.5	26.5	22	23.4
10.17	17.2	9.5	14.6	69	30.2	68	26.5
10.83	18.3	10.3	16	165	31.7	164	27.2
11.58	20.3	10.95	17.1	330	33.1	330	27.7
12.33	21.4	22.25	24.7	670	33.9	670	29.1
24	28.5	68	26.9				
69	32.2	164	27.8				
165	33.8	330	28				
330	34.4	670	28.8				
670	34.8						

Table D.8 Statistical Analysis Results of Moduli from Curing Compound Analysis from PSPA

Variable	P-value
Aggregate type	**0.0178**
Compound	0.9353
Age	**0.0001**
n	58
r^2	0.7176

Table D.9 Moduli of Top and Bottom 4 in. Cores from RF

Position	Moduli, Gpa			
	LS		SRG	
	Data	Avg.	Data	Avg.
Top	36	35.1	28.1	28.8
	35		27.3	
	34.6		27.8	
	35.1		28.6	
	33.6		32	
	36.1			
Bottom	37.3	38.2	31.8	30.9
	36.4		31.4	
	37.7		28.3	
	40.2		30.9	
	38.7		31.9	
	39.1			

Table D.10 Statistical Analysis Results of Moduli of Top and Bottom Cores from RF

Variable	All	LS	SRG
Position	**0.0003**	**0.0009**	0.0849
Aggregate type	**0.0001**	-	-
n	22	11	9
r^2	0.8857	0.6876	0.3257

Table D.11 Slab Modulus Values over Core Locations Using PSPA

Aggregate		Modulus, Gpa									
		Day 1		Day 3		Day 8		Day 14		Day 28	
		Data	Avg	Data	Avg	Data	Avg	Data	Avg	Data	Avg
4 in.	LS	27.9	28.3	32.3	32.4	35	33.4	35.3	34.9	34.7	35
		26.7		30.5		32.2		32.9		34.9	
		28.6		33		33.4		35.9		35.6	
		28.8		33.5		33.6		34.5		34.1	
		28.7		32.4		32.9		35.7		34.5	
		29.1		32.5		33.2		35.1		36.2	
	SRG	22.6	23.3	26.8	27.1	25.7	27.5	29.5	28.6	29.8	30.3
		23		29.5		26.9		27.6		31.2	
		24.1		27.4		28.1		28.6		30.1	
		22.9		26		26.5		28.7		30.3	
		22.3		26.1		29.5		29.3		28.6	
		24.7		27		28.4		27.9		31.6	
6 in.	LS					34.3	32.4			35.2	34.6
						30.9				31.9	
						31.5				36.6	
						31					
						34.5					
						32.4					
	SRG					27.5	27.5			31.2	29.4
						28.5				28.3	
						28.4				27.4	
						27.4				29.6	
						26.3				29.8	
						27				29.9	

Table D.12 Statistical Analysis Results of PSPA versus RF Tests

Variable	p-value
Aggregate	0.0001
Core Diameter	0.0507
Age	0.0001
Test Method	0.0001
n	163
r^2	0.9067

Table D.13 Moduli from Destructive Tests

Specimen	Agg.	Description	Modulus, Gpa									
			Day 1		Day 3		Day 7		Day 14		Day 28	
				Avg.		Avg.		Avg.		Avg.		Avg.
Sand-cured	LS		22	23	23	23	29	24	28	31	34	32
Cylinders			24		24		19		33		31	
	SRG		17	17	28	25	27	25	25	25	28	24
			17		22		24		25		19	
Water-cured	LS		20	19	31	26	31	31	33	32	33	33
Cylinders			19		22		32		30		33	
	SRG		18	18	23	20	25	23	22	23	28	28
			18		17		22		25		28	
4" Full Core	LS		23	22	32	32	18	18	29	26	26	41
			22		32				23		56	
	SRG		25	24	17	21	24	27	24	24	25	25
			23		25		29		24		24	
6" Full Core	LS						28	28			27	33
							28				38	
	SRG						26	24			24	23
							23				22	
4" Full Core	LS	Cardboard									28	34
											40	
	SRG										20	26
											32	
	LS	Tined									28	28
	SRG										23	23
											23	
4" Full Core	LS	S w/ Steel									44	35
w/ Steel											25	
		S w/out Steel									28	34
											40	
		D w/ Steel									25	29
											33	
		D w/out Steel									28	34
											40	

Appendix E. Construction Specifics for Small Slab Study II

Table E.1 Construction Sequence for Small Slab Study II Activities on March 28, 2001

Time		Description	
Begin	Complete	Action	Batch
11:03	11:12	Poured slab O	1
11:04	11:20	Poured slab N	1
11:11		Cast cylinders	1
11:13	11:31	Poured slab S	1
11:21	11:46	Poured slab 2	2
11:26	11:41	Poured slab 8	2
11:31		Cast cylinders	2
11:33	11:42	Poured slab P	2
12:02		Burlap finish	
12:12		Applied plastic sheeting	
12:05	12:08	Applied MMF on S, 2, and 8	
12:08		Weather station moved to new location	
12:15		Began ambient I-button	
12:35		Microwave sensors added	
1:01		Curing compound applied to section O	
2:21		Curing compound applied to section S	
4:35		Curing compound applied to section 2	
10:30		Curing compound applied to section 8	

Table E.2 Properties of Concrete Batches Used in Small Slab Study II

Description	Weight	
	Batch 1	Batch 2
Type I-II (lb)	2135	2130
3/4" Aggregate (lb)	12285	12260
Water (lb)	1033	882
Fly Ash (lb)	903	930
Air Entraining Agent (oz)	22	14
Sand (lb)	10120	10140
Water Reducer (lb)	304	304

Table E.3 Batch Mixes Used in Small Slab Study II

Batch	Slump (in.)	Air Content (%)	Unit weight (pcf)	Cylinders made
1	3	6		20
2	2 1/2	6	142.8	20

Appendix F. Raw Data Used in Nondestructive Tests of Small Slab Study I

Table F.1 Cylinder Strengths, Testing Times, and Equivalent Ages

'Age'	ID	Compr							Tensile						
		Time	Age,		Batch	Load,	Strength,		Time	Age,		Batch	Load,	Strength,	
			hrs.	Equiv.		lbs.	psi	avg.		hrs.	Equiv.		lbs.	psi	avg.
1	a	2:45	26.75	26	1	18890	668	752			*26*	1	9990	139	145
	b			*26*	1	20500	725				*26*	2	11000	153	
	c			*26*	2	24400	863				*26*	2	10300	143	
3	a	10:35	70.60	78		37180	1315	1380	9:40	69.70	76		23100	321	301
	b	11:56	72.00	79		38460	1360		9:50	69.80	76		21370	297	
	c	12:10	72.20	79		41450	1466		10:00	70.00	76		20620	286	
7	a	10:24	166.40	183	2	60400	2136	2002	8:53	164.88	182	1	22670	315	329
	b			*183*	1	61050	2159		9:10	165.17	182	2	27940	388	
	c			*183*	2	48400	1712				*182*	1	20500	285	
14	a	11:30	335.50	391	1	56500	1998	2431	11:05	335.08	390	1	19740	274	267
	b	12:35	336.58	392	1	75520	2671		11:11	335.18	390	1	17350	241	
	c	12:38	336.63	392	2	74200	2624		11:16	335.27	390	2	20640	287	
28	a	1:08			2	91790	3246	3182	10:59			1	33290	462	397
	b	1:10			2	92180	3260		11:05			1	25430	353	
	c	11:15			1	85970	3041		11:10			2	27010	375	

* *Italics* signify estimates

Table F.2 Tensile Strength, Testing Times, and Equivalent Age of 3-Day Cores

Slab ID			Time	Age	Load	Equiv. days			Predicted Strength	Actual/Predicted Strength		
				hrs.	lbs.	I-button	Meter	Used			avg. by depth	avg. by slab
N	a	w	12:40	72.6	3000	86		86	261	0.77	0.91	0.99
		x			3620		89	89	265	0.91	0.93	
		z			4680	93		93	270	1.16	1.13	
	b	w	1:00	73.0	3810	86		86	261	0.97		
		x			4140		89	89	265	1.04		
		z			3780	93		93	270	0.93		
	c	w	1:28	73.5	3900	86		86	261	1.00		
		x			3350		90	89	265	0.84		
		z			5280	93		93	270	1.31		
O	a	w	1:33	73.5	3470			80	253	0.91	0.95	1.13
		x			3540		99	80	253	0.93	1.03	
		z			4680	70		80	253	1.23	1.42	
	b	w	1:40	73.6	4240			80	253	1.12		
		x			3800		99	80	253	1.00		
		z			5280	70		80	253	1.39		
	c	w	1:49	73.8	3120			80	253	0.82		
		x			4340		99	80	253	1.14		
		z			6250	70		80	253	1.65		
S	a	w	10:18	70.3	2470			86	261	0.63	0.76	1.10
		x			2640		86	86	261	0.67	0.94	
		z			6230			86	261	1.59	1.60	
	b	w	10:26	70.5	2790			86	261	0.71		
		x			3970		86	86	261	1.01		
		z			6510			86	261	1.66		
	c	w	10:06	70.0	3690			86	261	0.94		
		x			4370		86	86	261	1.12		
		z			6080			86	261	1.55		
2	a	w	12:35	72.5	4400	84		84	258	1.14	1.01	1.10
		x			4540			89	265	1.14	1.05	
		z			5670	96		96	273	1.38	1.24	
	b	w	12:45	72.8	3460	84		84	258	0.89		
		x			4320			89	265	1.09		
		z			4520	96		96	273	1.10		
	c	w	1:00	73.0	3910	84		84	258	1.01		
		x			3600			89	265	0.91		
		z			5060	96		96	273	1.23		
8	a	w	12:26	72.5	5080	82		82	256	1.33	1.25	1.29
		x			5360		92	92	268	1.33	1.25	
		z			5330	95		95	272	1.31	1.36	
	b	w	12:16	72.8	5220	82.7		82.7	256	1.36		
		x			5360		92.5	92.5	269	1.33		
		z			6160	95		95	272	1.51		
	c	w	1:19	73.3	4080	82.5		82.5	256	1.06		
		x			4400		93	93	270	1.09		
		z			5150	95		95	272	1.26		
P	a	w	1:58	74.0	4460			109	289	1.03	0.99	1.12
		x			4040		109	109	289	0.93	0.99	
		z			6140			109	289	1.42	1.37	
	b	w	2:05	74.0	4650			109	289	1.07		
		x			4470		109	109	289	1.03		
		z			6210			109	289	1.43		
	c	w	2:13	74.3	3700			109	289	0.85		
		x			4390		110	109	289	1.01		
		z			5500			109	289	1.27		

Table F.3 Tensile Strength, Testing Times, and Equivalent Age of 7-Day Cores

Slab ID			Time	Age hrs.	Load, lbs.	Equiv. days I-button	Equiv. days Meter	Equiv. days Used	Predicted Strength	Actual/Predicted Strength	Actual/Predicted Strength avg. by depth	Actual/Predicted Strength avg. by slab
N	a	w	11:25	167.5	4120	212		210	382	0.72	0.71	0.92
		x			4630		208	210	382	0.81	0.83	
		z			4900	212		210	382	0.86	1.22	
	b	w	11:28	167.5	4000	212		210	382	0.70		
		x			4080		208	210	382	0.71		
		z			6140	212		210	382	1.07		
	c	w	11:35	167.5	4100	212		210	382	0.72		
		x			5510		208	210	382	0.96		
		z			9950	212		210	382	1.74		
O	a	w	2:00	170.0	4690			178	356	0.88	0.83	0.88
		x			4080		209.5	178	356	0.76	0.82	
		z			5730	146		178	356	1.07	0.97	
	b	w	2:20	170.3	4850			178	356	0.91		
		x			5160		210	178	356	0.97		
		z			5130	146		178	356	0.96		
	c	w	11:45	167.8	3770			178	356	0.71		
		x			3950		207.5	178	356	0.74		
		z			4740	144		178	356	0.89		
S	a	w	1:55	170.0	5490			197	372	0.98	0.86	0.94
		x			4540		196.5	197	372	0.81	0.79	
		z			6870			197	372	1.23	1.16	
	b	w	1:45	169.8	4450			197	372	0.80		
		x			3860		196.5	197	372	0.69		
		z			5500			197	372	0.99		
	c	w	1:39	169.7	4450			197	372	0.80		
		x			4760		196.5	197	372	0.85		
		z			7060			197	372	1.27		
2	a	w	2:31	170.5	3420	192		192	368	0.62	0.76	0.77
		x			4010			201	375	0.71	0.72	
		z			4250	209		209	381	0.74	0.83	
	b	w	2:34	170.5	4930	195		195	370	0.89		
		x			4170			203.5	377	0.74		
		z			4300	212		212	384	0.75		
	c	w	3:14	171.3	4320	195		195	370	0.78		
		x			3970			204	377	0.70		
		z			5690	212.3		212	384	0.99		
8	a	w	2:47	170.8	3440	198.8		198.8	373	0.61	0.62	0.85
		x			4500		211.3	211	383	0.78	0.72	
		z			7310	217.8		217.8	388	1.26	1.22	
	b	w	3:00	171.0	3630	199		199	373	0.65		
		x			4290		211.5	212	384	0.75		
		z			6970	218		218	388	1.20		
	c	w	2:50	170.8	3370	198.8		198.8	373	0.60		
		x			3600		211	211	383	0.63		
		z			7060	217.8		217.8	388	1.21		
P	a	w	2:23	170.3	5550			252	413	0.90	0.69	0.76
		x			4120		251.8	252	413	0.67	0.64	
		z			5180			252	413	0.84	0.96	
	b	w	3:02	171.0	3680			252	413	0.59		
		x			3080		251.5	252	413	0.50		
		z			6910			252	413	1.12		
	c	w	2:58	171.0	3550			252	413	0.57		
		x			4750		251.5	252	413	0.77		
		z			5750			252	413	0.93		

Table F.4 Tensile Strength, Testing Times, and Equivalent Age of 28-Day Cores

Slab ID			Time	Age	Load,	Equiv. days			Predicted Strength	Actual/Predicted Strength		
				hrs.	lbs.	I-button	Meter	Used			avg. by depth	avg. by slab
N	a	w	1:58	674.0	5090	725		725	649	0.52	0.56	0.66
		x			4410			715.5	645	0.46	0.58	
		z			8750	706		706	641	0.91	0.86	
	b	w	2:01	674.0	5640	725		726	649	0.58		
		x			6080			715.5	645	0.63		
		z			9270	706		707	642	0.96		
	c	w	2:04	674.0	5490	725		727	649	0.56		
		x			6340			715.5	645	0.66		
		z			6720	706		708	642	0.70		
O	a	w	1:20	673.3	7220			580.5	590	0.82	0.79	0.81
		x			6410		680	580.5	590	0.72	0.64	
		z			9110	481		580.5	590	1.03	1.00	
	b	w	1:54	674.0	7250			580.5	590	0.82		
		x			6050		680.5	580.5	590	0.68		
		z			7080	482		580.5	590	0.80		
	c	w	1:52	673.9	6630			580.5	590	0.75		
		x			4440		680.5	580.5	590	0.50		
		z			10380	482		580.5	590	1.17		
S	a	w	2:10	674.2	6740			684	633	0.71	0.68	0.73
		x			5420		683.6	684	633	0.57	0.61	
		z			9380			684	633	0.99	0.92	
	b	w	2:14	674.3	6300			684	633	0.66		
		x			5930		683.5	684	633	0.62		
		z			7500			684	633	0.79		
	c	w	2:59	675.0	6290			684	633	0.66		
		x			5900		685.5	684	633	0.62		
		z			9270			684	633	0.98		
2	a	w	2:49	674.8	6220	688.8		688.8	635	0.65	0.71	0.79
		x			6390			698.5	638	0.67	0.71	
		z			10680	708		708	642	1.11	0.96	
	b	w	2:52	674.9	7860	689		689	635	0.83		
		x			6980			699	639	0.73		
		z			6110	708		708	642	0.63		
	c	w	2:20	674.3	6110	688		688	634	0.64		
		x			6850			689	635	0.72		
		z			11040	708		708	642	1.15		
8	a	w	1:47	674.0	5870	679		679	631	0.62	0.63	0.80
		x			7920			692.5	636	0.83	0.74	
		z			11720	706		706	641	1.22	1.03	
	b	w	1:42	673.8	4790	679		679	631	0.51		
		x			5410			693	636	0.57		
		z			8560	706		706	641	0.89		
	c	w	1:38	673.6	7330	678		678	630	0.78		
		x			7710			692	636	0.81		
		z			9430	705		705	641	0.98		
P	a	w	1:28	673.5	6300							
		x			6060							
		z			13050							
	b	w	1:33	673.5	5580							
		x			7620							
		z			11240							
	c	w	3:04	675.0	6100							
		x			8580							
		z			10400							

Table F.5 Aquameter Readings from Open and Sheltered Pans

Concrete Mode				Calibration Mode						From Weight					
Open		Sheltered		Open			Sheltered			Open			Sheltered		
Age hrs.	Value	Age, hrs	Value	Age, hrs.	Value	/10	Age, hrs.	Value	/10	Age, hrs.	Weight	Moisture, %	Age, hrs.	Weight	Moisture, %
4.25	6.6	2.75	5.2	8.92	52	5.2	8.25	49	4.9	0.13	31.16	3.62	0.13	29.90	3.62
4.75	6.4	3.25	5.1	9.50	53	5.3	8.92	48	4.8	0.75	31.04	2.97	0.75	29.88	3.50
5.25	6.3	3.75	5.9	10.08	56	5.6	9.50	45.3	4.53	1.53	31.04	2.98	1.53	29.80	3.04
5.75	6.1	4.25	5.5	10.67	54.5	5.45	10.08	50.2	5.02	1.97	30.94	2.43	1.97	29.80	3.04
8.25	4.7	4.75	6.1	11.33	47.5	4.75	10.67	49	4.9	5.75	30.86	1.99	5.75	29.17	-0.79
8.92	5.3	5.25	5.2	12.00	56.2	5.62	11.33	51	5.1	6.63	30.84	1.88	6.63	29.30	0.02
9.50	4.8	5.75	5	14.58	41.8	4.18	12.00	50	5	7.50	30.86	1.99	7.50	29.76	2.80
10.08	5.5	6.75	5.2	15.00	45.6	4.56	25.00	60.6	6.06	8.50	30.88	2.10	8.50	29.74	2.69
10.67	3.2	7.75	4.4	17.83	50	5	26.00	57.9	5.79	9.50	30.88	2.10	9.50	29.74	2.69
11.33	3.3	8.25	3.8	18.83	52.4	5.24	27.17	58.6	5.86	10.50	30.84	1.88	10.50	29.68	2.33
12.00	5.5	8.92	3.6	25.00	55.6	5.56	29.00	55.5	5.55	11.50	30.84	1.88	11.50	29.68	2.33
13.58	4.5	9.50	3.3	26.00	54	5.4	30.00	50.6	5.06	18.00	30.86	1.99	18.00	29.70	2.45
14.58	1.4	10.08	4.4	27.17	52.6	5.26	31.33	55	5.5	19.00	30.78	1.54	19.00	29.72	2.57
15.00	2.6	10.67	5.5	29.00	51.9	5.19	34.83	52.8	5.28	20.00	30.78	1.54	20.00	29.62	1.97
15.75	3.4	11.33	4.8	30.00	51.6	5.16				21.00	30.74	1.32	21.00	29.54	1.49
17.83	3.7	12.00	3.5	31.33	51.2	5.12				22.00	30.70	1.09	22.00	29.62	1.97
18.83	4.2	21.75	7	34.83	54.6	5.46				23.00	30.68	0.98	23.00	29.58	1.73
21.75	5.2	23.00	6.9	43.58	54.8	5.48				24.00	30.70	1.09	24.00	29.62	1.97
23.00	5.5	24.00	7.7	44.85	57.9	5.79				25.00	30.78	1.54	25.00	29.58	1.73
24.00	5.3	25.00	7.1	46.70	55.8	5.58				26.08	30.74	1.32	26.08	29.58	1.73
25.00	5.4	26.00	6	50.50	60.6	6.06				27.00	30.74	1.32	27.00	29.60	1.85
26.00	5	27.17	6.3	54.70	56.6	5.66				28.00	30.74	1.32	28.00	29.62	1.97
27.17	4.5	29.00	5.4	65.50	50.3	5.03									
29.00	4.3	30.00	5.3	67.62	53.6	5.36									
30.00	4.2	31.33	5.2												
31.33	4.1	34.83	4.2												
34.83	5														
43.58	4.8														
44.85	5.8														
46.70	5.5														
50.50	7														
54.70	5.9														
65.50	3.9														
67.62	5														

Pan 1=	Open
Pan 2 =	Sheltered
Height =	6
Diameter =	12
Weight Mold (lb)=	13.23
Potential Water (%)=	0.0362

Table F.6 Concrete Mode Aquameter Readings

Date	Time	Hours	Slab							
			P	O	S	2	8	N	Pan 1	Pan 2
28	2:15	2.25		5.8	~~7.9~~			5.8		
	2:45	2.75		7.8	~~8.6~~		9.5	6		5.2
	3:15	3.25		6.4	~~6.3~~		9	5.2		5.1
	3:45	3.75		5.9	~~6.3~~		8.6	5		5.9
	4:15	4.25		6.2	~~6~~		9.4	5.5	6.6	5.5
	4:45	4.75		6.4	~~6~~		9.5	5.4	6.4	6.1
	5:15	5.25		5.6	~~6~~		8.3	5.5	6.3	5.2
	5:45	5.75		6.1	~~6~~	~~6.4~~	9.4	5.4	6.1	5
	6:45	6.75		5.3	~~6~~	~~5.6~~	8.1	5.3	~~6.1~~	5.2
	7:45	7.75		7.3	5.2	5.8	5	4.3	~~4.7~~	4.4
	8:15	8.25		6.2	4.8	3.5	4.5	5.9	4.7	3.8
	8:55	8.92		5.6	3.9	3.6	3.9	4.6	5.3	3.6
	9:30	9.50		5.2	3.8	4.3	4	5.5	4.8	3.3
	10:05	10.08		7	3.4	4.2	3.8	5.6	5.5	4.4
	10:40	10.67		6.5	4.3	6.1	~~3.8~~	6.2	3.2	5.5
	11:20	11.33		7.2	3.3	5	~~3.8~~	6.2	3.3	4.8
29	12:00	12.00		5.8	3.5	4.8	3.9	5.2	5.5	3.5
	1:35	13.58		6.5	3.2	4.4	4	5	4.5	
	2:35	14.58		5.9	3.4	3.9	3.7	2.3	1.4	
	3:00	15.00		6.2	4	3.8	3.9	4.8	2.6	
	4:45	15.75		5.6	2.8	3.8	4.2	5.2	3.4	
	5:50	17.83		5.1	2.7	2.8	4.1	4.3	3.7	
	6:50	18.83		6.2	3.6	4.5	5	5.5	4.2	
	9:45	21.75	5.7	9.3	5.8	7	6.2	5.3	5.2	7
	10:58	23.00	5.3	9.3	5.5	6.2	5.9	5.6	5.5	6.9
	11:56	24.00	5.3	9.8	5.2	7.2	7.9	7.2	5.3	7.7
	12:57	25.00	7.9	8.9	5.1	6	5.4	6.9	5.4	7.1
	2:05	26.00	6.2	8.6	5.3	5.9	5.4	6.3	5	6
	3:10	27.17	7.6	8.4	4.7	5.5	5.2	6.7	4.5	6.3
	5:00	29.00		8.1	4.2	4.6	4.7	5.8	4.3	5.4
	6:00	30.00		7.8	4.1	4.8	4.6	5.6	4.2	5.3
	7:20	31.33		7	3.8	4.9	4.7	5.4	4.1	5.2
	10:50	34.83		7	3.6	4.3	4.3	5.3	5	4.2
30	7:35	43.58		6.8	3.7	4.3	4.7	4.9	4.8	
	8:51	44.85	6.1		4.4	5	5	6	5.8	
	10:42	46.70	6.9	8.1	4.5	5.6	5.3	6	5.5	
	2:30	50.50	8.2	9.4	5.3	6.2	6.1	6.7	7	
	6:42	54.70	6.2	8.6	4.4	5.6	5	6.3	5.9	
31	5:30	65.50	5	6.6	2.6	3.8	4	4.1	3.9	
	7:37	67.62	6	6.8	3.5	3.8	4.7	5.5	5	

Table F.7 Humidity Sensor Data Results for Slab *N*

Sensor 1				Sensor A			
Date	Time	Age, hrs.	Humidity, percent	Date	Time	Age, hrs.	Humidity, percent
28 pm	1:10	1.17	69.05	28 pm	9:25	9.42	109.98
	1:20	1.33	66.39		10:00	10.00	109.99
	2:40	2.60	84.17		12:00	12.00	105.17
	3:20	3.33	86.3	29	2:02	14.03	106.35
	4:35	4.58	73.76		4:35	16.58	109.45
	5:27	5.50	89.24		5:46	17.77	110.6
	6:25	6.42	94.58		7:05	19.08	103.63
	7:45	7.75	99.32		8:50	20.83	84.79
	8:22	8.37	98.32		10:02	22.03	77.14
	11:05	11.08	99.72		11:00	23.00	77.53
29	1:03	13.00	73.82		12:00	24.00	74.83
	2:58	15.00	101.43		1:15	25.25	77.77
	5:27	17.45	101.53		2:16	26.27	73.42
	6:05	18.08	101.49		2:54	26.90	86.31
	7:15	19.25	94.31		4:43	28.72	98.53
	8:58	21.00	55.76		7:09	31.15	108.7
	10:12	22.20	82.46		11:01	35.02	110.41
	11:10	23.20	66.52	30 am	5:26	41.43	106.1
	12:06	24.10	71.21		7:20	43.33	100.77
	1:25	25.42	73.55	30 pm	5:46	53.77	106.29
	2:25	26.42	77.34	31 am	5:34	65.57	122.04
	3:05	27.08	85.79		7:48	67.80	97.87
	4:55	28.92	91.62				
	7:18	31.30	100.69				
	11:00	35.00	100.99				
30 am	5:38	41.63	96.72				
30 pm	5:53	53.88	103.17				
31 am	5:20	65.33	123.52				
	8:04	68.07	96.58				

Table F.8 Humidity Sensor Data Results for Slab *O*

Sensor 1				Sensor A			
Date	Time	Age, hrs.	Humidity, percent	Date	Time	Age, hrs.	Humidity, percent
28 pm	4:30	4.50	90.34	28 pm	7:50	7.83	108.84
	5:15	5.25	86.49		8:00	8.00	106.7
	6:10	6.17	98.67		8:47	8.78	107.63
	10:00	10.00	102.67		10:29	10.48	108.46
29	1:08	13.13	96.91		10:35	10.58	107.82
	3:05	15.08	101.45		11:45	11.75	108.82
	5:18	17.30	103.75	29	2:08	15.13	106.3
	6:15	18.25	100.51		4:50	16.83	109.28
	7:22	19.37	86.43		6:04	18.07	110.47
	9:05	21.08	58		7:12	19.20	86.36
	10:18	22.30	65.17		8:55	20.92	68.52
	11:14	23.23	67.29		10:06	22.10	80.36
	12:11	24.18	70.49		11:07	23.12	71.82
	1:26	25.43	72.81		12:03	24.05	73.39
	2:30	26.50	78.47		1:17	25.28	75.91
	3:08	27.13	73.16		2:21	26.35	77.99
	4:45	28.75	93.03		3:02	27.03	89.77
	6:48	30.80	97.42		4:54	28.90	94.55
	11:07	35.12	100.86		7:15	31.25	106.34
30 am	5:28	41.47	98.44		11:05	35.08	106.17
30 pm	6:05	54.08	102.36	30 am	5:40	41.67	106.09
31 am	5:34	65.57	122.42	30 pm	6:00	54.00	105.86
	7:50	67.83	95.93	31 am	5:30	65.50	122.57
					8:05	68.08	86.36

Table F.9 Humidity Sensor Data Results for Slab *S*

Sensor 1				Sensor A			
Date	Time	Age, hrs.	Humidity, percent	Date	Time	Age, hrs.	Humidity, percent
28	2:45	2.75	85.06	28	7:45	7.75	104.24
	3:02	3.03	82.32		8:05	8.08	105.93
	3:48	4.80	91.91		11:20	11.33	109.94
	4:55	4.92	81.69	29	2:15	14.25	105.95
	5:40	5.67	95.67		4:58	16.80	108.24
	9:40	9.67	102.98		6:13	18.22	106.26
	10:40	10.70	103.63		7:20	19.33	76.79
29	1:13	13.22	93.14		9:00	21.00	71.33
	3:12	15.20	101.39		10:14	22.23	79.24
	5:11	17.18	103.35		11:12	23.20	76.34
	6:25	18.42	98.34		12:08	24.13	75.72
	7:31	19.52	80.25		1:24	25.40	71.02
	9:12	21.20	69.45		2:28	26.47	87.86
	10:23	22.38	73.52		3:07	27.12	90.32
	11:17	23.28	69.94		5:13	29.22	101.8
	12:14	24.23	70.12		6:46	30.77	109.4
	1:34	25.57	69.17		11:09	35.15	108.81
	2:33	26.55	81.97	30 am	5:30	41.50	107.17
	3:19	27.32	82.42		6:10	42.17	106.58
	6:55	30.92	99.29	31 am	5:23	65.38	122.39
	11:11	35.18	102.84		7:52	67.87	95.64
30 am	5:43	41.72	99.58				
	6:15	42.25	99.56				
31 am	5:29	65.48	125.01				
	8:08	68.13	86.84				

Table F.10 Humidity Sensor Data Results for Slab *2*

Sensor 1				Sensor A			
Date	Time	Age, hrs.	Humidity, percent	Date	Time	Age, hrs.	Humidity, percent
28	4:01	4.02	86.82	29	2:20	14.33	104.59
	5:05	5.08	73.62		5:15	17.25	108.06
	5:20	5.33	91.23		6:23	18.38	101.53
	7:55	7.92	98.4		7:29	19.48	74.25
	8:52	8.87	101.58		9:08	21.13	76.2
	9:04	9.07	99.02		10:20	22.33	73.85
	10:18	10.30	101.38		11:15	23.25	72.25
	11:45	11.75	99.2		12:13	24.22	69.64
29	1:18	13.30	93.06		1:31	25.52	65.53
	3:20	15.33	101.25		2:31	26.52	82.91
	5:03	15.05	102.25		3:17	27.28	75.67
	6:35	18.58	77.8		6:53	30.88	106.32
	7:40	19.66	66.36		11:15	35.25	107.12
	9:22	21.37	70.16	30 am	5:45	41.75	106.49
	10:27	22.45	70.68		7:37	43.6	105.49
	11:21	23.35	67.37	31 pm	6:17	54.28333	105.07
	12:17	24.28	70.01	31 am	5:27	65.45	122.41
	1:44	25.73	64.84		8:14	68.23333	86.29
	2:40	26.67	78.31				
	3:23	27.38	83.71				
	7:00	31.00	98.38				
	11:17	35.28	102.11				
30 am	5:50	41.83	99.69				
	7:30	43.50	101.62				
30 pm	6:20	54.33	98.81				
31 am	5:22	65.37	123.96				
	8:09	68.15	88.64				

Table F.11 Humidity Sensor Data Results for Slab *8*

Sensor 1				Sensor A			
Date	Time	Age, hrs.	Humidity, percent	Date	Time	Age, hrs.	Humidity, percent
28	3:10	3.17	79.606	29	2:27	14.45	103.83
	4:16	4.27	84.57		5:08	17.13	108.35
	5:10	5.17	73.58		6:31	18.52	94.06
	6:00	6.00	91.53		7:36	19.60	77.5
	8:47	8.78	101.18		9:14	21.23	67.11
	9:27	9.45	102.06		10:25	22.42	65.07
	10:30	10.50	101.64		11:19	23.32	69.02
	11:30	11.50	88.27		12:17	24.28	68.28
	12:00	12.00	96.01		1:36	25.60	64.07
29	1:22	13.37	94.83		2:36	26.60	80.74
	3:27	15.45	97.44		3:21	27.35	85.4
	4:35	16.58	102.51		6:58	30.97	106.35
	6:45	18.75	86.4		11:17	35.28	106.75
	7:48	19.80	78.11	30 am	5:51	41.85	106.22
	9:45	21.75	65.09	30 pm	6:25	54.42	105.06
	10:31	22.52	65.4	31 am	5:20	65.33	122.15
	11:28	23.47	67.89		8:13	68.22	82.47
	12:23	24.38	63.09				
	1:10	25.17	56.95				
	2:07	26.12	61.52				
	2:45	26.75	71.96				
	7:05	31.08	98.96				
	11:19	35.32	105.46				
30 am	5:47	41.78	102.59				
30 pm	6:18	54.30	100.46				
31 am	5:26	65.43	125.27				
	8:10	68.17	88.07				

Table F.12 Humidity Sensor Data Results in Open Pan

Sensor 1				Sensor A			
Date	Time	Age, hrs.	Humidity, percent	Date	Time	Age, hrs.	Humidity, percent
28 pm	1:20	1.33	70.79	28 pm	9:05	9.1	110.05
	3:06	3.10	69.72		9:40	9.7	106.16
	4:40	4.66	72.37		10:15	10.3	105.85
	5:35	5.58	82.18		10:40	10.7	101.37
	6:35	6.58	90.4		12:15	12.3	100.69
	11:15	11.25	85.11		12:54	12.9	97.83
29	1:29	13.48	86.94	29	2:35	14.6	95.35
	2:28	14.47	89.69		3:29	15.5	104.6
	3:33	15.55	88.96		5:22	17.4	104.35
	4:45	16.75	99.94		6:41	18.7	102.48
	5:48	17.80	100.78		7:45	19.8	64.58
	7:07	19.12	69.49		9:53	21.9	71.44
	8:47	20.78	62.01		10:29	22.5	72.03
	10:05	22.08	74.87		11:22	23.6	68.92
	10:59	22.98	61.29		12:21	24.4	69.44
	11:59	23.98	68.01		1:10	25.16667	75.02
	1:16	25.27	73.39		2:05	25.08333	67.97
	2:14	26.23	69.76		3:26	27.43333	84.39
	2:58	26.97	65.82		7:03	31.05	106.53
	7:11	31.18	98.24				

References

Aïtcin, P., Miao, B., Cook, W. D., and D. Mitchell, “Effects of Size and Curing on Cylinder Compressive Strength of Normal and High-Strength Concretes,” *ACI Materials Journal*, Vol. 91, No. 4, July-August 1994, pp. 349–354.

ASTM, “Standard Practice for Estimating Concrete Strength by the Maturity Method,” C 1074–98.

Ahmed, A. E., “Does Core Size Affect Strength Testing?”, *Concrete International*, Vol. 21, No. 8, August 1999, pp. 35–39.

Bartlett, F. M., and J. G. MacGregor, “Effect of Core Diameter on Concrete Core Strengths,” *ACI Materials Journal*, Vol. 91, Sept.-Oct., 1994, pp. 460–470.

Bloem, D. L., “Concrete Strength in Structures,” *Journal of the American Concrete Institute*, March 1968, pp. 176–187.

Bloem, D. L., “Concrete Strength Measurement – Cores versus Cylinders,” *American Society for Testing and Materials. Proceedings*, Vol. 65, 1965, pp. 668–696.

Bloem, D. L, and S. Walker, “Effects of Aggregate Size on Properties of Concrete,” *Journal of the American Concrete Institute*, Title No. 57-13, Sept. 1960, pp. 283–297.

Bungey, J. H., “Determining Concrete Strength by Using Small-Diameter Cores,” *Magazine of Concrete Research,* Vol. 31, No. 107, June 1979, pp. 91–98.

Bungey, J. H., The Testing of Concrete in Structures, 2nd ed. Chapman and Hall, New York, 1989, pp. 94–110.

Campbell, R. H., and R. E. Tobin, “Core and Cylinder Strengths of Natural and Lightweight Concrete,” *Journal of the American Concrete Institute. Proceedings*, Vol. 64, No. 4, April 1967, pp. 190–195.

Carino, N. J., “Prediction of Potential Concrete Strength at Later Ages,” *ASTM Significance of Tests and Properties of Concrete and Concrete Making Materials*, STP 169 C, 1994, pp. 140–152.

Carrasquillo, P. M., “Concrete and Concrete Making Materials,” *ASTM Significance of Tests and Properties of Concrete and Concrete Making Materials*, STP 169 C, 1994, pp. 123–139.

Concrete Society, *Concrete Core Testing for Strength,* Technical Report No. 11 (including 1987 addendum), Ref. 53.056, London, 1987.

Date, C.G., and R. H.Schnormeier, “Day-to-Day Comparison of 4- and 6-in. Diameter Concrete Cylinder Strengths,” *Concrete International*, Vol. 6, No. 8, Aug. 1984, pp. 24–26.

Elimov, R., and G. C. Hoff, "Core Strength of High-Strength Concrete," *ACI. Proceedings* of the 3rd CANMET/ACI International Conference, Malaysia, SP 172-38, 1997, pp. 705–715.

Grater, Stephan F., "An Investigation toward Performance-Oriented Specifications for Portland Cement Concrete Pavement." Diss. The University of Texas at Austin, 1997.

Holland, T. C., "Using the Maturity Method to Predict Concrete Strength," *Concrete Construction*, V. 32, No. 10, Oct. 1987, pp. 867–869.

Keiller, A.P., "An Investigation of the Effects of Test Procedure and Curing History on the Measured Strength of Concrete," ACI Publication, SP-82, 1984, pp. 441–458.

Kesler, C.R., "Strength," *ASTM Significance of Tests and Properties of Concrete and Concrete Making Materials*, STP 169A, 1966, pg 144–159.

Légeron, F., and P. Paultre, "Prediction of Modulus of Rupture of Concrete," *ACI Materials Journal*, March-April 2000, Title No. 97-M25, Vol. 97, No. 2, pp. 193–200.

Munday, J. G. L., and R. K. Dhir, "Assessment of In Situ Concrete Quality by Core Testing," *American Concrete Institute*, Publication SP-82, Detroit, Michigan, 1984, pp. 393–410.

Lamond, J.F., "Making and Curing Concrete Test Specimens," *ASTM Significance of Tests and Properties of Concrete and Concrete Making Materials*, STP 169 C, 1994, pp. 71–76.

Malhotra, V.N., "Contract Strength Requirements - Cores versus In Situ Evaluation," *Journal of the American Concrete Institute*. *Proceedings*, Vol. 74, No. 4, April 1977, pp. 163–172.

Malhotra, V.M., "Nondestructive Tests," *ASTM Significance of Tests and Properties of Concrete and Concrete Making Materials*, STP 169 C, 1994, pp. 320–338.

Mather, B., and W. O. Tynes, "Investigation of Compressive Strength of Molded Cylinder and Drilled Cores of Concrete," *Journal of the American Concrete Institute. Proceedings*, Vol. 57, No. 7, January 1961, pp. 767–778.

McCullough, B. F., Zollinger, D., and T. Dossey, "Evaluation of the Performance of Texas Pavements Made with Different Coarse Aggregates," *Center for Transportation Research*, The University of Texas at Austin, Research Report 3925-1, September 1998, Revised June 1999.

McCullough, B. F., Zollinger, D., and T. Dossey, "Evaluation of the Performance of Texas Pavements Made with Different Coarse Aggregates: Project Summary Report," *Center for Transportation Research*, The University of Texas at Austin, Research Report 3925-S, September 1998.

Meininger, R. C., "Effect of Core Diameter on Measured Concrete Strength," *Journal of Materials,* Vol. 3, No. 2, June 1968, pp. 320–36.

National Climatic Data Center (NCDC), "Hourly Observation Table," March 1, 1999, Online, May 26, 2000.

Oluokun, F. A., Burdette, E. G., and J. H. Deatherage, "Early-Age Concrete Strength Prediction by Maturity- Another Look," *ACI Materials Journal*, Nov.-Dec. 1990, pp. 565–572.

Plowman, J. M., "Maturity and the Strength of Concrete," *Magazine of Concrete Research*, Vol. 8, No. 22, 1956, pp. 13–22.

Raphael, J. M., "Tensile Strength of Concrete," *Journal of the American Concrete Institute*, March-April 1984, pp. 158–165.

Rochefort, J. L., "Evaluation of the Effects of the Tining Operation on the Performance of Portland Cement Concrete Pavements," The University of Texas at Austin, 2000.

Schindler, A., "Implementation of Aggregate Thermal Properties to Improve Pavement Performance," Center for Transportation Research at The University of Texas at Austin, June 2001.

Senbetta, E., "Curing and Curing Materials," *ASTM Significance of Tests and Properties of Concrete and Concrete Making Materials*, STP 169 C, 1994, pp. 478–483.

Simons, B. P., "Compressive Strength Relationship Between Cylinder Tests and Core Tests," *Construction Materials Serviceability and Durability. Proceedings*, 1990, V. 1, pp. 223–232.

SAS Institute Inc., *SAS User's Guide: Statistics, Version 5 Edition*, Cary, NC: SAS Institute Inc., 1985. 965 pp.

Tanigawa, Y., and K. Yamada, "Size Effect in Compressive Strength of Concrete," *Cement and Concrete Research*, Vol. 8, No. 2, 1978, Pergamont Press Inc., pp. 181–190.

Wright, P. J. F., "Comments on an Indirect Tensile Test on Concrete Cylinders," *Magazine of Concrete Research*, Vol. 7, No. 20, London, July 1955, pp. 87–96.

Yip, W.K., and C. T. Tam, "Concrete Strength Evaluation Through the Use of Small Diameter Cores," *Magazine of Concrete Research*, Vol. 40, No. 143, 1988, pp. 99–105.

Yuan, D., Results from Seismic Tests on Small PCC Slab I Technical Memorandum. May 2001.